

# Modelling an inclined fallpipe for subsea rock placement.

Carried out for 'Great Lakes Dredge & Dock Company, LLC'

R.L.H. Vehmeijer

Thesis report









# **Modelling an inclined fallpipe for subsea rock placement.**

**Carried out for 'Great Lakes Dredge & Dock Company, LLC'**

THESIS REPORT

R.L.H. Vehmeijer

October 19, 2022

Faculty of Mechanical, Maritime and Materials Engineering (3mE) · Delft University of  
Technology

Student number: 4461142

Thesis committee:	Prof.dr.ir. C. van Rhee	TU Delft
	Dr.ir. S.A. Miedema	TU Delft
	Dr.ir. A.M. Talmon	TU Delft
	M. Beton	Great Lakes Dredge & Dock Company, LLC



The work in this thesis was supported by Great Lakes Dredging and Docking. Their cooperation is hereby gratefully acknowledged.



Copyright ©  
All rights reserved.





# Acknowledgements

---

This research is my final step in obtaining a master's degree in Offshore & Dredging engineering at the Delft University of Technology. This research has been done in collaboration with Great Lakes Dredge & Dock Company, LLC (GLDD). Within GLDD there was significant interest in my project and I hope my research will help them contribute to the US offshore wind industry to develop a more sustainable future.

First, I would like to thank Dr.ir. S.A. Miedema as being the person who has brought me in contact with GLDD. Together with Sape Miedema, I visited the office of GLDD in Houston for two weeks. During this stay, he guided me through the physics behind all the computer models that I made. As known for his expertise in Dredging technologies, his ingenuity helped me make a computer model for an inclined fallpipe for subsea rock installation.

Secondly, I would like to thank my daily supervisor from the TU Delft, Prof.dr.ir. Cees van Rhee. During the meetings I had with Cees van Rhee, he always knew to put me back on track whenever I was lost. Providing helpful feedback to keep the focus on the main subject. His knowledge was especially helpful for me to draw a conclusion from the data gathered from the experiments.

Moreover, I want to thank my supervisor from GLDD, Michael Beton who guided me during the entire process. During my stay in Houston, we looked into physics together to understand what we were trying to model. When having a meeting with Michael, he always knew to motivate me and come up with a different look on the situation due to his experience with this kind of project. I could not have had a more involved and dedicated supervisor than Michael Beton.

R.L.H.Vehmeijer,  
Delft, October 2022





# Abstract

---

Subsea rock installation is a process in offshore engineering where rocks are placed on the seabed or subsea structures using a fallpipe. An example of a subsea structure could be a cable or pipeline that must be protected. In this research, the main scope is rock installation for scour protection of the foundation of offshore wind turbines. As the US government is planning to build 30 gigawatts of offshore wind capacity by 2030, many rock installation projects are planned. This is where GLDD wants to contribute by being part of a more sustainable future by building a subsea rock installation vessel. This vessel with a 20.000 ton rock capacity is placing rocks using a solid fallpipe.

Accurate knowledge of how rocks are placed using a fallpipe is necessary to plan, manage and estimate the costs of a project. The main focus of this thesis project is to establish an optimal computer model for an inclined fallpipe for subsea rock installation. This model can be used to calculate rock velocity during operating the inclined fall pipe (IFP). Additionally, the particle concentration and the distribution of particles over the pipe's cross-sectional area can be determined. The velocity of particles is essential for future models calculating where the rocks settle down after leaving the fallpipe. Based on the literature two models were made: Vertical fallpipe model 1 (VFM1) and Sliding bed model 1 (SBM1), these models are improved based on data and observations from lab research. These improvements lead to Vertical fallpipe model 2 (VFM2) and Sliding bed model 2 (SBM2).

In the lab research, a scale model of a fallpipe is made. This is done by placing a transparent fallpipe in a 5x2.5x2 meter tank of water. This fallpipe is attached to a conveyor belt, making it possible to precisely control the amount of rocks per second placed in the fallpipe.





# Table of Contents

---

<b>Acknowledgements</b>	<b>i</b>
<b>1 introduction</b>	<b>1</b>
<b>2 Flow regimes</b>	<b>3</b>
2-1 The 8 flow regimes . . . . .	5
2-2 Applicable flow regimes . . . . .	6
<b>3 Rock placement using a vertical fallpipe</b>	<b>9</b>
3-1 Vertical fallpipe production . . . . .	9
3-2 Volumetric concentration . . . . .	9
3-3 Particle velocity . . . . .	10
3-3-1 Single-particle velocity . . . . .	10
3-3-2 Hindered settling . . . . .	11
3-3-3 Wall influenced settling velocity . . . . .	12
3-4 Influence of fallpipe diameter . . . . .	13
3-5 Normalized production with hindered settling . . . . .	13
3-5-1 Maximum concentration for given $\alpha$ . . . . .	14
3-6 Matlab model vertical fallpipe 1 . . . . .	16
<b>4 Rock placement using an inclined fallpipe</b>	<b>17</b>
4-0-1 The limit deposit velocity . . . . .	17
4-1 Sliding bed model . . . . .	19
4-1-1 Gravity force . . . . .	20
4-1-2 Friction force bed-fluid . . . . .	21
4-1-3 Friction force bed-pipewall . . . . .	21
4-1-4 Friction force water-pipewall . . . . .	22
4-1-5 Friction force water, in between bed, and pipewall . . . . .	22
4-1-6 Solving the equilibrium of forces . . . . .	23
4-1-7 Applying model, with known inputs . . . . .	24
4-2 Results sliding bed model 1 . . . . .	24
4-3 Conclusions of results . . . . .	27
4-4 Discussion of results . . . . .	28

<b>5</b>	<b>Lab research</b>	<b>29</b>
5-1	Aim of lab test . . . . .	29
5-2	Lab test setup and method . . . . .	29
5-3	Scaling . . . . .	31
5-4	Method lab research . . . . .	32
5-4-1	Measuring dispersion setup . . . . .	33
<b>6</b>	<b>Results lab research</b>	<b>35</b>
6-1	Result gathering . . . . .	35
6-1-1	Velocity . . . . .	35
6-1-2	Calculating remaining variables . . . . .	38
6-2	Results from labtest . . . . .	38
6-2-1	Dispersion results labtest . . . . .	41
6-3	Conclusion of lab research . . . . .	44
6-3-1	Backflow . . . . .	44
6-3-2	Concentration bed or flow is not constant . . . . .	44
6-3-3	Influence of high concentration . . . . .	45
6-3-4	Dispersion of rock . . . . .	45
6-4	Discussion of lab research results . . . . .	46
<b>7</b>	<b>Validating models with labtest results</b>	<b>47</b>
7-1	Validation sliding bed model . . . . .	47
7-2	Validation vertical pipe model . . . . .	49
<b>8</b>	<b>Model improvement based on lab research</b>	<b>51</b>
8-1	Sliding bed model 2 . . . . .	51
8-2	Vertical fallpipe model 2 . . . . .	54
<b>9</b>	<b>Conclusion</b>	<b>55</b>
<b>10</b>	<b>Discussion and recommendation</b>	<b>57</b>
10-1	When to use which model . . . . .	57
10-2	Different production . . . . .	57
10-3	Scaling models to full scale . . . . .	58

<b>A The back of the thesis</b>	<b>59</b>
A-1 Settling velocity in more detail . . . . .	59
A-2 Sliding bed formulas derived . . . . .	59
A-3 Rewriting the equilibrium . . . . .	61
A-4 Additional images lab research setup . . . . .	63
A-5 Remarkable observations lab research . . . . .	64
A-6 Spread of rock . . . . .	65
A-7 Observation of flow regime labresearch . . . . .	66
A-7-1 Observation of dispersion lab research . . . . .	79
<b>B Sliding bed model 1 code</b>	<b>83</b>
<b>C Sliding bed model 1 code: rewritten</b>	<b>85</b>
<b>D Sliding bed model 2 code</b>	<b>87</b>
<b>E Sliding bed model 2 code:rewritten</b>	<b>91</b>
<b>F Vertical model fallpipe code 1</b>	<b>93</b>
<b>G Vertical model fallpipe code 2</b>	<b>95</b>
<b>Bibliography</b>	<b>97</b>
<b>Glossary</b>	<b>99</b>
List of Acronyms . . . . .	99
List of Symbols . . . . .	99



# List of Figures

---

2-1	Flow regime 1 . . . . .	5
2-2	Flow regime 2 . . . . .	5
2-3	Flow regime 3 . . . . .	5
2-4	Flow regime 4 . . . . .	5
2-5	Flow regime 5 . . . . .	5
2-6	Flow regime 6 . . . . .	6
2-7	Flow regime 7 . . . . .	6
2-8	Flow regime 8 . . . . .	6
3-1	The Reynolds number as a function of the particle diameter . . . . .	12
3-2	Relative particle size . . . . .	13
3-3	Normalized rock production . . . . .	14
3-4	Maximum concentration for given $\alpha$ . . . . .	15
3-5	VFM1:input output . . . . .	16
4-1	Flow directions in pipe, no added water. . . . .	19
4-2	Force equilibrium sliding bed. . . . .	19
4-3	Schematic view cross section pipe . . . . .	20
4-4	Velocity sliding bed . . . . .	23
4-5	SBM1R:input output . . . . .	24
4-6	Velocity sliding bed, top view graph . . . . .	26
4-7	The average and standard deviation of critical parameters . . . . .	27
5-1	Perspective view: 3D model of lab test setup . . . . .	30
5-2	Side view: 3D model of lab test setup . . . . .	30
5-3	Rock collector . . . . .	33
6-1	The average and standard deviation of critical parameters . . . . .	37
6-2	Measure bed height . . . . .	38



6-3	Velocities measured labtest . . . . .	40
6-4	Bed or flow density . . . . .	40
6-5	Beta measured . . . . .	40
6-6	Run 19 spread . . . . .	41
6-7	Run 20 spread . . . . .	41
6-8	Run 21 spread . . . . .	41
6-9	Run 19 spread data . . . . .	42
6-10	Run 20 spread data . . . . .	42
6-11	Run 21 spread data . . . . .	42
6-12	Run 19 spread . . . . .	42
6-13	Run 20 spread . . . . .	42
6-14	Run 21 spread . . . . .	42
6-15	plumes . . . . .	42
6-16	Backflow in labtest: brown arrow is material flow, blue arrow is water backflow	44
6-17	Bed or flow density 2 . . . . .	45
7-1	Bed angle $\beta$ . . . . .	48
7-2	Particle velocity . . . . .	48
8-1	Bed angle $\beta$ SBM2 . . . . .	52
8-2	Particle velocity SBM2 . . . . .	52
10-1	Model advise flowchart . . . . .	57
A-1	The pipe figure and its 3D model . . . . .	60
A-2	Velocity sliding bed . . . . .	62
A-3	Lab setup scaffolding with conveyor belt . . . . .	63
A-4	Lab setup conveyorbelt . . . . .	63
A-5	Lab setup funnel feeding the fallpipe . . . . .	63
A-6	Difference in velocity due to local concentration . . . . .	64
A-7	Run 19 spread . . . . .	65
A-8	Run 20 spread . . . . .	65
A-9	Run 21 spread . . . . .	65
A-10	Side-view run 2 . . . . .	66
A-11	Side-view run 3 . . . . .	67
A-12	Side-view run 4 . . . . .	68
A-13	Side-view run 5 . . . . .	69
A-14	Side-view run 6 . . . . .	70

---

A-15 Side-view run 7 . . . . .	71
A-16 Side-view run 9 . . . . .	72
A-17 Side-view run 10 . . . . .	73
A-18 Side-view run 12 . . . . .	74
A-19 Side-view run 13 . . . . .	75
A-20 Side-view run 16 . . . . .	76
A-21 Side-view run 17 . . . . .	77
A-22 Side-view run 18 . . . . .	78
A-23 Run 19 observations . . . . .	79
A-24 Run 20 . . . . .	81



# List of Tables

---

3-1	Vertical fallpipe model 1 input . . . . .	16
4-1	Variables sliding bed. . . . .	20
4-2	Sliding bed model 1 input . . . . .	25
5-1	Scaled dimensions labtest . . . . .	31
6-1	Results lab test and Matlab model[small rock]. . . . .	38
6-2	Results lab test and Matlab model[Medium rock]. . . . .	39
6-3	Results lab test and Matlab model[large rock]. . . . .	39
6-4	Dispersion test . . . . .	41
8-1	Results lab test compared with Vertical fallpipe model 2 . . . . .	54
A-1	The mechanisms of four consensus filtering approaches . . . . .	60



---

# Chapter 1

---

## introduction

Worldwide the demand for renewable energy rises, so is offshore wind energy becoming increasingly important in the US. On March 29 2021, the White House convened leaders from across the Administration and announced a set of bold actions that will catalyze offshore wind energy. In addition, the Biden Administration has recently set a goal of reaching 30 gigawatts of offshore wind capacity by 2030 in the USA[The White House, 2021]. To place an offshore wind farm, several offshore operations must be completed to fulfil the task. After the base of a monopile is installed, the seabed around its base is covered with a layer of rock to prevent scouring. The part of subsea rock installation is what Great Lakes Dredge & Dock Company, LLC (GLDD) wants to do with their new vessel. This thesis report is a sequel to the literature research that is done. This literature research provided knowledge about the physics behind this vessel's fallpipe system, by understanding this key part of the ship future operations can be better organised. Based on the literature research 2 models are made to predict the particle velocity in a fallpipe. After these models were made, the importance of making and testing a scale model became clear to verify these models.

The main question of this literature research is defined as 'How to model the production for an inclined fallpipe used for subsea rock installation?' To answer this main question the following sub-questions were determined:

- Is the designed fallpipe capable of discharging the required production at every operational relevant pipe angle?
- Which flow regimes are expected in an inclined fallpipe during rock placement?
- Does a backflow of water occur in an inclined fallpipe while operating it? If so, at what angles?
- At which fallpipe angle, do the particles reach the highest velocity?
- Is there a relation between pipe angle and bed density?
- How far do the rocks spread out after leaving the fallpipe? And what does this spreading pattern look like?
- What factors influence the spreading of rock after leaving the fallpipe?



In chapter 2 the flow regimes are explained to better understand how material transported in a pipe behaves. When flow regimes are clear, the physics behind a vertical fallpipe is discussed in chapter chapter 3 which will lead to Vertical fallpipe model 1 (VFM1).

Where-after in chapter 4, physics behind an inclined fallpipe is discussed, based on a sliding bed flow regime Sliding bed model 1 (SBM1) is made. This computer model will provide a production limit and velocity of the particles. Thereafter a scale model is made to validate and improve these theoretical models to match with the lab research. In chapter 5 the layout of this lab research is explained, followed by results in chapter 6. These results are compared with the models in chapter 7 whereafter the results are implemented in the final models: Vertical fallpipe model 2 (VFM2) Sliding bed model 2 (SBM2) shown in chapter 8.

---

## Chapter 2

---

# Flow regimes

In slurry transport, it is common to distinguish different flow patterns, which are so-called flow regimes. These regimes originate from slurry transport, where many different particle types are used. In case of sub-sea rock placement, it is clear that 'rocks' are used, not fine particles such as clay and sand. A typical characteristic in rock placement is that gravity is causing the movement of particles. In slurry transport, water is used as a carrier causing particles to move in the same direction true a pipe. In addition, most often, water is moving slower than the rocks, whereas in slurry transport water is moving faster than the particles in a pipe. This difference in velocity is called 'slip'  $[V_{sl}]$ , which is defined as the difference between the velocity of mixture  $[V_m]$  and solids  $[V_s]$ . In this chapter eight flow regimes are discussed which occur for laboratory and real-life conditions [Miedema, b]. A visual display of how these eight different flow regimes look like is shown in 2-1. Every regime is visualised with two cross areas of a pipe, left with fine particles and right with coarse particles. These flow regimes are important to define the situation in a pipe and which equations can be applied to calculate friction forces in the pipe. With these friction forces, velocity of the particles can be determined.



## 2-1 The 8 flow regimes

### 1. Fixed bed without suspension.

A fixed bed with no suspension: all particles lay on the bed. This two-layer system where particles are settled at the bottom and above it is a flow of water, both layers usually have a different velocity. The bed slides due to friction between the two layers and the pressure working on the beds cross-section. A friction force between the layers occurs. This friction between the bed and fluid is expressed as the Darcy-Weisbach friction factor  $\lambda_{12}$ . This friction factor resulting in a force will be used in the sliding bed model and is expressed in equation

Further friction force in this regime is the bed/pipe-wall friction, known as  $F_{2,fr}$ .

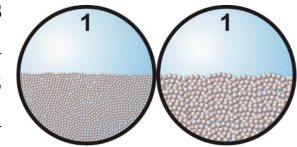


**Figure 2-1:**  
Flow regime 1

### 2. Fixed bed with suspension.

Flow regime 2 is a fixed bed with a suspension of particles that flow above the bed. The bed's density decreases to the top of the bed. The 'sheet flow' above the bed is similar to sliding bed but less dense, the sheet flow density also decreases.

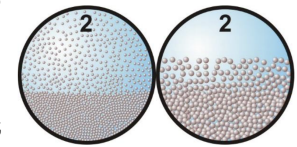


**Figure 2-2:**  
Flow regime 2

### 3. Fixed bed with suspension or sliding bed with sheet flow Constant $C_{vs}$ .

Under laboratory circumstances with a constant spatial volumetric concentration  $C_{vs}$ , for coarse particles the bed is sliding with sheet flow at the top, where the thickness of the sheet flow layer increases with an increasing velocity difference between the flow above the bed, while for fine particles the shear stress on the bed is not high enough to make it start sliding, but more and more particles will be in suspension as the line speed increases. For fine particles, the behaviour starts following the heterogeneous behaviour more and more with increasing line speed.

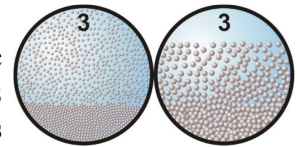


**Figure 2-3:**  
Flow regime 3

### 4. Fixed bed with the suspension of coarse particles. The bed is sliding with sheet flow. The thickness of the sheet flow layer increases at a higher particle velocity difference. For fine particles, the shear stress, between the bed and the mixture flow above it, is not high enough to create a sliding bed.

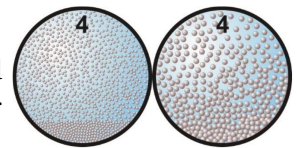


**Figure 2-4:**  
Flow regime 4

### 5. Heterogeneous transport $C_{vt} \approx C_{vs}$

Line speed increased further, the difference between spatial and delivered concentration becomes smaller. Due to the turbulence of the flowing water, turbulent forces interacting with the particles are not strong enough to create a uniform particle distribution. In both cases, for coarse and fine particles, a concentration gradient occurs along the vertical axis of the pipe. Highest concentration at the top, the lowest concentration at the bottom.

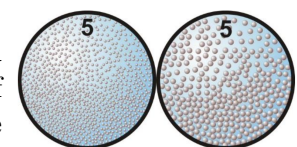


**Figure 2-5:**  
Flow regime 5

### 6. Homogeneous transport $C_{vt} \approx C_{vs}$

Similar to flow regime 5, even smaller difference between spatial and delivered concentration. For coarse and fine particles, the turbulent forces interacting with them are high enough to create a complete uniform distribution throughout the cross-section.

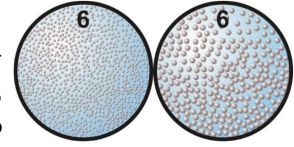


**Figure 2-6:**  
Flow regime 6

### 7. Sliding Flow.

For relative low concentrations and relatively small particle diameters, the sliding bed regime will transform into a heterogeneous regime at the intersection of the two regimes. This is caused by the lift forces not being large enough to lift particles from the bed. However, when particles are bigger and the lift forces are not large enough to lift the particles, a bed will form. This regime is called sliding flow, there is flow but the resistance on the bed is comparable with that of sliding bed friction.

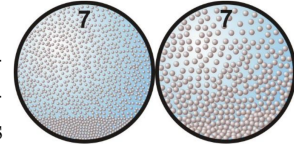


**Figure 2-7:**  
Flow regime 7

### 8. Fixed bed with suspension, constant $C_{vt}$ .

In this flow regime, constant volumetric transport concentration with decreasing line speed. An equilibrium arises between erosion and deposition of the bed. This equilibrium results in a certain bed height. This regime occurs if the relative excess hydraulic gradient is high enough to result in a sliding bed and so this will occur much more with small pipe diameters than with large pipe diameters.

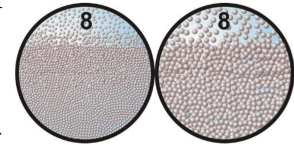


**Figure 2-8:**  
Flow regime 8

## 2-2 Applicable flow regimes

Much research has been done on flow regimes, however, this was for slurry transport and not for subsea rock installation (using an inclined fallpipe). The main difference is the driving force and grain size.

1. Driving force: for rock installation, this is gravity, for slurry transport, this is a pressure gradient. The pressure created by a pump creates a pressure difference causing water and particles to flow true the pipe. Water and particles are transported in the same direction. For a closed fallpipe where no water is added, this is not the case. Particles are moving down the pipe and water is staying in the pipe because it is not added. This is discussed in more detail in chapter 4.
2. Grain size: for rock installation relative large particles are used compared to slurry transport, this results in very large Reynolds numbers. A significant difference in

grain size results in different behaviour of particles, making empirical and pseudo-scientific equations less applicable. With a particle diameter of 100 mm and higher for rock placement the Reynolds number is far above 2000, so the particle will be in the turbulent region according to figure 4.3-2 in Miedema's book[Miedema, b].

These differences listed above make it difficult to predict which flow regime will occur in which situation. It is assumed that in the case of a vertical fallpipe, homogeneous transport applies. If the pipe is placed diagonally, it is assumed that a sliding bed or sliding flow occurs. The difference between a sliding bed and a sliding flow is that a bed is dense and a flow is not, a requirement of a bed is that it would be theoretically possible to walk on it[Miedema, b]. To determine which flow regime occurs in different situations, a scale model of a fallpipe is tested in a lab researchchapter 5.



# Rock placement using a vertical fallpipe

In this chapter the physics behind a vertical fallpipe is discussed to provide the information needed to make Vertical fallpipe model 1 (VFM1). The equations that are used for calculating the production of a vertical fallpipe is given in the first section 3-1. The different variables that are included in this equation will be further discussed in depth to give an insight in which variables influence the production of a fallpipe.

### 3-1 Vertical fallpipe production

In this section the production of a fallpipe will be discussed, it is expressed in kg/second or tons/hour. In this chapter it is assumed that water and stones will be added at the top (inlet section). The equation to calculate the production is given in Eq. (3-1).

$$P_o = \rho_s \cdot c \cdot u_p \cdot A_p \quad (3-1)$$

In Eq. (3-1) there are four variables that influence the production of a fall pipe. To maximise the production and increase the efficiency of a rock dumping process we look closer to this formula. The first variable is  $\rho_s$ , this is a material property of rock. This can differ depending on what kind of rock is used but is constant for a chosen rock type. The second variable is the volumetric concentration  $c$ . It is the ratio between rock and water that flows true the pipe, this ratio can be changed. This will be further discussed in section 3-2. Particle velocity  $u_p$  can be increased resulting in higher production, increasing  $u_p$  has its own pros and cons and will be discussed in the section 3-3. Finally, there is the fourth variable  $A_p$ , which is the crosssectional surface area of the pipe, this will be discussed in section 3-4.

### 3-2 Volumetric concentration

As can be read from Eq. (3-1), increased Volumetric concentration of rocks in a fallpipe lead to higher production. However the concentration has its limits, when the concentration of rock in a fallpipe is too high it will clog and production will drop to zero. When a higher



concentration of material is wanted in the fallpipe, more water should be added at the top to prevent clogging the system. A clear overview of concentration operating limits with various amounts of added water to the fallpipe ( $\alpha$ ), is shown in Figure 3-3

### 3-3 Particle velocity

Obviously, a higher particle velocity results in a higher fallpipe production. Despite striving for a maximum production, a particle velocity that is 'too high' is not desired. When rocks reach a high velocity and shoot out of the end of the fallpipe, this can lead to more rock penetration, damaging structures and rocks ending up in a different location than planned. More about the consequences of high particle velocity is discussed in the appendix. The particle velocity  $[u_p]$  in a fallpipe is relative to the velocity of the water around it [Van Rhee, 2018]. Therefore the water velocity  $[u_w]$  in the pipe is added to the settling velocity  $[w_s]$ .

$$u_p = u_w + w_s \quad (3-2)$$

The velocity of the water can be expressed as:

$$u_w = \alpha \cdot w_{0,p} \quad (3-3)$$

$u_w$  is the average water velocity due to added water at the inlet of the pipe based on  $\alpha$  which is a dimensionless factor used to describe the amount of water added to the pipe. In the following subsections, different particle velocities will be discussed, it will depend on the situation which one to use. Eventually, Eq. (3-11) will be used to take into account hindered settlement and wall influences.

#### 3-3-1 Single-particle velocity

In this part, only the single settling velocity of the sphere is discussed. This results in equation Eq. (3-4), this is a general equation of the one-dimensional settling velocity.

$$w_0 = \sqrt{\frac{4\Delta g d}{3C_D}} \quad (3-4)$$

Where  $C_D$  is dependent on the Reynolds number of a particle, in the case of subsea rock installation, where large rocks are used  $C_D$  is equal to 0.4. The settling velocity of a single particle is  $w_0$  and can be calculated by Eq. (3-4).

However, if it is uncertain which flow regime is applicable, it can be determined by:

$$\begin{aligned}
Re_p < 1 C_D &= \frac{24}{Re_p} \\
1 < Re_p < 2000 C_D &= \frac{24}{Re_p} + \frac{3}{\sqrt{Re_p}} + 0.34 \\
Re_p > 2000 C_D &= 0.4
\end{aligned} \tag{3-5}$$

First one for the laminar, second for transition and the third for the turbulent regime. Reynolds number  $Re_p$ , is expressed in Eq. (3-8).

### 3-3-2 Hindered settling

When multiple particles settle in a confined space, the particles hinder each other due to the water flow around each particle influencing the other particles. [Richardson and Zaki, 1997]

$$w_s = w_0 \cdot (1 - c)^n \tag{3-6}$$

The exponent  $n$  in Eq. (3-6) is dependent on the Reynolds number and can be expressed as:

$$n = \frac{4.7 + 0.41 \cdot Re_p^{0.75}}{1 + 0.175 \cdot Re_p^{0.75}} \tag{3-7}$$

In the case of coarse particles this results in 'high' Reynolds numbers: 2000+ then  $n$  in Eq. (3-7) is 2.4 and for fine particles, it is 4.65 [Rowe, 1987].

The Reynolds number can be expressed as:

$$Re_p = \frac{w_0 \cdot d}{\nu} \tag{3-8}$$

The plot in figure 3-1 shows the particle Reynolds number as a function of the particle diameter for sands and gravels, using the Ruby & Zanke(1977) equation.

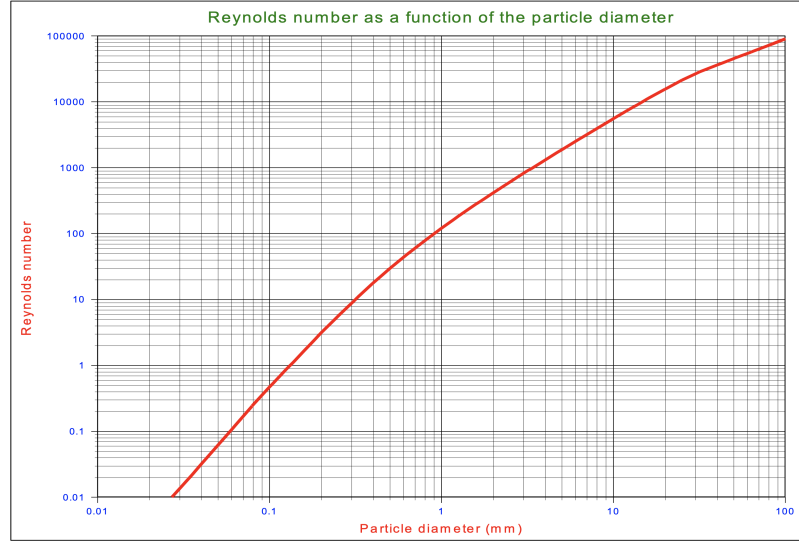


**Figure 3-1:** The Reynolds number as a function of the particle diameter

### 3-3-3 Wall influenced settling velocity

The velocity reduction of a material that flows true a pipe and is influenced by the pipe wall is given in equation Eq. (3-9).

$$\frac{w_{0,p}}{w_0} = (1 - \lambda_w^2) \cdot \sqrt{1 - 0.5\lambda_w} \quad (3-9)$$

When a large particle falls true a pipe filled with water, the water that flows around the object causes friction. This friction slows down the falling object, when the object has nearly the same diameter as the pipe the effect becomes large and the velocity approaches zero. In that case the particle behaves almost like a piston. The equation for hindered settling velocity shows that  $\lambda_w$ , the ratio between the particle and pipe diameter, has a significant influence on the settling velocity and thereby on the production. In figure 3-2 this relation between relative particle size and reduction in velocity is shown.

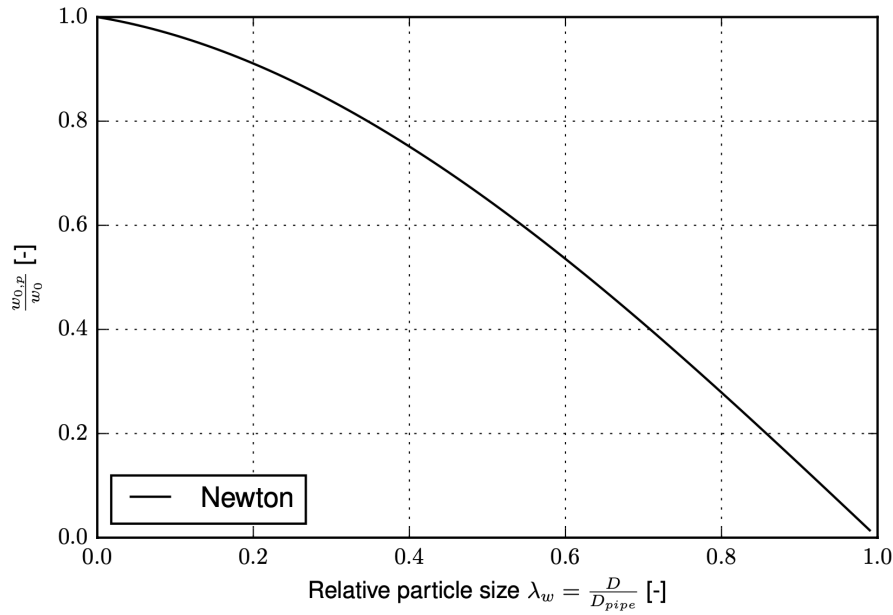


Figure 3-2: Relative particle size

### 3-4 Influence of fallpipe diameter

Increasing the fallpipe diameter increases production in two ways. A larger diameter results in a larger surface area of the pipe  $A_p$  as shown in Equation 3-10 the production of material that can flow true the pipe.

$$A_p = \frac{\pi}{4} \cdot D \quad (3-10)$$

Another influence of pipe diameter is the wall influence of a particle and the pipe Figure 3-2. As shown in Eq. (3-9), the ratio between rock diameter and pipe diameter  $\lambda_w$  influences the settling velocity in a pipe.

### 3-5 Normalized production with hindered settling

Assuming that water, together with the rocks is added to the fallpipe, Equation 3-11 can be written based on Eq. (3-2), Eq. (3-9) and Eq. (3-3).

$$P_s = c \cdot (\alpha + (1 - c)^n) \cdot (\rho_s \cdot A_p \cdot w_{0,p}) \quad (3-11)$$

In the equation Eq. (3-11) the hindered settling exponent  $n$  is set on 2.4 based on high Reynolds numbers applied in Eq. (3-7). This value is chosen for relative large rock particles

with high Reynolds numbers. With this value set, the production of the fallpipe can be determined based on particle concentration  $c$  and different values for  $\alpha$ . The production curve for  $\alpha = 0, 0.1, 0.28, 0.4$  is given by graph in Figure 3-3. This graph clearly shows how to achieve maximum production for a fallpipe in different circumstances. When no water is added to the fallpipe and  $\alpha$  is zero, maximum production can be achieved at a concentration around 30%. A higher or lower concentration leads to lower production. When the concentration passes the critical value of about 30/35%, the flow velocity will drop at that point in the pipe. When the local flow velocity drops the local concentration will rise and can eventually block the fallpipe.

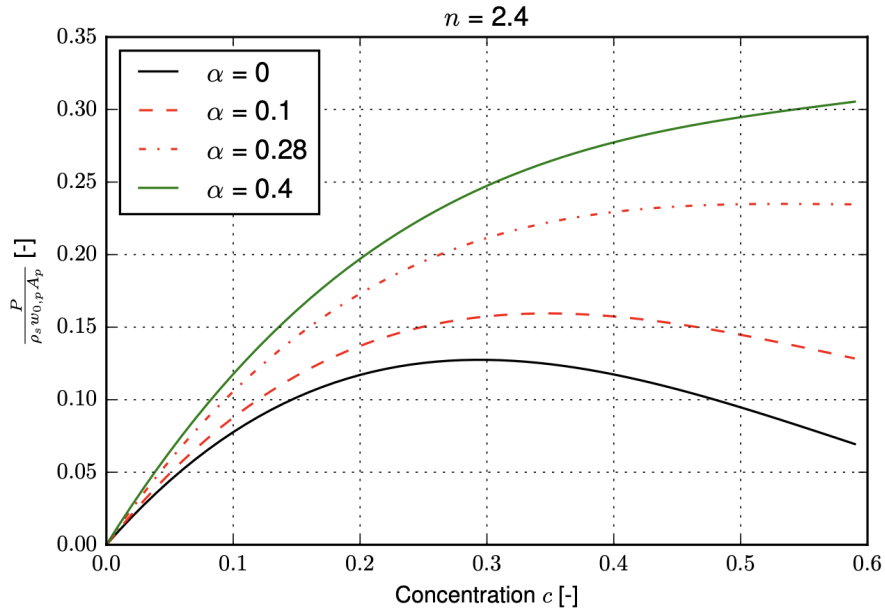


**Figure 3-3:** Normalized rock production

When no water is added to the inlet of the fallpipe the situation can become unstable, as local concentration in the pipe can fluctuate. When the concentration exceed 0.28% the pipe can be blocked. Therefore, when no water can be added caution is needed and the concentration must be kept under the maximum to prevent the pipe from clogging.

### 3-5-1 Maximum concentration for given $\alpha$

When equation 3-11 is derived over the concentration the maximum production can be found by setting the normalized rock production equal to zero for different values of  $\alpha$ .

$$\frac{d\tilde{P}_s}{dc} = \alpha + (1 - c)^n - c \cdot n(1 - c)^{n-1} \quad (3-12)$$

Where The value chosen for the hindered settling exponent  $n = 2.4$ , which is a value for high particle Reynolds numbers [Van Rhee, 2018] When assuming  $n = 2.4$ , the maximum concentration can be found by setting equation 3-12 equal to zero. Plotting  $\alpha$  and the maximum concentration results in the following graph:

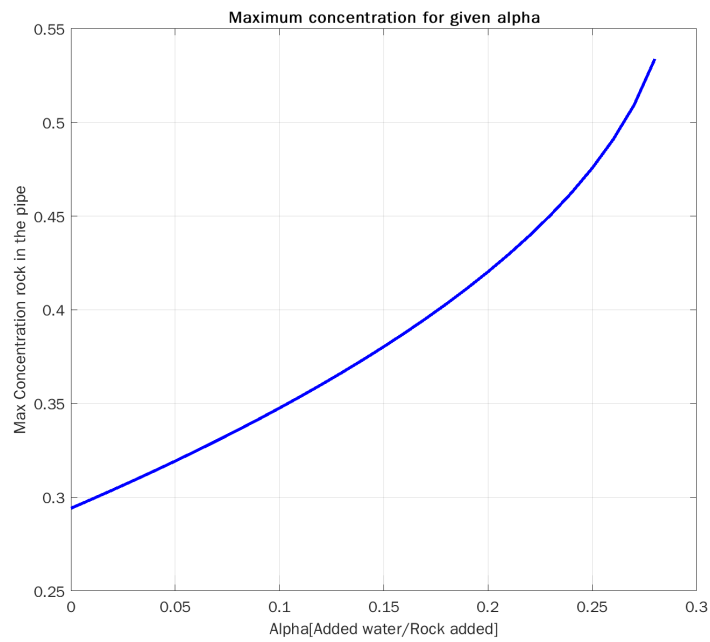


**Figure 3-4:** Maximum concentration for given  $\alpha$

### 3-6 Matlab model vertical fallpipe 1

Combining concentration hindered settling and wall influences the VFM1 is setup, the code for it can be found in the Appendix F. Aswell as in the Sliding bed model 1 (SBM1), the equation for calculating production of the fallpipe must be rewritten to have production as an input instead of an output of the model. The main output of the model is concentration, which can be judged as acceptable according to Figure 3-3. As long as there no water added to the fallpipe, it is advised to keep the concentration below 0.2 to prevent the change of blocking the pipe. This concentration is eventually used to calculate the hindered settling velocity of the particles.



**Figure 3-5:** VFM1:input output

The following velocities are calculated using the VFM1 shown Table 3-6. The concentration (c) shown in the table is set based on the production that is required, in this case, production of 0.48 was used because that was the production that was used in the lab research, scaled from the desired production on full-scale operational vessel.

Batch #	$d_{50}$	c	$w_0[m/s]$	$w_{0,p}[m/s]$	$w_c [m/s]$
1	0.008 [m]	0.072	0.46	0.44	0.37
2	0.015 [m]	0.052	0.63	0.59	0.52
3	0.022 [m]	0.039	0.76	0.67	0.60

Constant properties:  $\rho_s = 2600 [kg/m^3]$   $\alpha = 90 [^\circ]$   $D_p = 0.094 [m]$

**Table 3-1:** Vertical fallpipe model 1 input

As shown in the table above, the velocity difference between single particle- and wall-influenced velocity is larger as the particle diameter increases. For small, medium and large particles the velocity decreases 4%, 6% and 12% due to interaction with the pipe-wall. When adding the influence of particles hindering each-other the settling velocity drops again with 16%, 12% and 10%, despite the low concentrations it makes a significant difference.

# Rock placement using an inclined fallpipe

In chapter 2, different flow regimes are distinguished. One of them, sliding bed, is being explained in more depth in this chapter. For a sliding bed regime, it is common to use the Wilson method [K.C.Wilson et al., 1992], this is what Miedema has applied when modelling a sliding bed regime at low line speeds [Miedema, a]. In this chapter, this method is adjusted and applied for Sliding bed model 1 (SBM1)

### 4-0-1 The limit deposit velocity

To form a 'sliding bed' the particles in the pipe must settle and not be in suspension. In Hydraulic Engineering it is assumed that particles stay in suspension when the so-called shear velocity equals the settling velocity of the particles:

$$U_* \geq w_c \quad (4-1)$$

Where  $w_c$  is the hindered settling velocity and  $U_*$  can be determined with :

$$U_* = \sqrt{\frac{\tau_{2,fl}}{\rho_l}} \quad (4-2)$$

Where  $\tau_{2,fl}$  is the shear stress between bed and pipewall, further described in Equation 4-8 [Miedema, 2013]

Furthermore, there is the limit deposit velocity, this is the velocity below which the first particles start to settle and a bed will be formed at the bottom of the pipe[Miedema, b]. This bed can be fixed, fixed with suspension or sliding as a whole. This is described in the subsection about flow regimes 2-1. The limit deposit velocity is calculated by equation 4-3

$$V_{ls,ldv} = F_L \cdot \sqrt{2 \cdot g \cdot D_p \cdot R_{sd}} \quad (4-3)$$

Where  $F_L = 1.34$  to  $2.2$  for coarse particles and  $R_{sd}$  is relative submerged density.



$$R_{sd} = \frac{\rho_s - \rho_l}{\rho_s} \quad (4-4)$$

The equations 4-1 & 4-3 are applicable when a material is transported in a horizontal pipe, where a liquid is flowing and a direction force between the liquid and the particles is created.

## 4-1 Sliding bed model

In a vertical placed fallpipe, rocks discharged at the inlet of the pipe will settle down vertically. The vertical pipe situation is previously discussed in chapter 3. When the pipe is placed at a steep angle, close to vertical, particles are still 'falling' and not sliding. In this chapter, the physics behind a 'sliding bed' will be discussed. At which angle this transition takes place is not clear and will be estimated. For future research it is useful to investigate this in more depth.

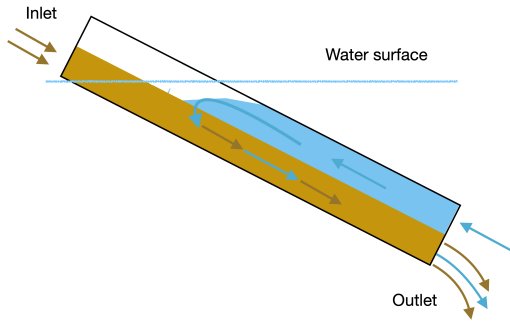


**Figure 4-1:** Flow directions in pipe, no added water.

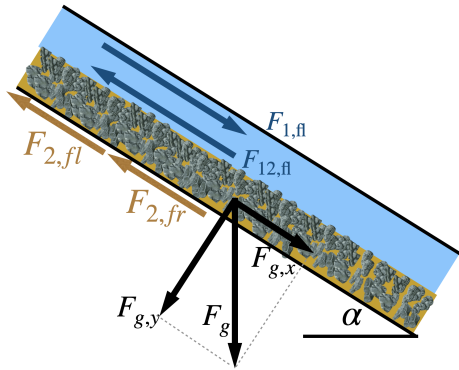


**Figure 4-2:** Force equilibrium sliding bed.

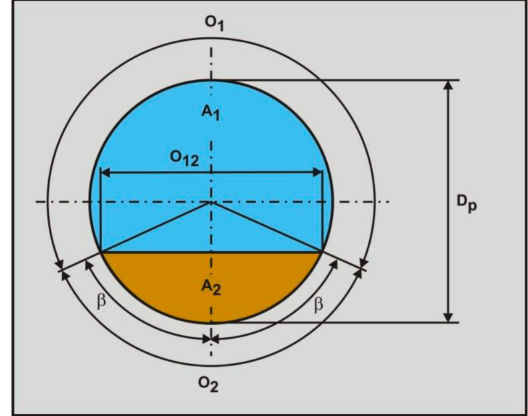
As rocks and water mix together at the inlet of the pipe, the water filling the pores is dragged with the water out of the pipe. The water needed to 'fill' the pores between rocks must come from somewhere, as the opening of the pipe is above water, the water comes from the other side of the pipe. The rocks dragging the water out the pipe cause the water level in the pipe to drop. This water drop causes a pressure difference between the inside and the outside of the pipe. This pressure difference causes water to come from the outlet of the pipe causing a flow in the opposite direction of the sliding bed movement. This flow of water is named the 'backflow'.

Figure 4-1 visualizes what happens. The forces acting on the system will create an equilibrium where a certain velocity is reached. In an inclined fallpipe, gravity is the driving force to make particles slide down; gravity force is straight down. Therefore it must be factorised to be parallel to the direction of the pipe, this vector is defined as  $F_{g,x}$ . The other four forces created by friction between the bed, the pipe and water are:

1.  $F_{12,fl}$ : Friction force bed-fluid.
2.  $F_{2,fr}$ : Friction force bed-pipewall.
3.  $F_{1,fl}$ : Friction force water-pipewall.
4.  $F_{2,fl}$ : Friction force water, in between bed, and pipewall.

This gravity force and the four friction forces will reach an equilibrium at a certain velocity which is the average particle velocity in the pipe.

In the following subsections, the relevant forces are discussed which lead to the equilibrium of forces in the pipe. Therefore the basic dimension of the pipe must be clear, following as shown in figure 4-3:



**Figure 4-3:** Schematic view cross section pipe

**Table 4-1:** Variables sliding bed.

Parameter	Description	Equation
$\beta$	Angle of the bed height [Rad]	[-]
$O_1$	Contact arc-length water and pipe [m]	$O_1 = D_p \cdot (\pi - \beta)$
$O_2$	Contact arc-length bed and pipe [m]	$O_2 = D_p \cdot \beta$
$O_{12}$	Width contact bed and water in pipe [m]	$O_{12} = D_p \cdot \sin(\beta)$
$A_p$	Cross sectional area pipe [m <sup>2</sup> ]	$A_p = \frac{\pi}{4} \cdot D_p^2$
$A_2$	Cross sectional area bed [m <sup>2</sup> ]	$A_2 = \frac{D_p^2}{4} \cdot (\beta - \sin(\beta) * \cos(\beta))$
$A_1$	Cross sectional area water above bed [m <sup>2</sup> ]	$A_1 = A_p - A_2$
$V_1$	Velocity of water above bed [m <sup>2</sup> ]	$V_1 = \frac{A_2 \cdot (1 - C_{vb}) \cdot V_2}{A_1}$
$V_2$	Velocity of sliding bed [m <sup>2</sup> ]	See eq 4-4

#### 4-1-1 Gravity force

In the sliding bed, gravity,  $F_g$  is the driving force. It can be vectorized in two forces: one force parallel and one perpendicular to the pipe. The gravity force vector parallel to the pipe is given by:

$$F_{gx} = F_g \cdot \sin(\alpha) \quad (4-5)$$

Where  $F_g$ , the submerged weight of the bed is given by calculating the volume of the bed multiplied by the relative density:

$$F_g = \rho_{fl} \cdot g \cdot L_{pipe} \cdot R_{sd} \cdot C_{vb} \cdot A_2 \quad (4-6)$$

Where  $\rho_{fl}$  is the liquid density,  $R_{sd}$  relative submerged density and  $C_{vb}$  the volumetric bed density.

#### 4-1-2 Friction force bed-fluid

The friction between water in the pipe and the sliding bed is given as  $F_{12,fl}$ . The shear stress between the sliding bed and water in the pipe is described as  $\tau_{12,fl}$ .

$$F_{12,fl} = \tau_{12,fl} \cdot L_{pipe} \cdot O_{12} \quad (4-7)$$

$$\tau_{12,fl} = \frac{\lambda_{12}}{4} \cdot \frac{1}{2} \cdot \rho_{fl} \cdot (V_1 + V_2)^2 \quad (4-8)$$

In the equation above, the velocity  $V_1$  and  $V_2$  are added instead of subtracted because the direction is opposite increasing the relative velocity between bed and fluid.

With:

$$\lambda_{12} = \frac{\alpha_{Wilson} \cdot 1.325}{\left( \ln \left( \frac{0.27 \cdot d_{50}}{D_H} + \frac{5.75}{Re^{0.9}} \right) \right)^2} \quad (4-9)$$

Where  $\alpha_{wilson}$  is 2.75 as described in Wilsons latest book [K.C.Wilson et al., 1992].

$$Re = \frac{V_1 \cdot D_H}{\nu_{fl}} \quad (4-10)$$

Where  $\nu_{fl}$  is the fluid viscosity. In the equation, previously mentioned  $V_1$  can be extracted from the equation which can be used to determine the production of the fallpipe.

#### 4-1-3 Friction force bed-pipewall

Friction forces between the bed and the pipe wall are caused by the shear stress;  $\tau_{2,fr}$

$$F_{2,fr} = \tau_{2,fr} \cdot O_2 \cdot L_{pipe} \quad (4-11)$$

Where  $\tau_{2,fr}$  exists of

$$\tau_{2,fr} = \frac{\mu_{fr} \cdot \rho_{fl} \cdot g \cdot \cos(\alpha) \cdot R_{sd} \cdot C_{vb} \cdot A_p}{\beta \cdot D_p} \cdot \frac{(\beta - \sin(\beta) \cdot \cos(\beta))}{\pi} \quad (4-12)$$

Where  $\mu_{fr}$  is the sliding friction factor between the pipe wall and particles. Miedema uses a value of +/- 0.4 for a sliding bed, this could vary depending on type and shape of rocks[Miedema, b].

#### 4-1-4 Friction force water-pipewall

Friction forces between water in the pipe and the pipe wall are caused by the 'backflow'. This force is given by:

$$F_{1,fl} = \tau_{1,fl} \cdot O_1 \cdot L_{pipe} \quad (4-13)$$

Where the shear stress is given by:

$$\tau_{1,fl} = \frac{1}{8} \cdot \lambda_1 \cdot \rho_{fl} \cdot V_1^2 \quad (4-14)$$

In this shear stress, the Moody friction factor is given by  $\lambda_1$ . This factor is necessary to define the shear stress between water flow and the pipe wall. In this equation  $\epsilon$  is the absolute roughness of the pipe material, divide this by the hydraulic diameter  $D_H$  and the relative roughness is obtained.

Where  $\lambda_1$  is the well-known Darcy Weisbach equation[Miedema, a]. Over the whole range of Reynolds numbers above 2320 the Swamee Jain equation gives a good approximation for the friction coefficient:

$$\lambda_1 = \frac{1.325}{\left( \ln \left( \frac{0.27 \cdot \epsilon}{D_H} + \frac{5.75}{Re^{0.9}} \right) \right)^2} \quad (4-15)$$

#### 4-1-5 Friction force water, in between bed, and pipewall

As the sliding bed exists of rock and water, which slide over the wall of the pipe, both create a shear stress between the pipe and the bed. In this part, the water in the bed sliding over the wall of the pipe is modelled.

Where  $F_{2,fl}$  is given by

$$F_{2,fl} = \tau_{2,fl} \cdot O_2 \cdot L_{pipe} \quad (4-16)$$

Where  $\tau_{2,fl}$ :

$$\tau_{2,fl} = \frac{\lambda_2}{4} \cdot \frac{1}{2} \cdot \rho_{fl} \cdot V_2^2 \quad (4-17)$$

$$\lambda_2 = \frac{1.325}{\left( \ln \left( \frac{0.27 \cdot \varepsilon}{d} + \frac{5.75}{Re^{0.9}} \right) \right)^2} \quad (4-18)$$

#### 4-1-6 Solving the equilibrium of forces

When material in the pipe moves at constant speed, the previous mentioned forces are in equilibrium and 4-19 can be used.

$$F_{gx} = F_{12,fl} + F_{1,fl} + F_{2,fr} + F_{2,fl} \quad (4-19)$$

By elaborating the equation and rewriting it, the production of the fallpipe is given in equation/figure 4-4. How this simplification and rewriting is done can be found in section A-3.

This equation seems very complex, that is because it is written in its most detailed form. Every variable such as  $O_1$ ,  $O_{12}$ ,  $O_2$  etc is expressed in  $\beta$ , resulting in:

$$V_2 =$$

$$\sqrt{\frac{g \cdot \sin(\alpha) \cdot R_{sd} \cdot C_{vb} \cdot A_2 - \frac{\mu_{fr} \cdot g \cdot \cos(\alpha) \cdot R_{sd} \cdot C_{vb} \cdot A_p}{\beta \cdot D_p} \cdot \frac{(\beta - \sin(\beta) \cdot \cos(\beta))}{\pi} \cdot \beta \cdot D_p}{\frac{1}{8} \cdot D_p \cdot \left( \frac{\alpha_{Wilson} \cdot 1.325}{\left( \ln \left( \frac{0.27 \cdot d}{D_H} + \frac{5.75}{Re^{0.9}} \right) \right)^2} \cdot \left( \frac{A_2 \cdot (1 - C_{vb})}{A_1} + 1 \right)^2 \cdot \sin(\beta) + \frac{1.325}{\left( \ln \left( \frac{0.27 \cdot \varepsilon}{D_H} + \frac{5.75}{Re^{0.9}} \right) \right)^2} \cdot \left( \frac{A_2 \cdot (1 - C_{vb})}{A_1} \right)^2 \cdot (\pi - \beta) + \frac{1.325}{\left( \ln \left( \frac{0.27 \cdot \varepsilon}{d} + \frac{5.75}{(Re)^{0.9}} \right) \right)^2} \cdot \beta \cdot (1 - c_{vb}) \right)}$$

**Figure 4-4:** Velocity sliding bed

When the velocity of the bed is known, the production of the fallpipe can be determined with:

$$P_o = V_2 \cdot A_2 \cdot C_{vb} \cdot \rho_s \quad (4-20)$$

#### 4-1-7 Applying model, with known inputs

The equilibrium of forces that result in a particle velocity Figure 4-4, is theoretically correct but cannot be used with the known input variables. During a subsea rock installation project, the Pipe-angle ( $\alpha$ ), production in/out ( $P_i/P_o$ ), particle diameter ( $d_{50}$ ) and other variables concerning viscosity and further rock properties are assumed to be fairly constant. What should be determined using the model is whether the pipe can cope with the production by calculating the volumetric concentration in the pipe. Therefore  $P_i$  must equal  $P_o$  otherwise the pipe gets blocked. Furthermore, the model must provide the velocity of particles sliding/falling true the pipe and the height of the sliding bed or flow.

To achieve this, Equation 4-21 is setup.

$$V_2 = \frac{P_i}{A_2 \cdot C_{vb} \cdot \rho_s} \quad (4-21)$$

This function can be solved by a program such as Matlab using 'vpasolve' function, finding the  $\beta$  that provides an equilibrium. When  $\beta$  is known, it can be used to calculate  $V_2$  with Equation 4-21, (the adjusted code of SBM1 is shown in Appendix C)

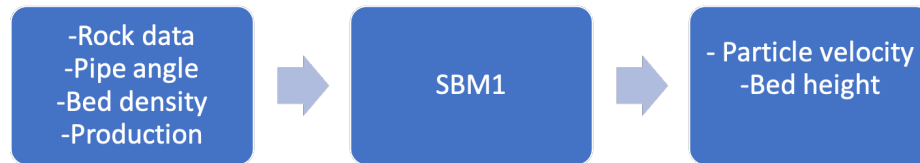


**Figure 4-5:** SBM1R:input output

## 4-2 Results sliding bed model 1

The properties/dimensions that are used for the model are in line with the properties/dimensions of the scale model used in the lab research discussed in chapter 5. The most important variables that are used in the Matlab model to calculate the velocity using Figure 4-4 are shown in Table 4-2.

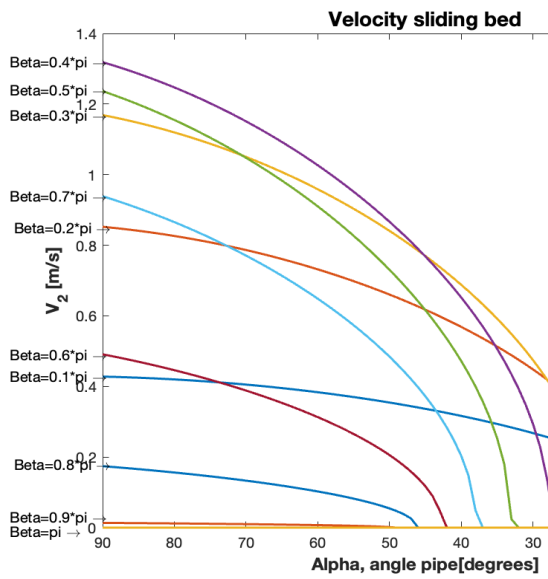
Variable	Value	Notes
Small particles $d_{50}$	0.008 [m]	Batch 1: Average particle size: 'Small stone' batch was 0.0058-0.01 [m] so 0.008 was used.
Medium particles $d_{50}$	0.015 [m]	Batch 2: Average particle size: 'Medium stone' batch was 0.01-0.02 [m] so 0.015 was used.
Large particles $d_{50}$	0.022 [m]	Batch 3: Average particle size: 'Medium stone' batch was 0.02-0.025 [m] so 0.022 was used.
$D_p$	0.094 [m]	Inner pipe-diameter used in lab was 0.094 [m]
$C_{vb}$	0.4 [-]	Density of sliding bed [-]
$C_{fr}$	0.416	friction-coefficient between rock and pipe, (PVC in labtest)
$C_{rgh}$	$0.0015 \cdot 10^{-3} [m]$	Roughness of material*
$\rho_s$	2612 [kg/m <sup>3</sup> ]	Density of rocks**

\* For the entire code that is used for the 'first sliding bed model', see Appendix B.

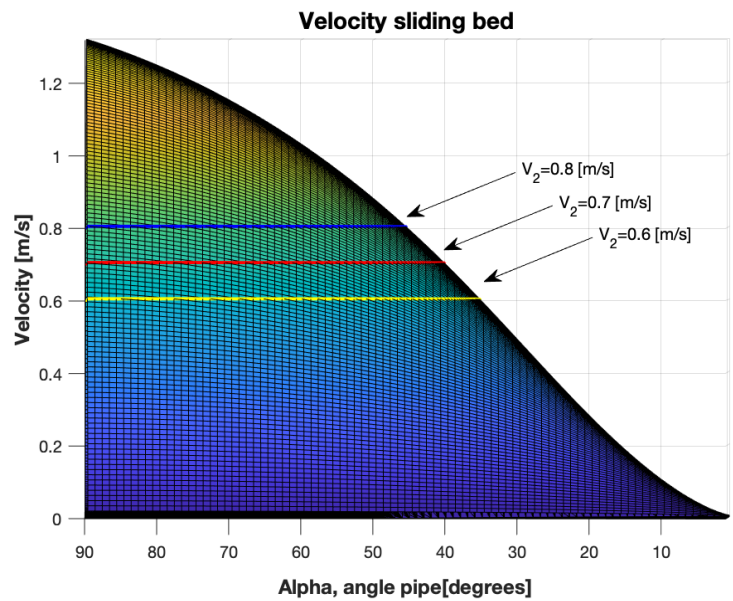
**Table 4-2:** Sliding bed model 1 input

The values from ?? are used to plot the graphs Figure 4-6 and Figure 4-7 using the equation for particle velocity  $V_2$  given in Figure 4-4 and production  $P_o$  as calculated with Equation 4-20. In the figures Figure 4-6 and Figure 4-7, all the mathematically possible velocities and productions are shown. For every pipe angle from 0 to 90 degrees ( $\alpha$ ) and every bed angle  $\beta$  from 0 to  $\pi$ , the results are plotted. Plotting the velocity equation based on different  $\alpha$  and  $\beta$  provides a 3D plot. The first 3 images of Figure 4-6 show the  $V_2$ , from which the first two images are similar. The difference is that Figure 4-6a exists of ten different  $\beta$ -values and Figure 4-6b exist of a mesh connecting 314 lines together. The third image Figure 4-6c is a top-view of the velocities plotted, where blue is a small number and increases to yellow/orange.

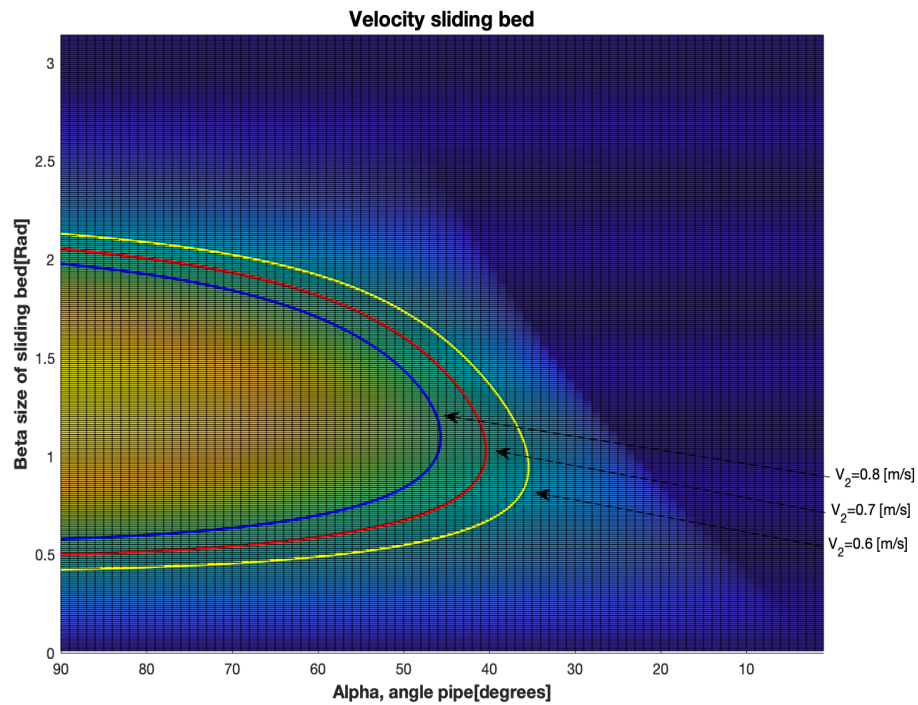




(a) Velocity particles plotted for 10 values of  $\beta$ , from  $0.1 \cdot \pi$  to  $\pi$  side view graph



(b) Velocity particles plotted for every value of  $\beta$ , from 0 to  $\pi$  side view graph



(c) Velocity: view 3

**Figure 4-6:** Velocity sliding bed, top view graph

In the figures Figure 4-6 and Figure 4-7, all the mathematically possible velocities and productions are shown. For every pipe angle from 0 to 90 degrees( $\alpha$ ) and every bed angle  $\beta$  from 0 to  $\pi$ , the results are plotted. By doing this it shows that for every velocity and every production there are two combinations possible. For example: see Figure 4-6c, when the fallpipe is operating at an angle alpha ( $\alpha$ ) of  $60^\circ$  there are two coordinates in the graph that shows a particle velocity  $V_2$  of  $0.6 \text{ m/s}$ . The first one is at  $\beta = 0.49$  and the other one is at  $\beta = 1.91$ . These two options are possible as the first one is with a relatively empty pipe and the other one is with a nearly blocked pipe. Therefore the lowest possible option is desired to prevent the pipe from getting blocked.

Based on the velocity that results from the equation in Figure 4-4 used in the Matlab model, production can be calculated with Equation 4-20.

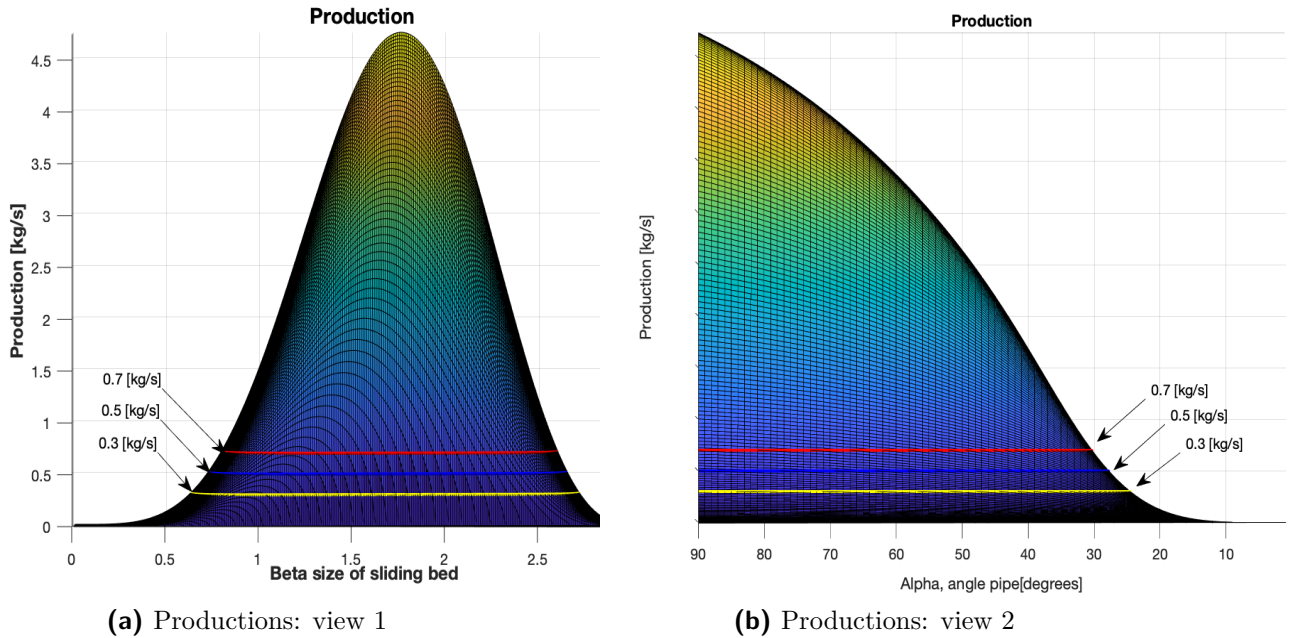


**Figure 4-7:** Results of sliding bed model: Production

### 4-3 Conclusions of results

The shape of velocity and production graph are similar because production  $P_o$ , is based on  $V_2$  multiplied by  $A_2 C_v b$  and  $\rho_s$  see (4-20).

The somewhat parabolic shape that occurs, can be explained due to the increasing  $\beta$  leading to a larger bed  $A_2$  with a larger mass. Due to the larger mass, gravity on the bed is a dominating force in the equilibrium causing a peak. However, when  $\beta$  increases further and

the bed is almost filling the entire pipe, friction forces become more dominant causing the velocity to drop. As shown in Figure 4-6b the velocity is steadily increasing as the angle of the pipe increases, this is due to the friction force  $F_{2,fr}$  is reaching zero and the other forces do not change that much.

## 4-4 Discussion of results

First of all, it must be clear that this model is assuming that the particles stay in a bed and the graphs show every combination of  $\alpha$  and  $\beta$ , this is a distorted view. Not every combination is actually possible to occur. For example, at a pipe-angle  $[\alpha]$  of  $90^\circ$  the particles are not more in a 'bed' but fall uniform across the pipe. In the Matlab model, some variables are assumed based on the literature. For example  $C_{vb}$  is estimated at 0.4 [Miedema, b], meaning that the bed's volumetric concentration is 40% rock and 60% water. That this value was an overestimation will become clear from the lab research results in chapter 6, changing  $C_{vb}$  into a variable depending on bed height or pipe angle will drastically change the shape of the velocity and production graphs.

---

# Chapter 5

---

## Lab research

In the chapter 2 flow regimes are discussed, where-after two models are made in Matlab: a vertical fallpipe in chapter 3 and in chapter 4 a sliding bed model. In the upcoming chapters, the main focus will be to validate these models based on a scale model that is built and tested in a lab research. In this chapter, the research questions are stated and the layout of the lab-research will be discussed. Then in 6 the results are discussed which are compared with the two models in 7. Finally, the results and observation gathered from the lab research is used to improve the models and bring them in line with reality in chapter 8.

### 5-1 Aim of lab test

Based on the results of this lab research the following research questions are answered:

- Does a backflow of water occur in a closed inclined fallpipe during underwater rock installation?
- What is the influence of fallpipe angle, on particle velocity, bed height and bed density?
- Which flow regime occurs in a fallpipe?
- Can the Sliding bed model 1 (SBM1) be used to calculate the bed height and particle velocity?
- How do the results of SBM1 compare to the labtest results?
- Is the model reliable for larger scale? What must be changed to be so?
- What does the spread of rocks look like after leaving the fallpipe? What is the influence of fallheight on that dispersion?

### 5-2 Lab test setup and method

#### setup Labtest

The tank that is used for the labtest is 5 by 2 by 2.5 meters, it has transparent glass on the sides. Next to the tank scaffolding is placed to support the conveyor belt and fallpipe.

This conveyor belt feeds the fallpipe with rocks true a funnel. As shown on 5-1 the pipe is connected with ropes to two crossbars above the tank. The length of these ropes can be adjusted to change the angle of the pipe. Dimensions in Figure 5-1 are in shown in centimeters.

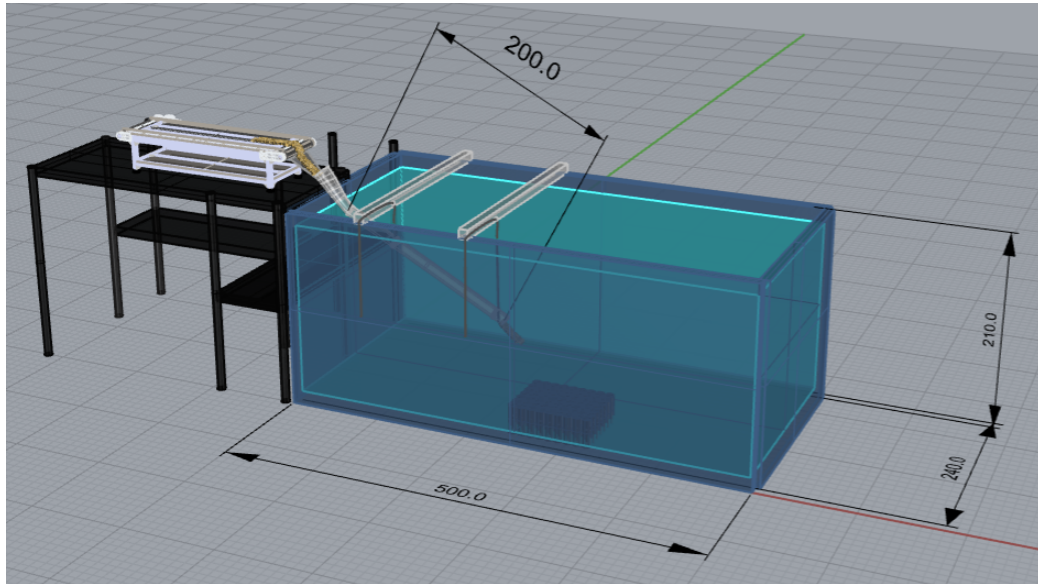


**Figure 5-1:** Perspective view: 3D model of lab test setup

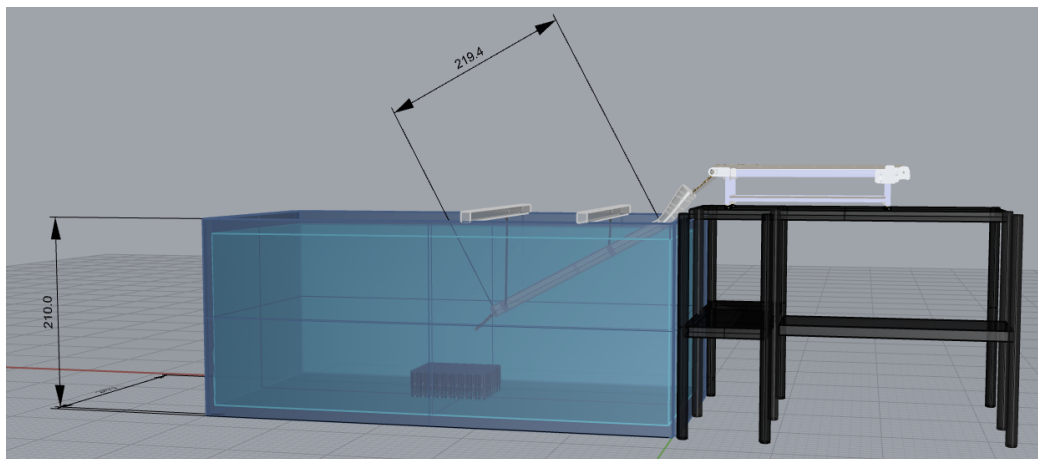


**Figure 5-2:** Side view: 3D model of lab test setup

For more images of the layout of the lab-research setup see Figure A-3.

### 5-3 Scaling

Assuming that a full-scale fallpipe has an inner diameter of 1.5 meters, in this lab test a pipe with an inner diameter of 0.092 m was used. Based on these dimensions a scale factor was set:  $\frac{0.092}{1.5} = \frac{1}{16.3}$ . All length dimensions are scaled based on this scale ratio. [de Jong, ] To keep dynamic similarity, in general this means that the Froude-number must stay constant in the following Equation 5-1

$$F_n^2 = \frac{V^2}{g \cdot L} \quad (5-1)$$

so

$$\frac{V_p}{\sqrt{g \cdot L_p}} = \frac{V_m}{\sqrt{g \cdot L_m}} \quad (5-2)$$

From Equation 5-2 can be concluded that if the length is scaled with scale factor  $\frac{1}{16.3}$ , that velocity scales with  $\frac{1}{\sqrt{16.3}}$ .

#### Example:

When the length is scaled with  $\frac{1}{16.3}$  and we take  $V_p$  1 then:  $\frac{1}{\sqrt{9.81 \cdot 0.092}} = \frac{V_m}{\sqrt{9.81 \cdot 1.5}}$  results in model velocity ( $V_m$ ) of  $\sqrt{16.3}$  so velocity is scaled with a squared root of the scale factor. When production is scaled, first must be investigated how 'production' is defined:  $P_o = V_2 \cdot A_2 \cdot c \cdot \rho_p$ . Concentration is dimensionless, and the density of rock/solids  $\rho_s$  is constant and cannot be scaled/changed. This results in a scale factor depending on velocity and surface area, velocity was scaled with  $\frac{1}{\sqrt{16.3}}$  and surface area is length multiplied by length so scale factor squared. Multiplying all these scale-factors lead to  $\frac{1}{\sqrt{16.3}} \cdot \frac{1}{16.3^2} = \frac{1}{16.3^{2.5}}$ . An overview of all the scalefactors are shown below in Table 5-3

	Full scale	Scale-factor	Scaled dimension	Lab test
<b>Length pipe</b>	63 [m]	/16.3	3.86[m]	2 [m]
<b>Diameter pipe</b>	1.5 [m]	/16.3	0.092 [m]	0.092[m]
<b>Particle Diameter</b>	24 - 434 [mm]	/16.3	1.47 - 26.6 [mm]	5.8 -25 [mm]
<b>Production</b>	1500 [ton/h]	/16.3 <sup>2.5</sup>	1.4 [ton/h]	1.4 [ton/h]
<b>Production</b>	416.7 [kg/s]	/16.3 <sup>2.5</sup>	0.388 [kg/s]	0.388 [kg/s]

**Table 5-1:** Scaled dimensions labtest

## 5-4 Method lab research

During the lab test, 3 batches of rock sizes are used; small: (5.8-10 mm), medium: 10-20 and large: 20-25 mm. These different batches are tested for at least four different pipe angles, 48°, 59°, 70° and 80°. After these test are done, some additional test are done to determine the spread of particles.

- Step 1: Rocks are placed on a conveyor belt.
- Step 2: Minimum of 1 slow-motion and one standard video camera is set in place. One for filming the entire pipe and one for a detailed view of a part, see A-7 for the camera views.
- Step 3: Conveyor belt feeds the rocks to a funnel which the rocks in a transparent pipe.
- Step 4: The pipe will be placed at an angle varying from 48 to 90 degrees in steps of +/- 10 degrees.
- Step 5: Measure particle velocity and bed height using video analysis software 'Tracker'.
- Step 6: Calculate bed density from bed height, production and velocity.
- Step 7: Additionally, the dispersion of the rocks is determined using the steel grid with containers.

### 5-4-1 Measuring dispersion setup

In this section, the setup for measuring the dispersion of rocks will be discussed. Rocks that will flow out of the pipe and spread out, and how this dispersion of rocks happens will be measured with a steel grid filled with containers. By catching the rocks in a container, afterwards can be determined how the dispersion is distributed by weighing the content of each container

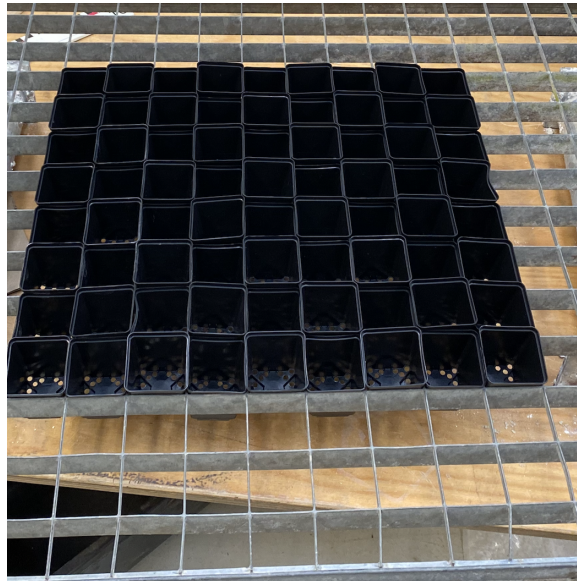


**Figure 5-3:** Rock collector





---

## Chapter 6

---

# Results lab research

In this chapter, the measured data and observations from the labtest will be discussed. First will be explained how the lab test was recorded, thereafter will be explained how the video footage was processed with video analysis software to measure particle velocity. After that the bed height of rocks in the pipe was measured manually. In addition to measuring velocity and bed height, particle dispersion was measured after leaving the fallpipe.

### 6-1 Result gathering

Every 'run' is filmed with 2 or 3 cameras, two of them being a GoPro HERO 9 on linear lens mode. According to the manufacturer, *this leads to 'Linear field of view (referred to as "lens" on HERO 9 captures a straight horizon with a more natural perspective. This mode eliminates the barrel distortion (fish-eye effect) typically captured by your GoPro's wide-angle lens, without compromising image quality.*

The resolution was set at 4K (2160x3840 pixels) with 240 frames per second. This high resolution and many frames per second were desired for having the best possible quality for analysing of the footage. During the lab test, the pipe angle, particle size, added water and input of rocks [kg/s] is varied, the data obtained from the video footage is particle velocity, bed height and observation of particle behaviour. Based on these measurements bed concentration can be calculated and based on visual observation flow regime can be determined.

**Production** First step is to determine production, this is done by weighing the amount of rocks placed on the conveyor belt divided by the time it took to empty it, providing kilogram rock going true the pipe per second.

#### 6-1-1 Velocity

Velocity of the particles is measured using 'Tracker', which is a video analysis and modeling tool built on the Open Source Physics (OSP) Java framework. It is designed to be used in physics education. Tracker video modeling is a powerful way to combine videos with computer modeling.

How to use this program is explained by the following eight steps:

**Step 1: Upload video file in tracker** Step (1), Simply drag a video in the program, in this research mp4 files are used.

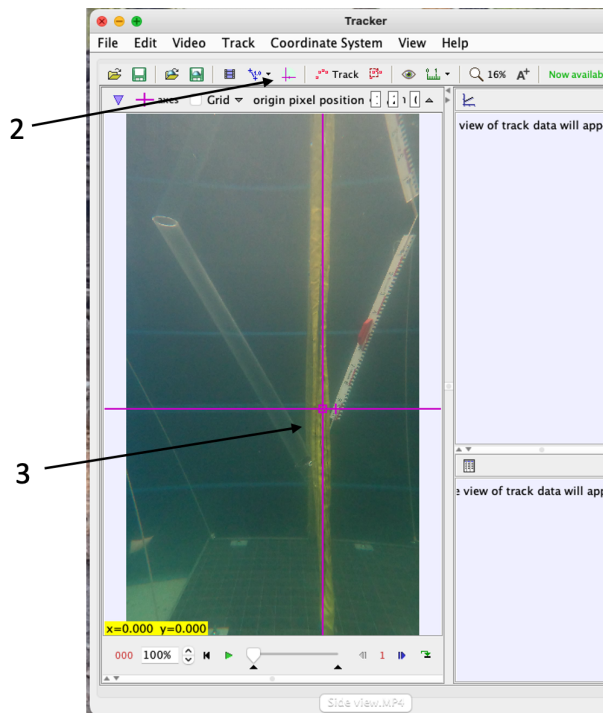
**Step 2 & 3: Create x-y axis** Step (2) adding x/y axis, this makes it possible for the program to define the position of a particle, difference in position from frame to frame is used to determine velocity and acceleration. The camera filming the setup is placed outside the tank, this causes the light refract and deform the image slightly. Therefore middle-point of the x/y axis is placed near the centre of the image where deformation is minimal(step 2). The axes are aligned with the horizontal and vertical beams in the tank, assuming these are placed in a  $90^\circ$  angle.

**Step 4& 5: Create calibration stick** A calibration stick is used to define length in the program, the 1 meter ruler is used to define 1 meter in the program. It is important that this calibration stick is in the same plane as the the movement of particle.

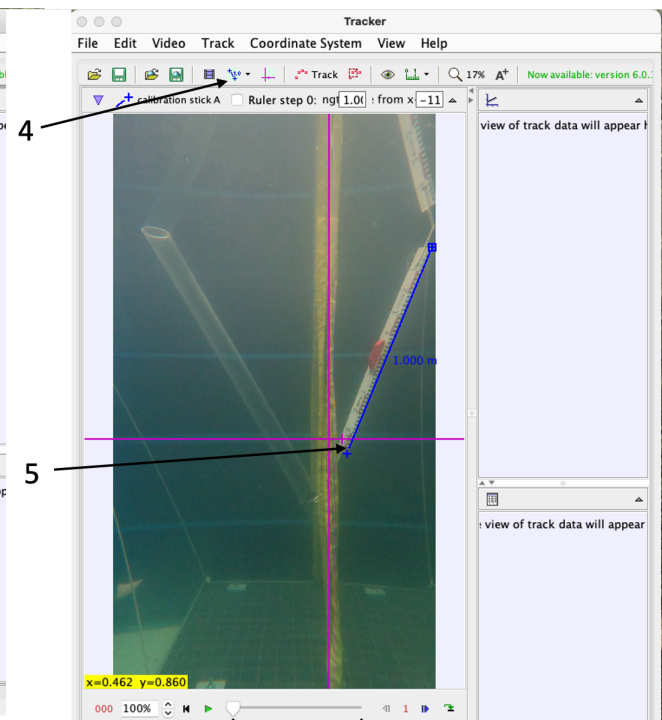
**Step 6: Define a point mass** Define a point mass to start tracking, in this case particles are so small that point mass is best suited. When zoomed in to one particle, it becomes blurry therefore an outstanding particle is chosen to make it easier to track it every frame. An odd coloured particle is mostly chosen, very dark, very light for example.

**Step 7 & 8: start tracking frame by frame** Now the file is ready to start tracking a particle, select a particle and select it in the middle holding shift, automatically the next frame will be shown and the particle has moved. Select the particle in the next frame, and continue this process. Every step, automatically the x/y coordinate is reported of the selected point. As the frame-rate is 60 frames per seconds, the program automatically calculated the particle velocity based on the difference in its position. Velocity is calculated and shown on the right of Figure 6-1d, these values can be exported and average velocity can be calculated from all values.

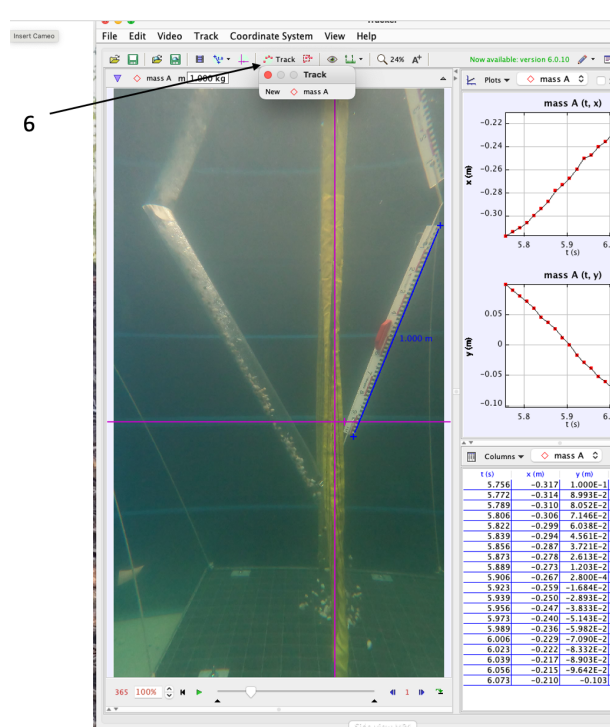
To determine the average particle velocity of a 'run' the following steps are repeated at least 5 times to receive an accurate average velocity.



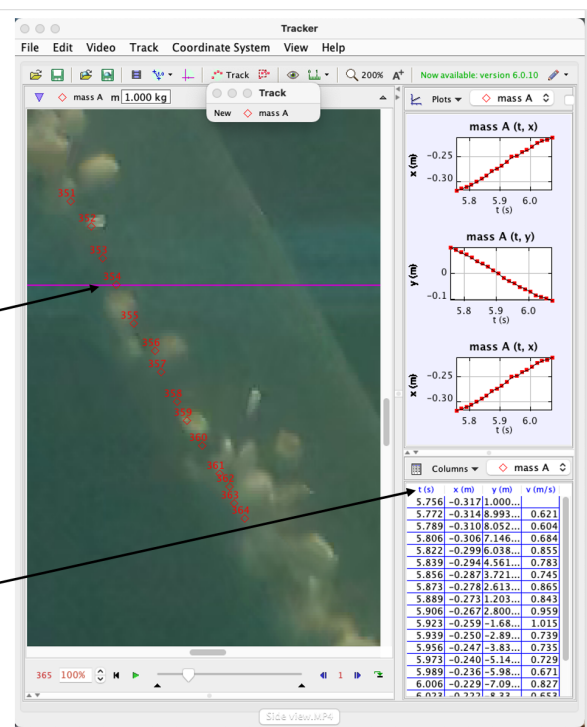
(a) Tracker step 2 and 3



(b) Tracker step 4 and 5



(c) Tracker step 6



(d) Step 7 &amp; 8

Figure 6-1: Explanation using 'Tracker' video analysis software

### 6-1-2 Calculating remaining variables

#### Bed height $\rightarrow A_2$

To determine  $\beta$ , bed height is measured as shown on Figure 6-2. The average height (H) was measured by placing a parallel line over the video footage and estimating the average height of the sliding bed/flow. As the particles are sliding and rolling down the pipe, some particles are in suspension and are above the average bed height calculated. With this height,  $\beta$  can be calculated:

$$\beta = \cos^{-1}\left(-\frac{H \cdot 2}{D_p} + 1\right) \quad (6-1)$$

When  $\beta$  is known,  $A_2$  can be calculated with Table 4-1.

In the process of measuring the bed height, it was clear that within a millimetre (on video footage, so not on model scale size) the bed height can be measured accurately. This inaccuracy is maximum 6%, using these values of H to calculate  $\beta$  this inaccuracy rises to

**Concentration of particles** Production is known, velocity is measured using video analysis and  $A_2$  is calculated using bed height. The volumetric concentration of particles in the sliding bed or sliding flow can be determined using all the known variables. It can be calculated by rewriting Equation 4-20 into Equation 6-2

$$C_{vb} = \frac{P_o}{V_2 \cdot A_2 \cdot \rho_s} \quad (6-2)$$

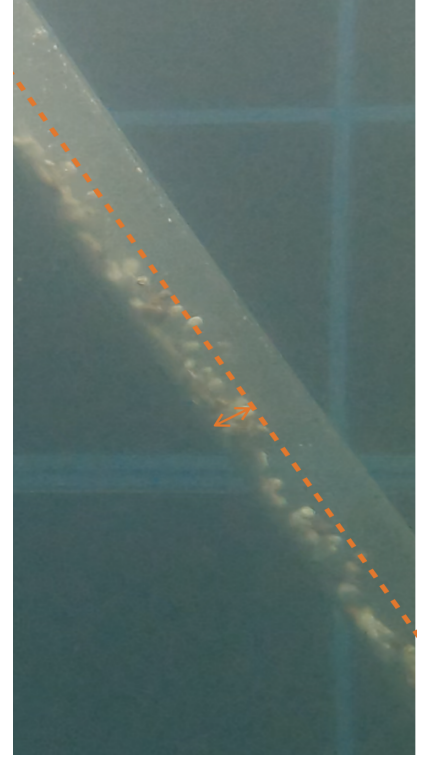


**Figure 6-2:** Measure bed height

## 6-2 Results from labtest

As described in section 6-1 all the data measured is shown in the Table 6-1, 6-2 and 6-3.

**Table 6-1:** Results lab test and Matlab model[small rock].

General				Lab Test		
Run	Pipe angle	D Stone	$P_o$ [kg/s]	$V_2$ [m/s]	$\beta$ [rad]	$C_{vb}$
4	48	5.8-10	0.46	0.65	1.14	0.16
7	59	5.8-10	0.43	0.64	1.27	0.12
12	70	5.8-10	0.48	0.52	1.51	0.11
23	80	5.8-10	0.48	0.57	1.57	0.09

**Table 6-2:** Results lab test and Matlab model[Medium rock].

General			Lab Test			
Run	Pipe angle	D Stone	$P_o$ [kg/s]	$V_2$ [m/s]	$\beta$ [rad]	$C_{vb}$
2	48	10-20	0.47	0.73	1.23	0.12
5	59	10-20	0.48	0.87	1.51	0.07
17	59	10-20	0.48	0.84	1.43	0.08
19	60	10-20	0.45	0.84	1.52	0.06
25	60	10-20	0.43	0.83	1.49	0.07
9	71	10-20	0.48	0.77	1.64	0.06
13	78	10-20	0.50	0.72	1.82	0.06
16	86	10-20	0.48	0.62	2.42	0.05

**Table 6-3:** Results lab test and Matlab model[large rock].

General			Lab Test			
Run	Pipe angle	D Stone	$P_o$ [kg/s]	$V_2$ [m/s]	$\beta$ [rad]	$C_{vb}$
3	48	20-25	0.50	0.68	1.45	0.09
6	59	20-25	0.43	0.75	1.51	0.07
18	71	20-25	0.48	0.70	1.85	0.06
24	80	20-25	0.50	0.70	2.01	0.05

The particle velocity measured in each run, is plotted against the pipe angle in Figure 6-3. From the data, it seems that there is no direct correlation between particle size and particle velocity in an inclined fallpipe. When the pipe is completely vertical, larger particles do have a higher velocity. However, any effect, of the fact that larger particles have a higher single settling velocity is cancelled out by the sliding flow. In a sliding flow, particles have a higher absolute velocity because water in the bed is moving in the same direction reducing drag forces on the particles. From the labtest observations, it is concluded that smaller particles are more influenced by the sliding flow and backflow. This could be an explanation why there is no direct correlation in particle size and velocity. Runs where the small particles are used, the  $\beta$  tends to be smaller than the runs with larger particles. This smaller  $\beta$  results in a denser flow see Figure 6-4 resulting in a relative high velocity. This is assumed to be the reason why in Figure 6-3 the medium particles have the highest velocity, still forming a relative dense flow but due to the larger particle size having the highest velocity at a pipe angle of 60 and 70 degrees.

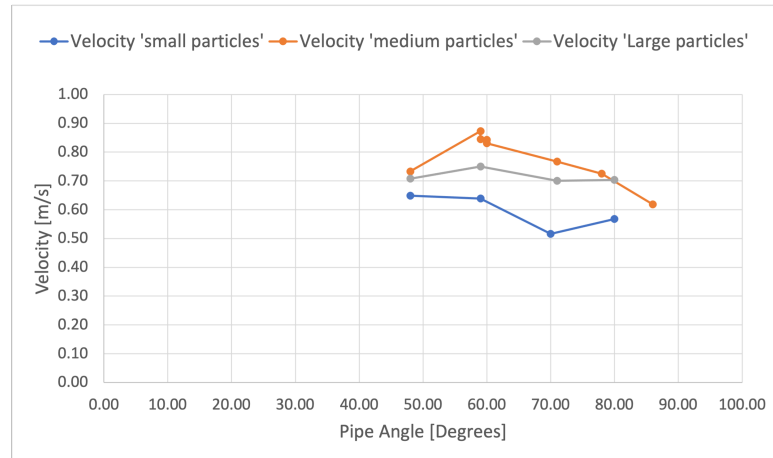


**Figure 6-3:** Velocities measured labtest

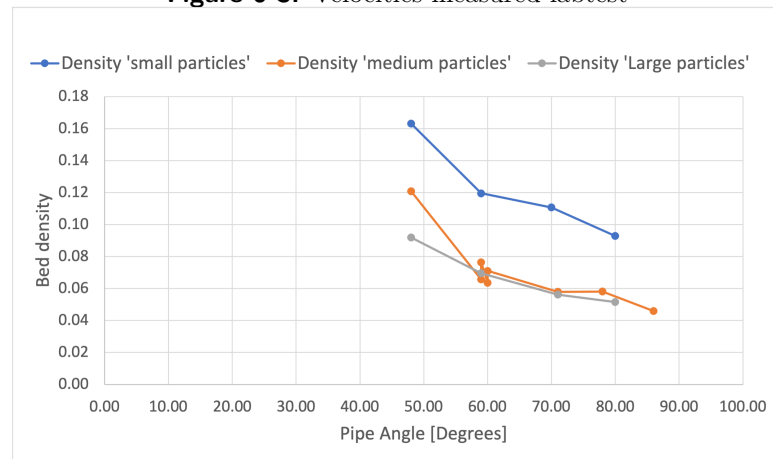


**Figure 6-4:** Bed or flow density

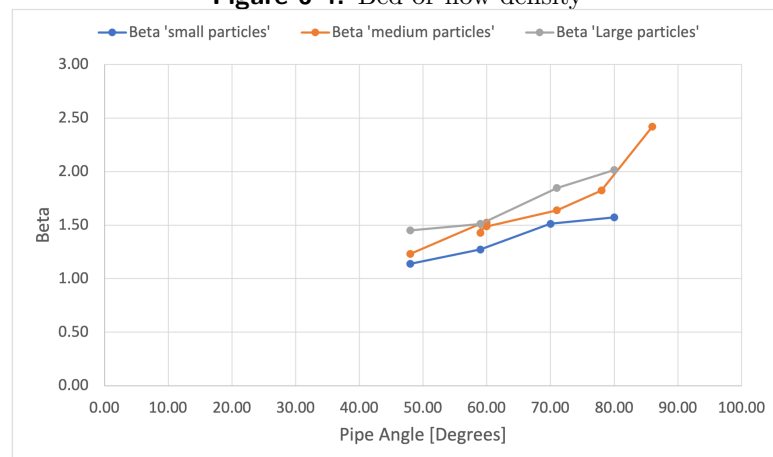


**Figure 6-5:** Beta measured

### 6-2-1 Dispersion results labtest

As measuring dispersion was not part of the main scope of this thesis project, it was not investigated extensively. At the end of the lab research, 3 runs where used to measure dispersion for three scenarios. These

Run	Angle pipe	Height pipe	Production [ $kg/s$ ]
19	$60^\circ$	$0.32m = 3.4 \cdot D_p$	0.45
20	$60^\circ$	$0.42m = 4.5 \cdot D_p$	0.33
21	$87^\circ$	$0.32m = 3.4 \cdot D_p$	0.25

**Table 6-4:** Dispersion test

In the Figure 6-6 /6-7 /6-8 the results are shown from the rocks spreading out, the blue/white circle shows where the pipe outlet was located above the steel grid with containers.



**Figure 6-6:** Run 19 spread



**Figure 6-7:** Run 20 spread



**Figure 6-8:** Run 21 spread

Each plastic bucket is weighed, resulting in a weight per bucket shown in a bar chart in Figure 6-9 ,6-10 and 6-11. In these charts, all the buckets are given a number from 1 to 24, each bucket contains a amount of rock defined in Kg shown on the left of each bar chart.



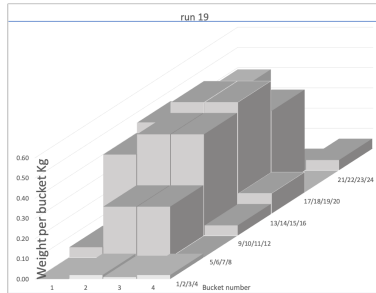


**Figure 6-9:** Run 19 spread data

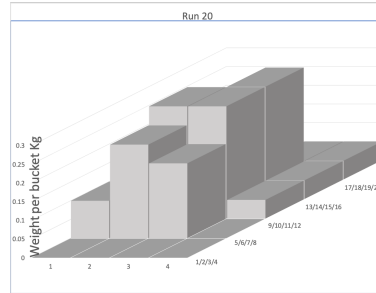


**Figure 6-10:** Run 20 spread data

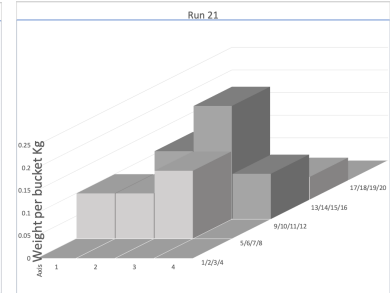


**Figure 6-11:** Run 21 spread data

Defining where the rocks ended up is divided into two circles, one circle wherein all the material ended up and one circle where the majority of the rocks ended up. By weighing each container it can be determined which percentage of rock ended in each circle.

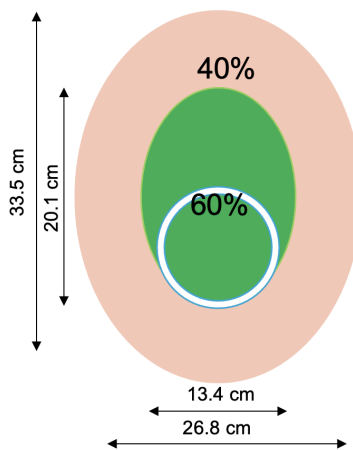


**Figure 6-12:** Run 19 spread

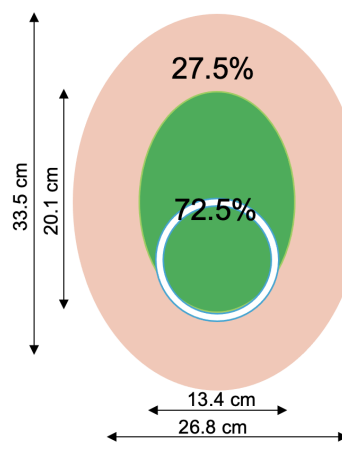


**Figure 6-13:** Run 20 spread

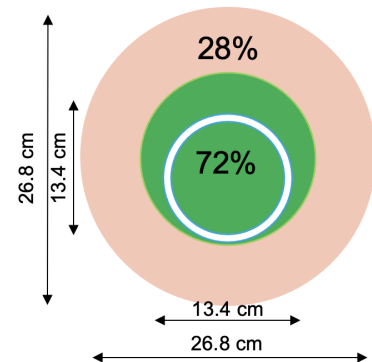


**Figure 6-14:** Run 21 spread

Observing the videos from the plumes of rock exiting the fallpipe, it was noticed that particles leaving the fallpipe experience a two-phase path. First, the particles travel in the same direction as the pipe similar to a jet stream leaving a jet. After which the flow mixture of water/rock mixes up with the surrounding water resulting in the particles settling down. Based on observations, the length of the first phase, the so-called 'jetting zone' is dependent on the velocity and the density of the mixture. And the spread of the second phase, the 'settling' phase looks like a normal distribution. This means that

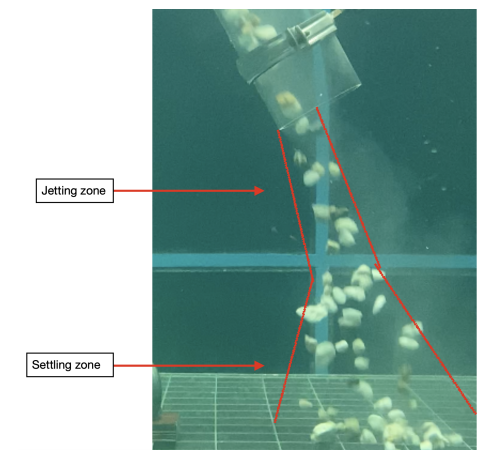


**Figure 6-15:** plumes

the material keeps spreading out further when the fall height increases but most of the rocks will end up in the centre.

This two-phase system can explain the results of the lab research, run 19 showed less concentrated dispersion than run 20 despite having a smaller height from the steel grid.

## 6-3 Conclusion of lab research

### 6-3-1 Backflow

As expected a 'backflow' occurs in the pipe, as rock is feed into the pipe it is mixed with water and the mixture flows down the pipe. As there is no water added to the top inlet of the pipe it must come from the outlet, this is when the backflow occurs. This is clearly visible on the video footage, and visualised in Figure 6-16. In the original model for the sliding bed, this backflow was assumed to be exactly equal to the water in the bed. In the original model the volume of water in the bed was calculated by  $A_2 \cdot (1 - C_{vb})$ . However, from the lab results, it is calculated that  $C_{vb}$  ranges from 0.16 to 0.05 and it is not likely that such a low concentration of particles will cause a 'perfect' water circulation. It seems that there is a relative velocity in  $A_2$  between the particles moving down and the water in that area. This velocity difference between the mixture velocity and particle velocity is called 'slip'. To understand 'slip' the solid velocity  $V_s$ , mixture velocity  $V_m$ , spatial volumetric concentration  $C_{vs}$  and volumetric transport concentration  $C_{vt}$  must be clear.

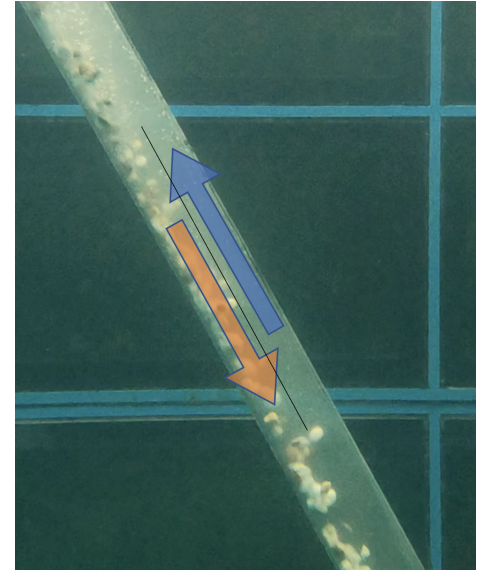


**Figure 6-16:** Back-flow in labtest: brown arrow is material flow, blue arrow is water backflow

$$V_{sl} = V_m - V_s \quad (6-3)$$

$$C_{vs} = \frac{V_s}{V_m} \quad (6-4)$$

Difference is that  $C_{vb}$  from Equation 6-2, is the density of the sliding bed only and  $C_{vs}$  is the spatial volumetric concentration.

$$C_{vs} = \frac{\rho_m - \rho_l}{\rho_s - \rho_l} \quad (6-5)$$

### 6-3-2 Concentration bed or flow is not constant

From first observations it is clear that the bed of flow density is not constant. When the pipe is placed in a 'low' angle, such as  $48^\circ$  particles are less in suspension than when the pipe is placed in a high angle ( $80^\circ$ ).

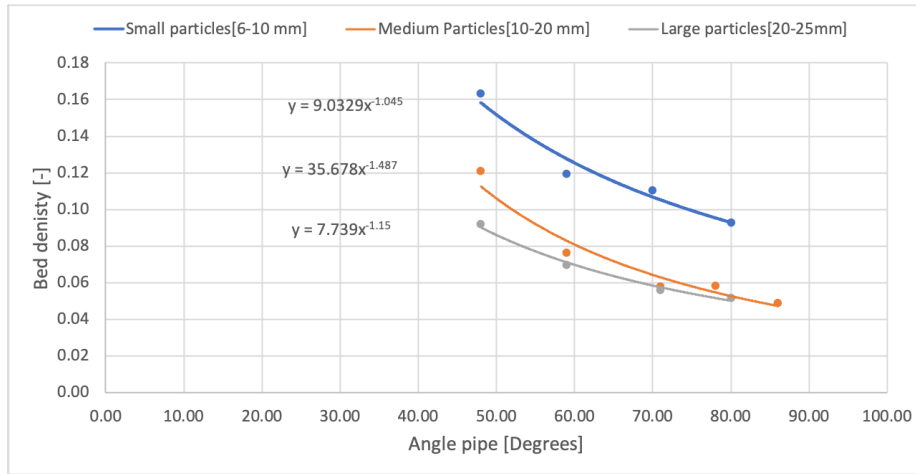


**Figure 6-17:** Bed or flow density 2

By curve-fitting bed density from Figure 6-4 the relation between  $C_{vb}$  and pipe inclination is defined as:

- Small particles[5.8-10 mm]:  $C_{vb} = 9.0 \cdot \alpha^{-1.05}$
- Medium particles[10-20 mm]:  $C_{vb} = 35.5 \cdot \alpha^{-1.49}$
- Large particles[20-25 mm]:  $C_{vb} = 7.7 \cdot \alpha^{-1.15}$

\*These values are based on the production used in the lab test, this was aimed to at 0.48 kg/s.

### 6-3-3 Influence of high concentration

Higher concentrations lower the settling velocity when a pipe is vertical, due to the effect of hindered settling. However, in the case of sliding bed or flow, high concentrations seem to have a higher velocity than sections where the velocity is lower. This is shown in Figure A-6

### 6-3-4 Dispersion of rock

A key element of a subsea rock installation project is that rocks end at the desired location on the seabed. To get a better understanding of how the rocks spread after leaving the fallpipe, the dispersion pattern is measured under different circumstances.

Logically, the dispersion of rock from a fallpipe increases when the height increases. However, what was remarkable was that the influence of production played a significant role. 6-13 shows a more concentrated resu

## **6-4 Discussion of lab research results**

Inaccuracy in measurements is high when tracking the smallest particles, it is impossible to follow one particle frame by frame due to turbulence and particles moving in front of each other before the next frame. Due to this inaccuracy, the results from the 'medium' and 'large' particles is more accurate.

---

## Chapter 7

---

# Validating models with labtest results

In this chapter, the results from the lab test are compared with the original models in Matlab. First, the sliding bed model is compared. Comparing the results will provide an indication of how far the models are off from reality and eventually implement results to calibrate the models.

### 7-1 Validation sliding bed model

To compare the results of the Sliding bed model 1 (SBM1) with the labtest the pipe angle  $\alpha$  and production are used as data-points to find the corresponding particle velocity and bed height. All other variables and properties used in the SBM1 are the same as used in the lab test. Variables such as rock properties, pipe dimensions, densities etc.

In Figure 7-1 the green lines show the measured  $\beta$ , and the red lines show the  $\beta$  from the SBM1. Clearly, the calculated  $\beta$  is much smaller, also it is nearly similar for every particle size. The first observation of Figure 7-1 is that  $\beta$  is too small. This can be explained by the fact that in the SBM1 uses a bed-density( $C_{vb}$ ) of 0.4 while in Figure 6-3-2 it was concluded that  $C_{vb}$  is variable depending on pipe angle. Using a too high bed density also explains the velocity  $V_2$  being too large in the SBM1 compared to the lab results, see Figure 7-2

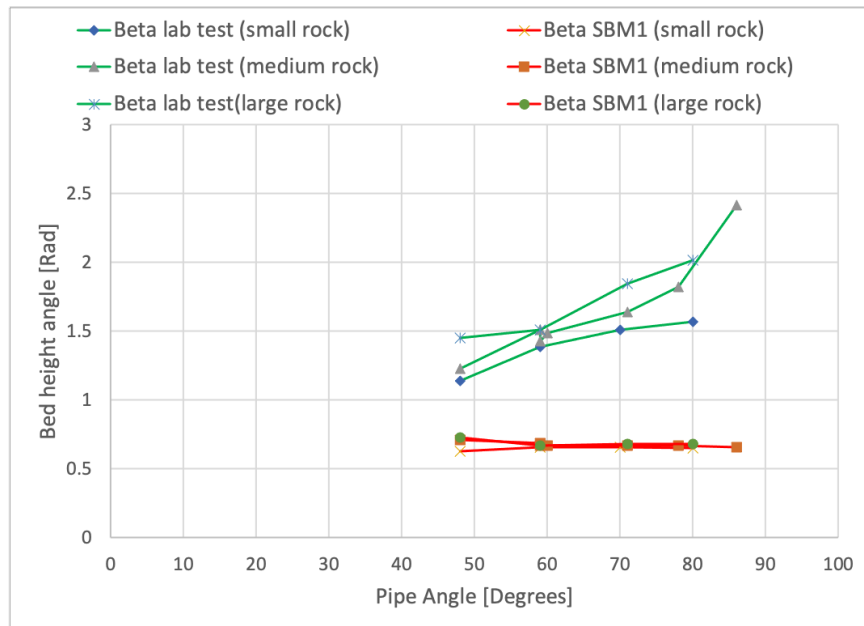


**Figure 7-1:** Bed angle  $\beta$

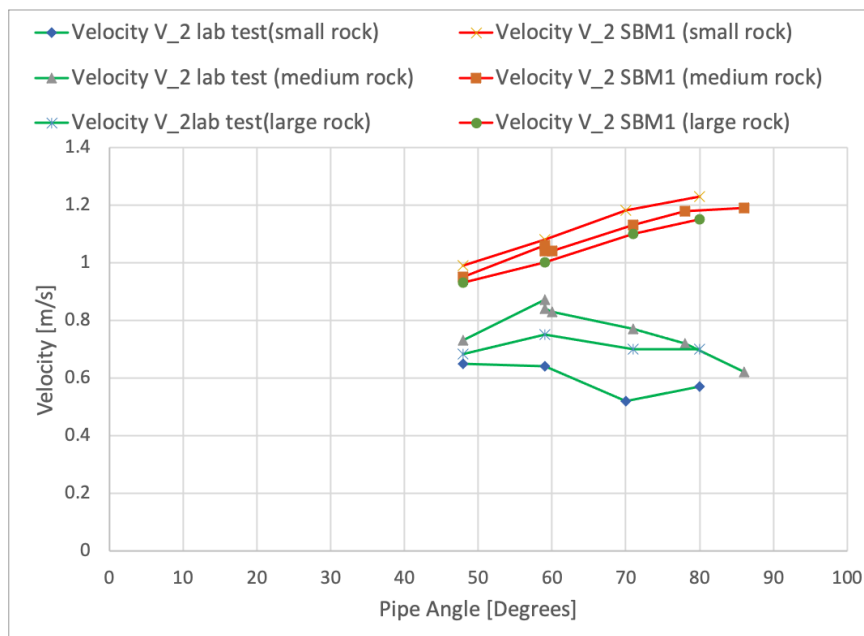


**Figure 7-2:** Particle velocity

## 7-2 Validation vertical pipe model

The Vertical fallpipe model 1 (VFM1) has some different outputs than SBM1, most important difference is that VFM1 assumes a uniform distribution of particles over the cross-area of the fallpipe. The outputs of VFM1 are pipe density and particle velocity.

The VFM1 cannot be validated exactly because 90 degree vertical fallpipe has not been tested in the labtest. This was not done due to operating limits of the test setup, the fallpipe is therefore placed at a maximum angle of  $86^\circ$  in run 16 using the batch of rocks with medium particle size (10-20 mm). The results from this run are given in Table 6-2.

The particle velocity measured in the labtest was 0.62 m/s compared with 0.40 m/s from the model, this shows a significant difference of 35%.

From observing the video footage it was remarkable that a backflow was generated due to the particles settling mainly on the bottom side of the pipe. Particles, were settling at the bottom-side also had higher velocity than in the middle part of the pipe. This means that particles settle faster being in each others drag, meaning that the concentration had positive influence on settling velocity. This increase in particle velocity due to concentration influence is applied in Vertical fallpipe model 2 (VFM2) and explained in section 8-2.





# Model improvement based on lab research

## 8-1 Sliding bed model 2

The original model for calculating the velocity and production of a inclined fallpipe is improved by making adjustments to the code:

- Change  $C_{vb}$  to a variable depending on pipe angle:

Small particles:  $C_{vb} = 9.0 \cdot \alpha^{-1.05}$

Medium particles:  $C_{vb} = 35.5 \cdot \alpha^{-1.49}$

Large particles:  $C_{vb} = 7.7 \cdot \alpha^{-1.15}$

- Adding a loss factor in the backflow calculation: to make backflow smaller at a larger pipe angle:  $e = 2.5 \cdot C_{vb} \cdot \cos(0.5 \cdot \beta)$  In the first model for a sliding bed, the velocity of the backflow was based on the volumetric production of water in the bed ( $A_2$ ) divided by the correctional area of the pipe minus  $A_2$  subsection 6-3-1
- Based on measurements from the lab research,  $C_{fr}$  due to rocks rolling and instead of only sliding a slightly lower friction factor is applied. Rolling instead of sliding significantly reduces friction forces, therefore a  $C_{fr}$  of 0.2 is used.

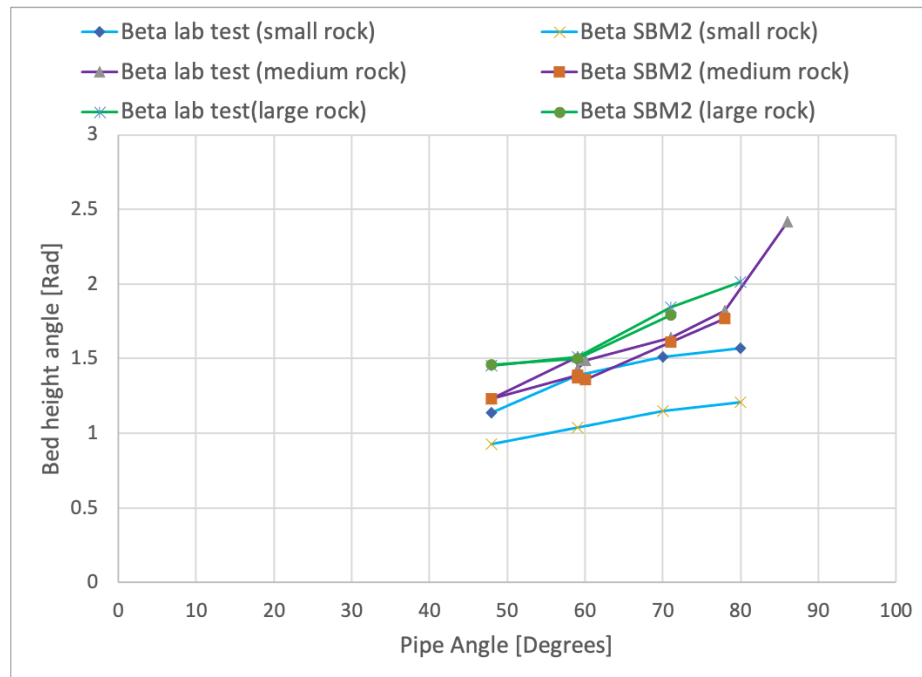


**Figure 8-1:** Bed angle  $\beta$  SBM2

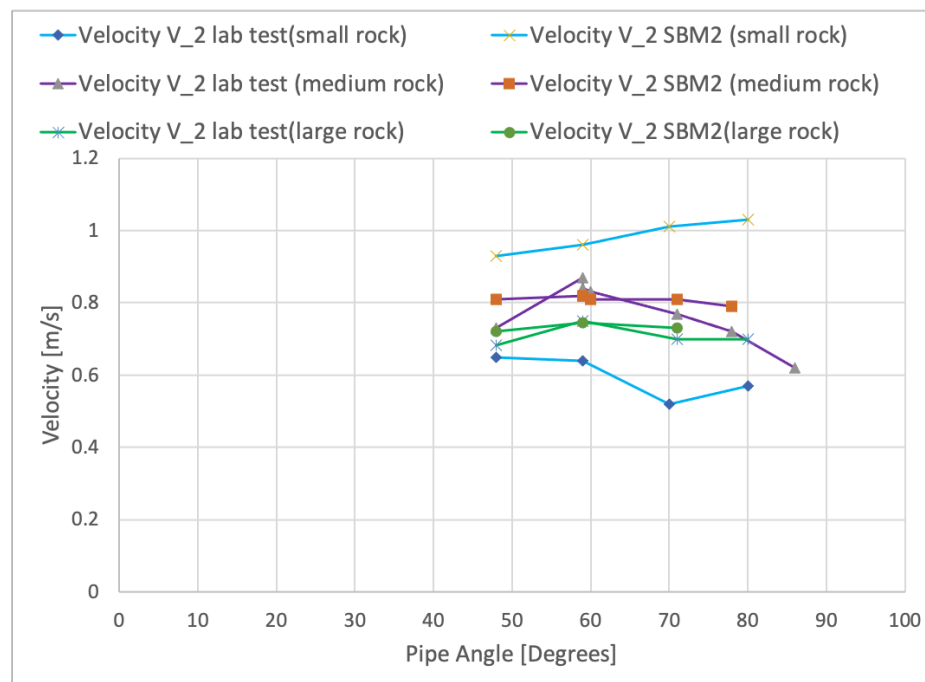


**Figure 8-2:** Particle velocity SBM2

The results of the modifications of Sliding bed model 1 (SBM1) into Sliding bed model 2 (SBM2) are shown in Figure 8-1 and Figure 8-2. Clearly, the results of SBM2 are much more similar to the results of the lab research, but still, the SBM2 does not have a perfect overlap with the lab test results. Especially the batch with the smaller stones is still not accurate. A reason for this could be that the in the SBM2 particle size does not play a significant role as the sliding bed is modelled as a whole. However, when the density of this bed becomes as low as in this situation, it can be that the particles experience an additional force that has a large influence. This could be a drag force resulting in a velocity reduction. Another cause of the difference could be a consequent mistake in measuring the bed height. From the lab-research video footage, it was noticed that especially the smaller particles were more in suspension and caught more often by the backflow, flowing back in the pipe. Therefore the bed height was measured for only the particles that flowed continuously downwards. This can cause the bed height to be measured smaller than it was, resulting in a higher bed density. This bed density was later used to define  $C_{vb} = 9.0 \cdot \alpha^{-1.05}$  which was used as an input for the SBM2. Furthermore, the velocity calculated with 'Tracker' is most inaccurate for the runs using small rocks, as it is not possible to follow one particle on the video footage. This was not a problem for the 'medium' and 'large' rock batches.

## 8-2 Vertical fallpipe model 2

The original model for calculating the velocity and production of a vertical fallpipe is improved by making adjustments to the code:

- If pipe angle  $\alpha$  is less than 87, then use the change equation of hindered settling velocity from  $W_s = W_0 \cdot (1 - c)^n$  to  $W_s = W_{0p} \cdot (1 + c)^n$ .
- Use vertical component of gravity by multiplying by  $\sin(\alpha) \rightarrow g \cdot \sin(\alpha)$

These adjustments resulted in very close predictions of particle velocity as shown in ?? In a range of 5%. (shown in Table 8-1)

**Table 8-1:** Results lab test compared with Vertical fallpipe model 2

General				Lab Test		Matlab model 2		
Run	Pipe angle	D Stone	$P_o$ [kg/s]	$V_2$ [m/s]	$C_{vb}$	$w_s$ [m/s]	c	$V_2/w_s$
16	86	10-20	0.48	0.62	0.05	0.65	0.04	104%
23	80	5.8-10	0.48	0.57	0.09	0.54	0.6	95%
24	80	20-25	0.50	0.70	0.05	0.74	0.04	104%
13	78	10-20	0.5	0.72	0.06	0.64	0.046	89%
18	71	20-25	0.48	0.70	0.06	0.72	0.04	100%
12	70	5.8-25	0.48	0.52	0.11	0.50	0.062	96%
6	59	20-25	0.43	0.75	0.07	0.68	0.04	91%
25	60	10-20	0.43	0.83	0.07	0.64	0.044	77%
7	59	5.8-10	0.43	0.64	0.16	0.47	0.058	73%

The table above is ordered in decreasing angle because the Vertical fallpipe model 2 (VFM2) is a model designed for a vertical fallpipe but modified to be used for high angles(close to 90° vertical). Due to being based on settling velocity, it is most accurate for a vertical fallpipe. VFM2 does not take into account that a backflow that occurs resulting in a sliding bed or flow increasing particle velocity. That is why this model is not so accurate for smaller particles at lower angles(the situation where a sliding flow occurs).

---

## Chapter 9

---

# Conclusion

The main objective of this research is to develop a model that can simulate the most efficient production levels of an inclined fallpipe, used for subsea rock installations.

After initial literature study two models have been developed that model a fallpipe, one simulating a diagonal fallpipe and one simulating a vertical fallpipe. These are the Sliding bed model 1 (SBM1) and Vertical fallpipe model 1 (VFM1). Where Model VFM1 was not designed to be used in other situations than completely vertical flow regimes, model SBM1 assumes particles to operate in the flow regime 'sliding flow' and 'sliding bed'. The use of model VFM1 showed a limitation due to the assumption of only a vertical situation, a fully suspended flow regime. On the other side, it was not clear under which flow angles the SBM1 model would be most accurate.

To gather information about the occurring flow regimes and particle velocity a scale model of a fallpipe was tested in a lab. The measurements and observations of these tests have been used to validate and calibrate the models which had to follow the operating limits and requirements of Great Lakes Dredge & Dock Company, LLC (GLDD). Based on the results of these tests the models were calibrated and Sliding bed model 2 (SBM2) and Vertical fallpipe model 2 (VFM2) have been made.

These final models are able to predict average particle velocity, the SBM2 model can provide particle velocity in 5% accurate from pipe angle 48° up to 86° for rock sizes from 10-25 mm. Smaller diameters that were tested seem to result in a larger deviation. This is best explained by a combination of inaccurate velocity measurements from the video footage due to small particle size and an overestimation of particle density that have thereafter been used in SBM2. The VFM2 provides results within 10% range accurate for a vertical pipe(90°) down to +/- 70°.

Remarkable is the influence of concentration in a vertical fallpipe model, as long as the fallpipe is completely vertical a higher concentration lowers the settling velocity. However, when the pipe is placed in an angle, starting at 87° a higher concentration increases the average particle velocity. When the pipe angle decreases even more, the particles start sliding over the pipe wall. Eventually, at a pipe angle below 60°, the friction force between the pipe and the particles becomes significant slowing it down. The highest velocity is reached at a pipe angle of 60° using 'medium-sized particles. At this angle medium particles still move in a sliding flow regime but are not slowed down significant by wall-friction, resulting in the maximum velocity measured. Furthermore, a reassuring confirmation is

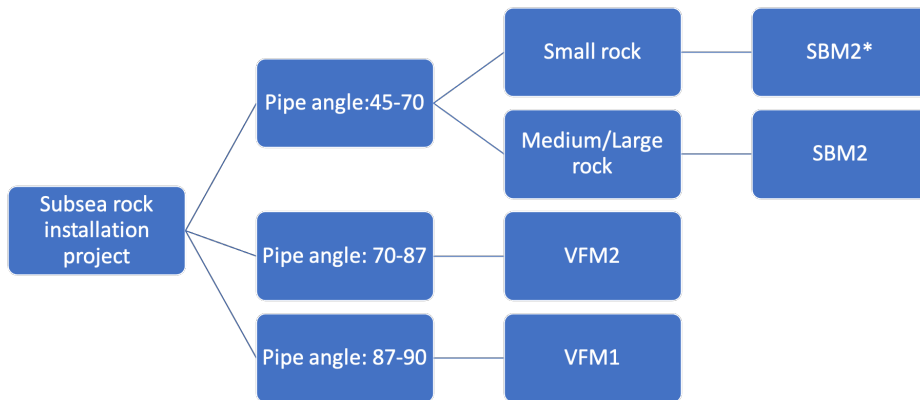
that the dimensions of the fallpipes provided by GLDD are large enough to cope with the estimated production limits. The scale model was mostly tested with a production of 0.48 [kg/s] which is comparable with 1850 ton/hour on full scale. Despite being not being validated, using the models SBM2 and VFM2 on lower productions, a credible output is given by the models, both providing a velocity close to single the settling velocity.

Concluding, this report shows that both the SBM2 and the VFM2 model can provide a good estimation of production levels for a fallpipe (used for subsea rock installations) when used in the correct and representative flow regime. Therefore, these results provide insights that can be used for future subsea rock operations by GLDD.

# Discussion and recommendation

## 10-1 When to use which model

After comparing the two final models Sliding bed model 2 (SBM2) and Vertical fallpipe model 2 (VFM2) with the results from the experiment done in the lab research, it became clear that each model operates optimally in certain situations. To decide which model to use at which pipe angle for which particle size, the flowchart in Figure 10-1 provides an overview.



\* Using small rocks in SBM2 is not accurate and not validated

**Figure 10-1:** Model advise flowchart

## 10-2 Different production

In SBM2 the bed density was determined based on the results from the lab research:

- Small particles:  $C_{vb} = 9.0 \cdot \alpha^{-1.05}$
- Medium particles:  $C_{vb} = 35.5 \cdot \alpha^{-1.49}$
- Large particles:  $C_{vb} = 7.7 \cdot \alpha^{-1.15}$



This will probably be different for different productions. To cover the most important production values, future lab research can be done using a lower production. This can be done by changing the amount of rock on the conveyor belt or changing the time it takes to empty the belt.

### 10-3 Scaling models to full scale

It is expected that VFM2 can be scaled without problems as it is built based on the single particle settling velocity. In this equation, particle size is used in the equation for a single settling velocity. Variables that need attention before scaling VFM2: Drag coefficient ( $C_D$ ) 1-2 for gravel → if using rough mined rock this value would be around 2[Miedema, b].

In contrast to SBM2, where particle size does not play a significant role in calculating particle velocity. Also, it can be that a drag force must be added to SBM2, as the particles are scaled, so does the velocity. Due to the low concentrations in the fallpipe that Great Lakes Dredge & Dock Company, LLC (GLDD) will probably using, a sliding bed does not occur. Therefore the rocks falling/rolling true the pipe will experience frontal drag force. These forces are not taken into account. As this force increases to a 2nd power as velocity increases ( $F_{drag} = 0.5 \cdot C_D \cdot A \cdot V^2$ ), it can be that this did not play a role in a scale model but does have significant influences at full scale.

---

# Appendix A

---

## The back of the thesis

### A-1 Settling velocity in more detail

For one-dimensional settling the particle velocity  $v_p$  is computed with:

$$(V_p \rho_s + M_a) \frac{dv_p}{dt} = A_p C_D \frac{1}{2} \rho_w |v_w - v_p| (v_w - v_p) + V_p g (\rho_s - \rho_w) \quad (\text{A-1})$$

Where  $V_p$  = Volume of particle,  $\rho_s$  = density of particle,  $\rho_w$  = density of water,  $v_p$  = velocity of particle,  $v_w$  = velocity of water surrounding particle,  $M_a$  = added mass coefficient,  $A_p$  = Surface area of particle in flow direction. The added mass is determined with

$$M_a = C_m \rho_w V_p \quad (\text{A-2})$$

For a stationary situation  $\left(\frac{dv_p}{dt} = 0\right)$  and stagnant flow conditions ( $v_w = 0$ ) this expression reads:

$$v_p = \sqrt{\frac{2\Delta g V_p}{C_D A_p}} \quad (\text{A-3})$$

Where the specific density  $\Delta$  is defined as:

$$\Delta = \frac{\rho_s - \rho_w}{\rho_w} \quad (\text{A-4})$$

For a sphere with diameter  $d$  this reduces to the well-known general equation for the settling velocity for a single sphere:

$$w_0 = \sqrt{\frac{4\Delta g d}{3C_D}} \quad (\text{A-5})$$

### A-2 Sliding bed formulas derived

In this section, the rewriting of the sliding bed force equilibrium equations will be described in more detail. First, we start with the basic assumption that all material in the pipe is

moving at a constant velocity. When the material is moving with a constant velocity, the forces in the pipe are in equilibrium. This equilibrium is defined by:

$$F_{gx} = F_{12,fl} + F_{1,fl} + F_{2,fr} + F_{2,fl} \quad (\text{A-6})$$

Shown in figure below:

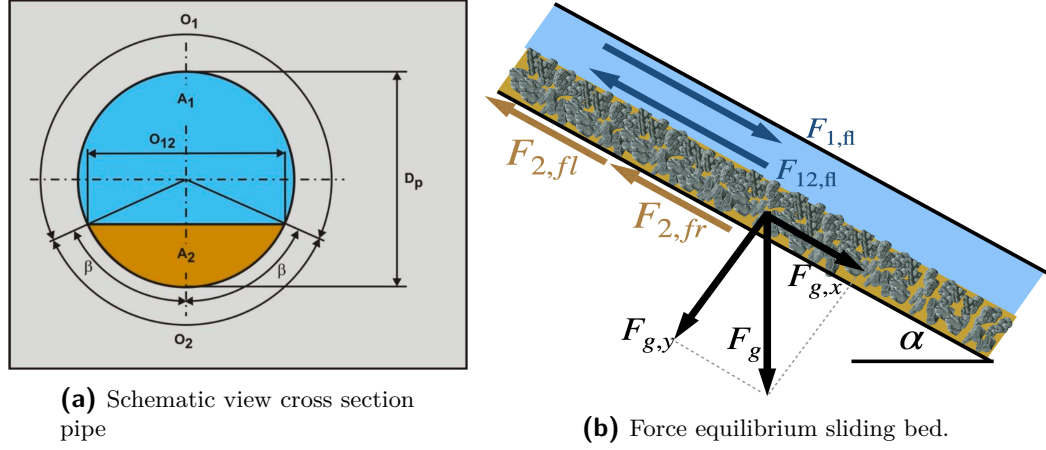


**Figure A-1:** The pipe figure and its 3D model

**Table A-1:** The mechanisms of four consensus filtering approaches

Paramater	Description	Equation
$\beta$	Angle of the bed height [Rad]	[-]
$O_1$	Contact arc-length water and pipe [m]	$O_1 = D_p \cdot (\pi - \beta)$
$O_2$	Contact arc-length bed and pipe [m]	$O_2 = D_p \cdot \beta$
$O_{12}$	Width contact bed and water in pipe [m]	$O_{12} = D_p \cdot \sin(\beta)$
$A_p$	Cross sectional area pipe [m <sup>2</sup> ]	$A_p = \frac{\pi}{4} \cdot D_p^2$
$A_2$	Cross sectional area bed [m <sup>2</sup> ]	$\frac{D_p^2}{4} \cdot (\beta - \sin(\beta) \cdot \cos(\beta))$
$A_1$	Cross sectional area water above bed [m <sup>2</sup> ]	$A_1 = A_p - A_2$

### A-3 Rewriting the equilibrium

The equilibrium of forces of a sliding bed is given in Eq. (A-7)

$$F_{gx} = F_{12,fl} + F_{1,fl} + F_{2,fr} + F_{2,fl} \quad (\text{A-7})$$

The following three forces are dependent on  $V_1$  and  $V_2$ , where  $V_1$  can be rewritten as Eq. (A-8).

$$V_1 = \frac{A2 \cdot (1 - C_{vb}) \cdot V_2}{A1} \quad (\text{A-8})$$

**Rewrite  $F_{12,fl}$  :**

$$F_{12,fl} = \frac{\alpha_{Wilson} \cdot 1.325}{\left(\ln\left(\frac{0.27 \cdot d}{D_H} + \frac{5.75}{Re^{0.9}}\right)\right)^2} \cdot \frac{1}{8} \cdot (V_1 + V_2)^2 \cdot \sin(\beta) \cdot D_P \quad (\text{A-9})$$

Substitute  $V_1$  with Eq. (A-8) and extract  $V_2^2$  from equation gives:

$$F_{12,fl} = \frac{\alpha_{Wilson} \cdot 1.325}{\left(\ln\left(\frac{0.27 \cdot d}{D_H} + \frac{5.75}{Re^{0.9}}\right)\right)^2} \cdot \frac{1}{8} \cdot \left(\frac{A2 \cdot (1 - C_{vb})}{A1} + 1\right)^2 \cdot \sin(\beta) \cdot D_P \cdot V_2^2 \quad (\text{A-10})$$

**Rewrite  $F_{1,fl}$  :**

$$F_{1,fl} = \frac{1}{8} \cdot \frac{1.325}{\left(\ln\left(\frac{0.27 \cdot \varepsilon}{D_H} + \frac{5.75}{Re^{0.9}}\right)\right)^2} \cdot (V_1)^2 \cdot (\pi - \beta) \cdot D_P \quad (\text{A-11})$$

Substitute  $V_1$  with Eq. (A-8) and extract  $V_2^2$  from equation gives:

$$F_{1,fl} = \frac{1}{8} \cdot \frac{1.325}{\left(\ln\left(\frac{0.27 \cdot \varepsilon}{D_H} + \frac{5.75}{Re^{0.9}}\right)\right)^2} \cdot \left(\frac{A2 \cdot (1 - C_{vb})}{A1}\right)^2 \cdot (\pi - \beta) \cdot D_P \cdot V_2^2 \quad (\text{A-12})$$

$$F_{2,fl} = \frac{1.325}{\left(\ln\left(\frac{0.27 \cdot \varepsilon}{d} + \frac{5.75}{(Re)^{0.9}}\right)\right)^2} \cdot \frac{1}{8} \cdot \beta \cdot D_P \cdot (1 - c_{vb}) \cdot V_2^2 \quad (\text{A-13})$$

Now the forces that were dependent on  $V_2$  are on the right side of the equation and on the left side are  $F_{gx}$  and  $F_{2,fr}$  that is not dependent on the velocity of the bed( $V_2$ ).

$$F_{gx} - F_{2,fr} = (F_{12,fl} + F_{1,fl} + F_{2,fl}) \cdot V_2^2 \quad (\text{A-14})$$

Can be written as:

$$\frac{F_{gx} - F_{2,fr}}{F_{12,fl} + F_{1,fl} + F_{2,fl}} = V_2^2 \rightarrow \sqrt{\frac{F_{gx} - F_{2,fr}}{F_{12,fl} + F_{1,fl} + F_{2,fl}}} = V_2 \quad (\text{A-15})$$

$V_2 =$

$$\sqrt{\frac{g \cdot \sin(\alpha) \cdot R_{sd} \cdot C_{vb} \cdot A_2 - \frac{\mu_{fr} \cdot g \cdot \cos(\alpha) \cdot R_{sd} \cdot C_{vb} \cdot A_p}{\beta \cdot D_p} \cdot \frac{(\beta - \sin(\beta) \cdot \cos(\beta))}{\pi} \cdot \beta \cdot D_p}{\frac{1}{8} \cdot D_p \cdot \left( \frac{\alpha_{Wilson} \cdot 1.325}{\left( \ln \left( \frac{0.27 \cdot d}{D_H} + \frac{5.75}{Re^{0.9}} \right) \right)^2} \cdot \left( \frac{A_2 \cdot (1 - C_{vb})}{A_1} + 1 \right)^2 \cdot \sin(\beta) + \frac{1.325}{\left( \ln \left( \frac{0.27 \cdot \varepsilon}{D_H} + \frac{5.75}{Re^{0.9}} \right) \right)^2} \cdot \left( \frac{A_2 \cdot (1 - C_{vb})}{A_1} \right)^2 \cdot (\pi - \beta) + \frac{1.325}{\left( \ln \left( \frac{0.27 \cdot \varepsilon}{d} + \frac{5.75}{(Re)^{0.9}} \right) \right)^2} \cdot \beta \cdot (1 - c_{vb}) \right)}}$$

**Figure A-2:** Velocity sliding bed

To get a production of the fallpipe, the following equation can be used:

$$P_i(Kg/s) = P_o = V_2 \cdot A_2 \cdot C_{vb} \cdot \rho_s \quad (\text{A-16})$$

## A-4 Additional images lab research setup

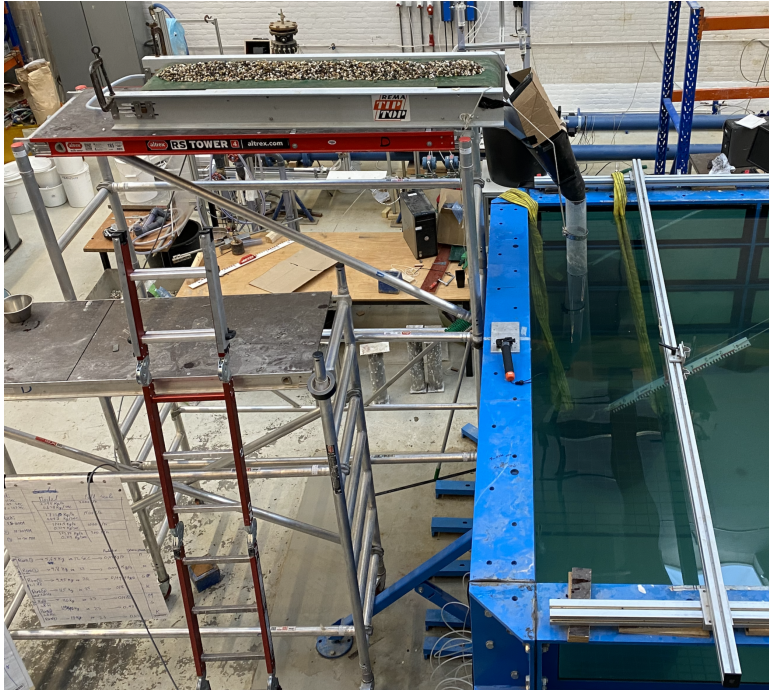


**Figure A-3:** Lab setup scaffolding with conveyor belt



**Figure A-4:** Lab setup conveyor belt

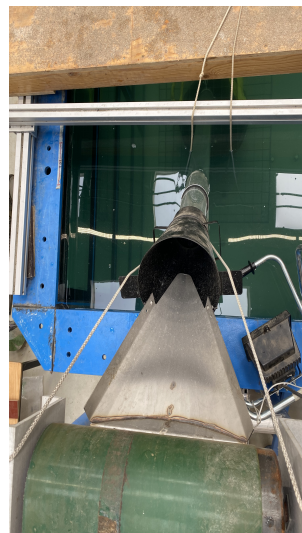


**Figure A-5:** Lab setup funnel feeding the fallpipe

## A-5 Remarkable observations lab research

It was noticed that there is a difference in velocity between a high concentration section and a low concentration section in the pipe. Particles that are sliding/flowing together move faster than particles that are not.

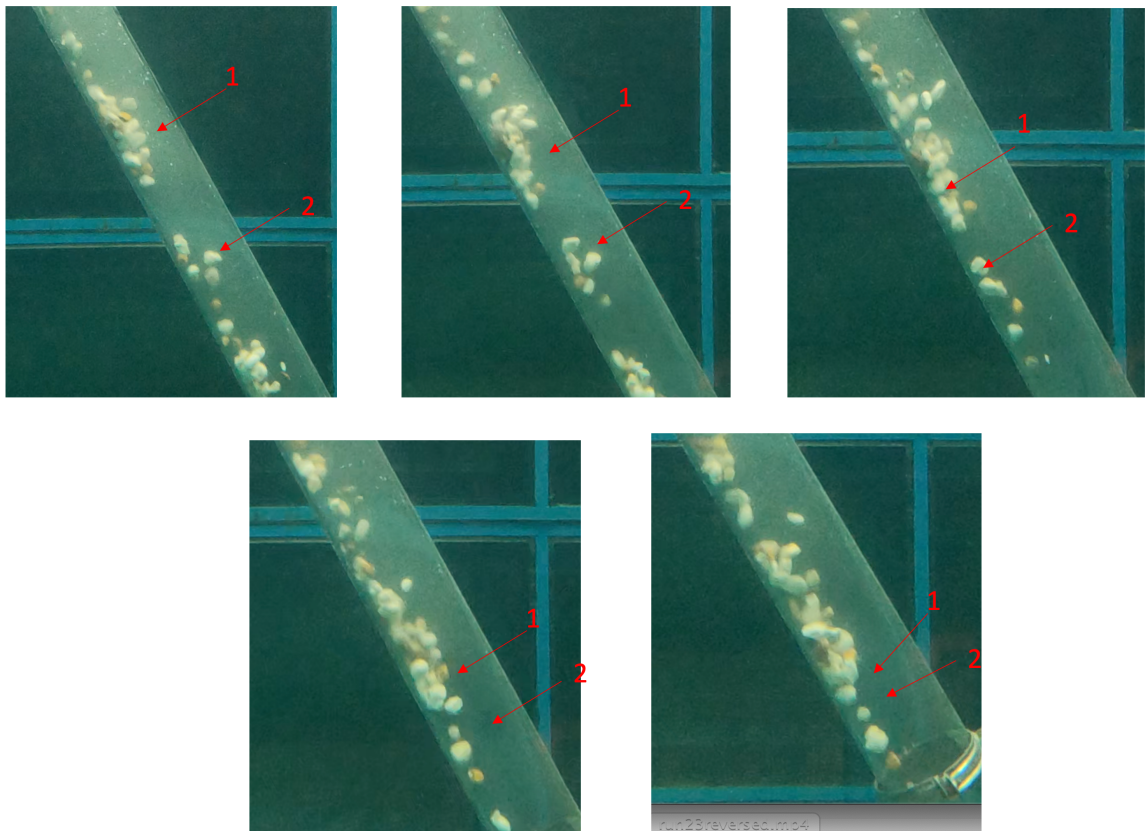


**Figure A-6:** Difference in velocity due to local concentration

In Figure A-6 5 frames are shown, with a region of high concentration particles numbered with '1' and a low concentration section numbered with '2'. Frame by frame it is clear that the cluster of particles with a high concentration gets closer to the particles that are moving alone.





**Figure A-7:** Run 19  
spread



**Figure A-8:** Run 20  
spread



**Figure A-9:** Run 21  
spread

## A-6 Spread of rock

Container Number	Weight test 1	Weight test 2	Weight test 3
1	0	0.00	0
2	0.02	0.00	0
3	0.01	0.00	0
4	0.02	0.00	0
5	0.05	0.10	0.1
6	0.25	0.25	0.1
7	0.25	0.20	0.15
8	0	0.00	0
9	0.4	0.10	0
10	0.5	0.30	0.15
11	0.5	0.30	0.25
12	0.05	0.05	0.1
13	0.45	0.05	0
14	0.55	0.15	0
15	0.55	0.30	0
16	0.1	0.05	0.05
17	0.1	0.00	0
18	0.5	0.05	0
19	0.4	0.05	0
20	0	0.05	0
21	0	0	0
22	0.25	0.00	0
23	0	0.00	0
24	0.05	0.00	0



## A-7 Observation of flow regime labresearch

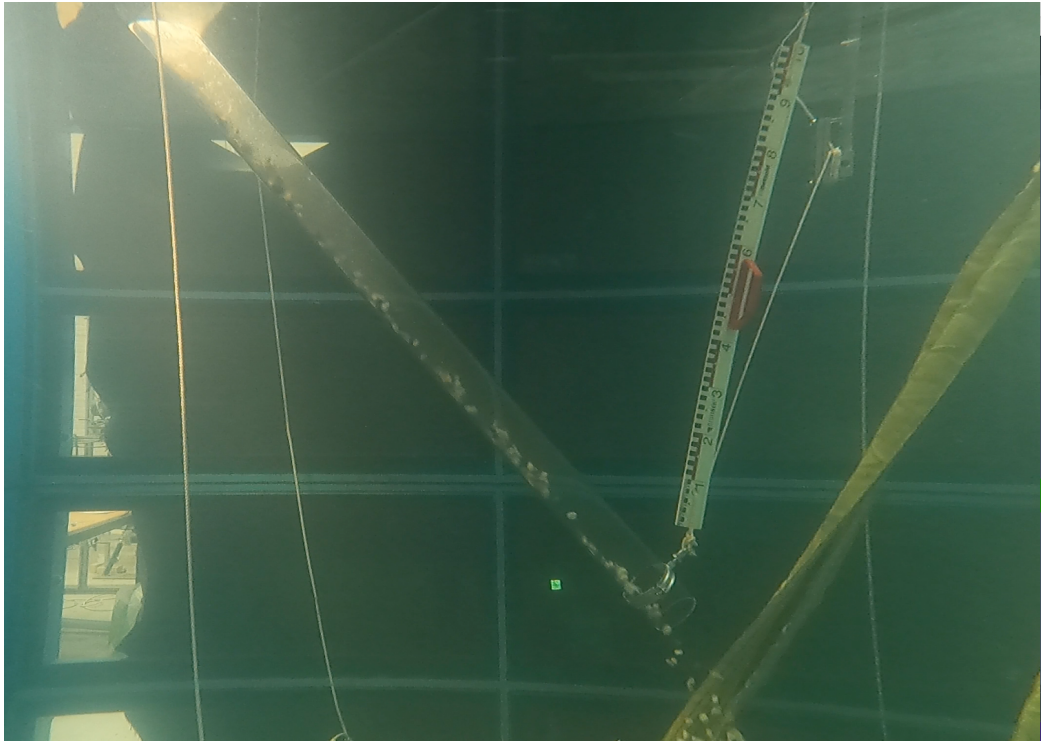


**Figure A-10:** Side-view run 2

### Run 2

- Angle pipe:  $48^\circ$
- Particle size: medium  $\rightarrow$  10/20 mm
- Production pipe: 0.47 kg/s
- Average velocity particles: 0.733 m/s

**Observations run 2** Particles are rolling and sliding down the pipe, a sliding bed forms and particles seem to cluster together. Clusters that are getting too high are separated by the 'back flow', between clusters there is some space.

**Two layer system:** Yes

**Sliding flow:** Yes

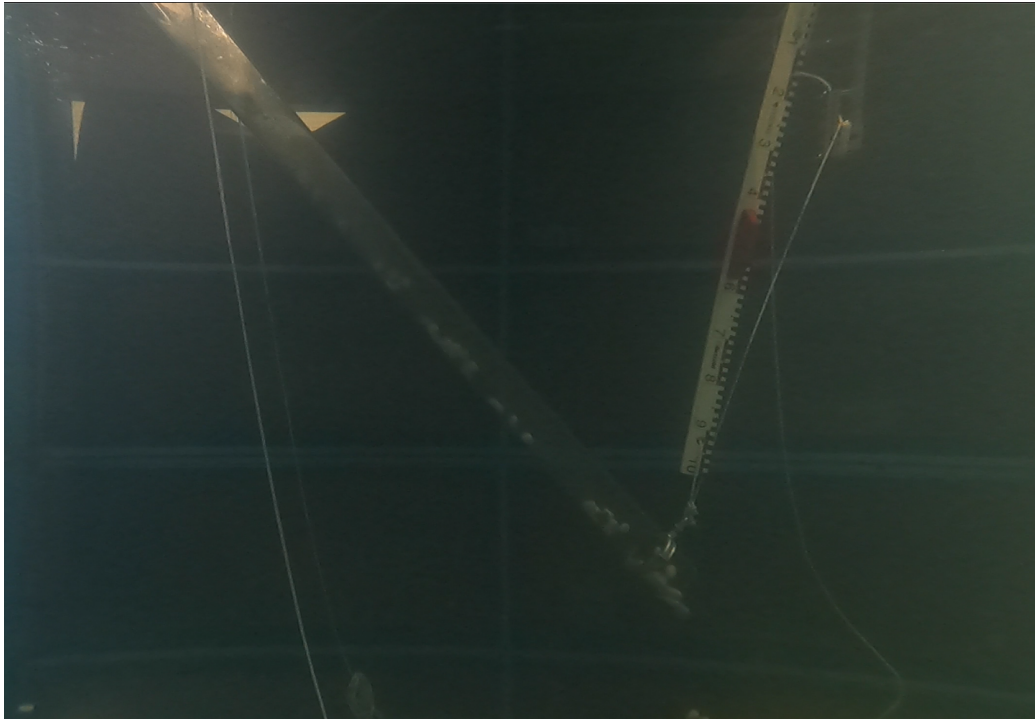


**Figure A-11:** Side-view run 3

### Run 3

- Angle pipe:  $48^\circ$
- Particle size: large  $\rightarrow$  20/25 mm
- Production pipe: 0.5 kg/s
- Average velocity particles: 0.708 m/s

**Observations run 3** Particles are rolling and sliding down the pipe, a sliding bed forms and particles seem to cluster together. Clusters are separated by the 'back flow', between clusters there is some space. Due to the large particle size, a uniform bed can not be formed. Particles are moving more individual than as a formed bed compared with run 2.

**Two layer system:** Yes

**Sliding flow:** Yes

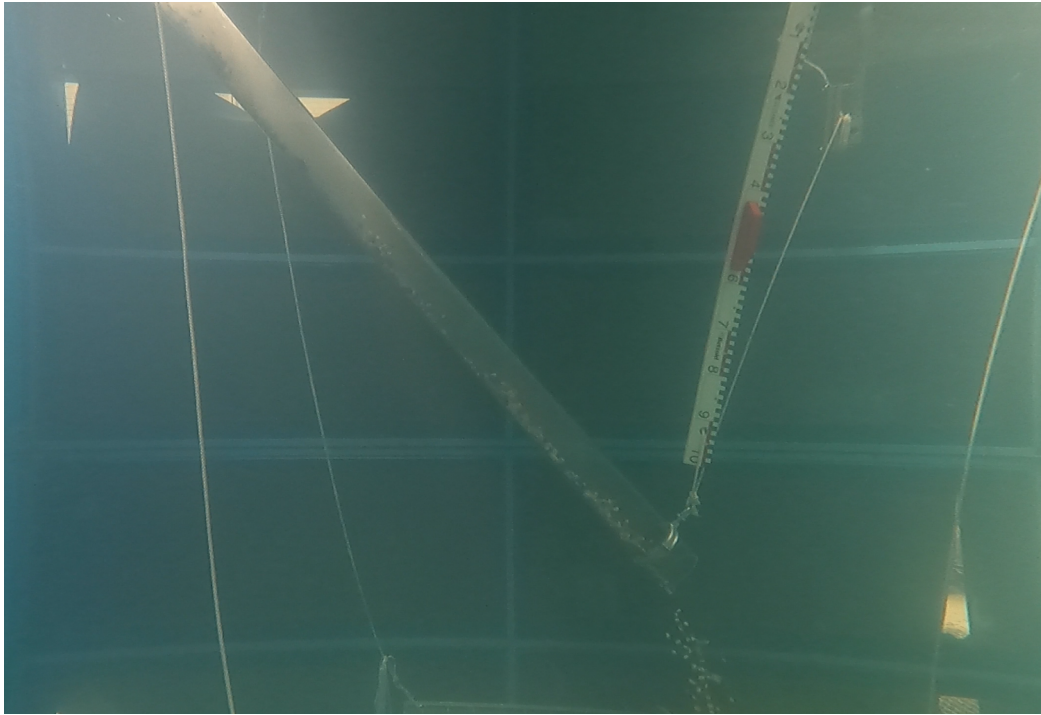


**Figure A-12:** Side-view run 4

#### **Run 4**

- Angle pipe:  $48^\circ$
- Particle size: small  $\rightarrow$  5.8/10 mm
- Production pipe: 0.46 kg/s
- Average velocity particles: 0.649 m/s

**Observations run 4** Particles form a bed instantaneous when entering the pipe. A more uniform flow is formed than in run 2 & 3. Bed height seems to be more stable than in run 2 & 3.

**Two layer system:** Yes

**Sliding flow:** Yes

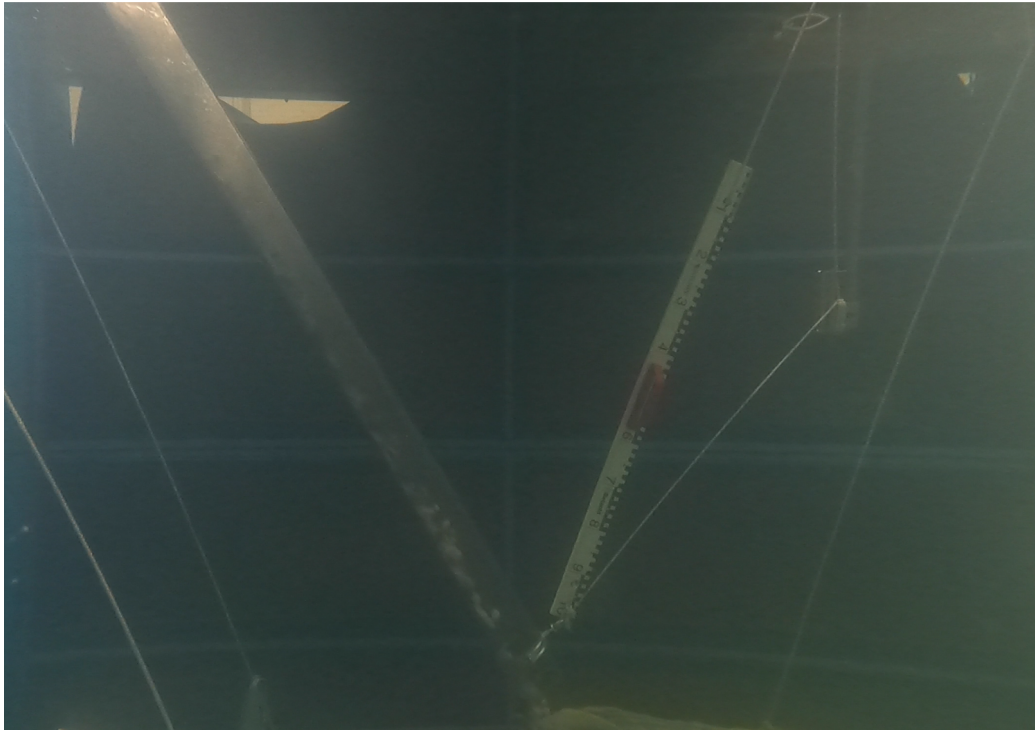


**Figure A-13:** Side-view run 5

### Run5

- Angle pipe:  $59^\circ$
- Particle size: medium  $\rightarrow$  10/20 mm
- Production pipe: 0.48 kg/s
- Average velocity particles: 0.873 m/s

**Observations run 5** Almost similar observation as run 2. Particles are rolling and sliding down the pipe, sliding flow forms and particles seem to cluster together. Clusters are separated by the 'back flow', between clusters there is some space.

**Two layer system:** Yes

**Sliding flow:** Yes

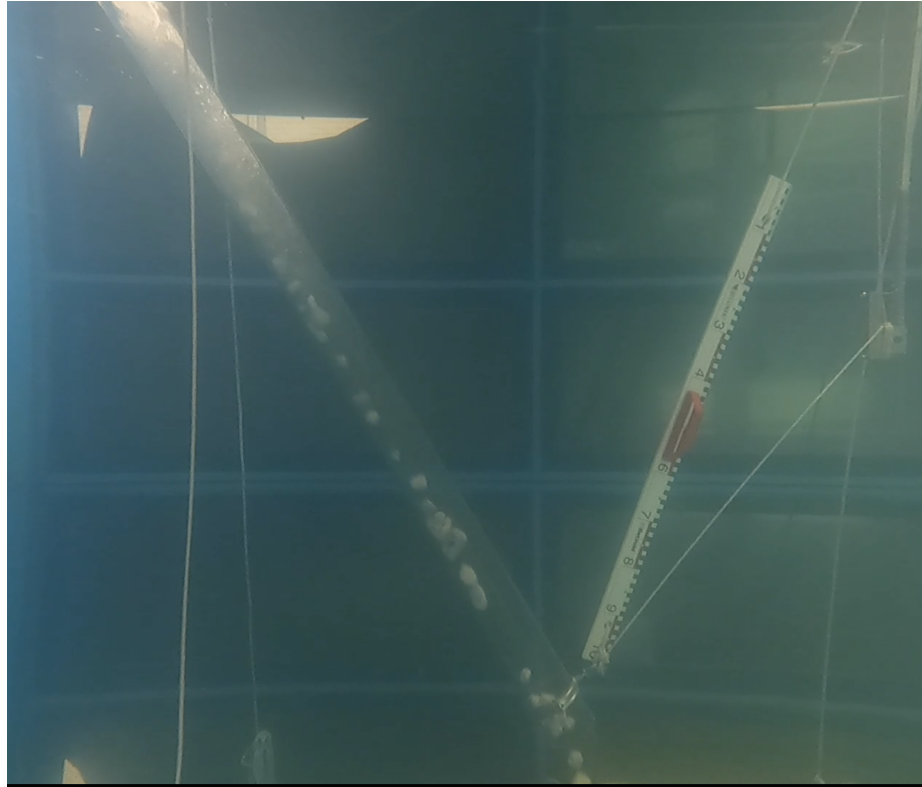


**Figure A-14:** Side-view run 6

### Run 6

- Angle pipe:  $59^\circ$
- Particle size: large  $> 20/25$  mm
- Production pipe: 0.43 kg/s
- Average velocity particles: 0.75 m/s

**Observations run 6** Almost similar as run 3, particles are rolling and sliding down the pipe, a sliding bed forms and particles seem to cluster together. Clusters are separated by the 'back flow', between clusters there is some space. Due to large particle size, a uniform bed can not be formed. Particles are moving more individual than as a formed bed compared with run 2.

**Two layer system:** Yes

**Sliding flow:** Yes



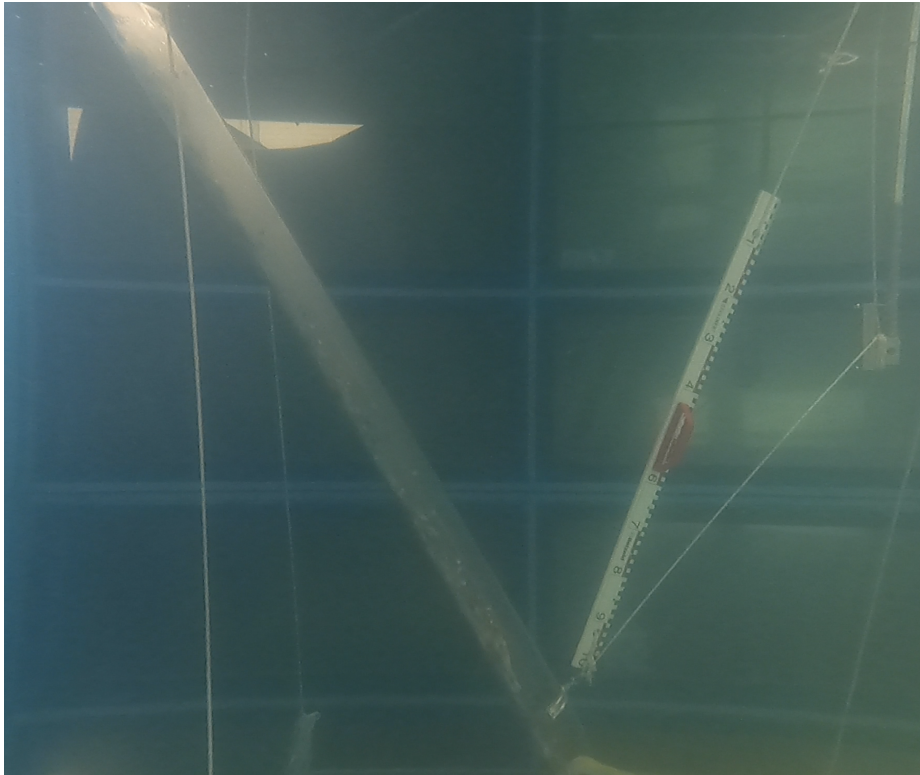


**Figure A-15:** Side-view run 7

### Run 7

- Angle pipe:  $59^\circ$
- Particle size: small  $\rightarrow$  5.8/10 mm
- Production pipe: 0.43 kg/s
- Average velocity particles: 0.639 m/s

**Observations run 7** Almost similar as observation in run 4. Particles form a bed instantaneous when entering the pipe. A more uniform bed is formed than in run 2 & 3. Bed height seems to be more stable than in run 2 & 3. Different seems to be that there is more suspension of particles as angle of the pipe increases.

**Two layer system:** Yes

**Sliding flow:** Yes

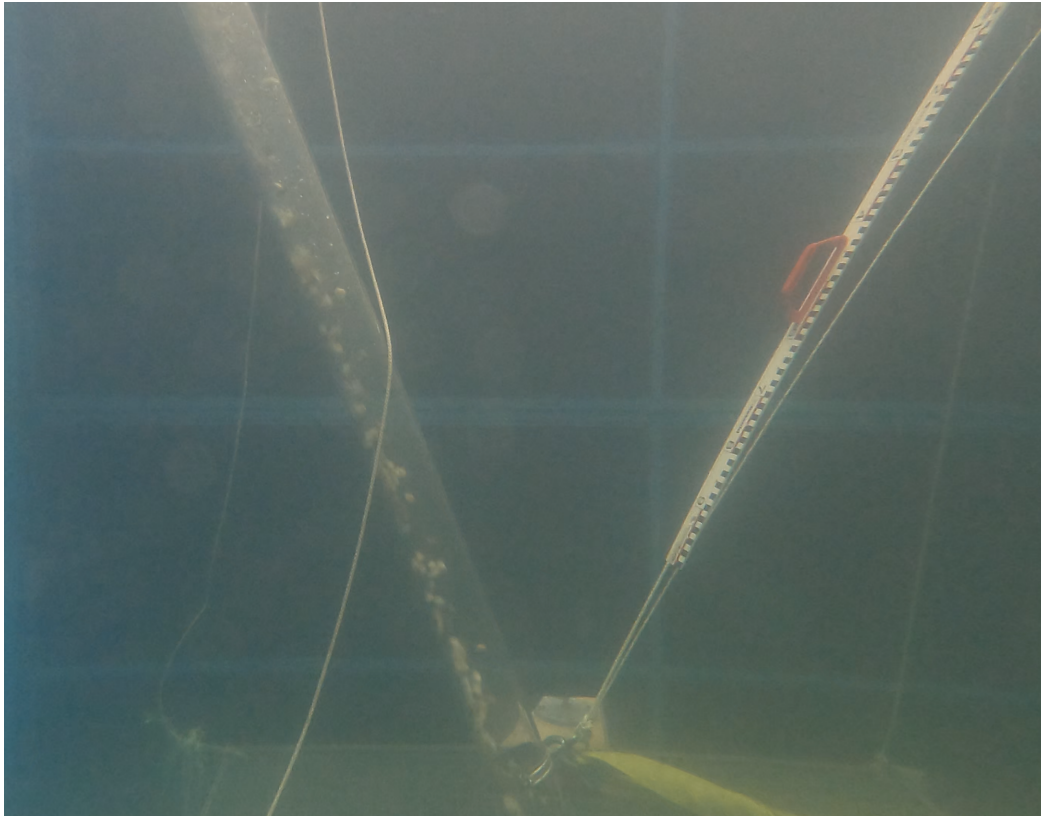


**Figure A-16:** Side-view run 9

**Run 9**

- Angle pipe:  $71^\circ$
- Particle size: medium  $\rightarrow$  10/20 mm
- Production pipe: 0.43 kg/s
- Average velocity particles: 0.737 m/s

**Observations run 9** Compared with run 9, (same rock size, other angle) the velocity seems to drop due to more suspension of particles and being caught by the 'backflow'. Two layer system is still present but less obvious.

**Two layer system:** Yes

**Sliding flow:** Yes

**Run 10****Figure A-17:** Side-view run 10

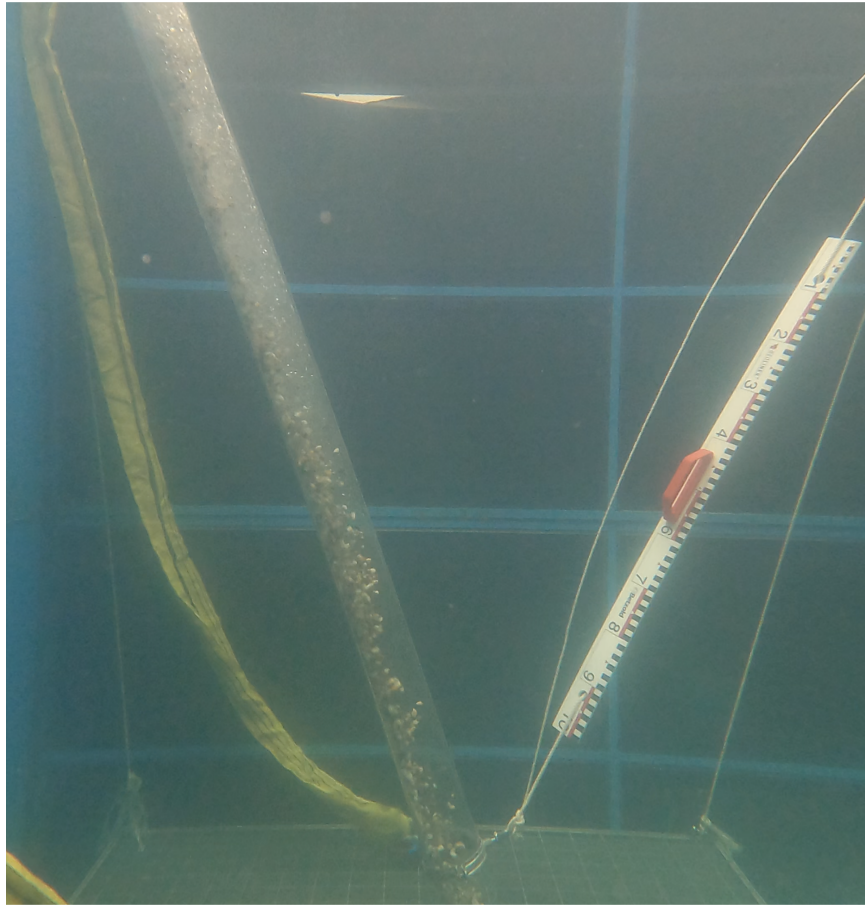
- Angle pipe:  $71^\circ$
- Particle size: medium  $\rightarrow$  20/25 mm
- Production pipe: 0.43 kg/s
- Average velocity particles: 0.834 m/s

**Observations run 10** Bad visibility, curtain fell off during video. Despite the bad quality, it can be seen that the large particles are rolling and tumbling down, not clearly sliding. Velocity of the particles is high, there is not much sliding friction  $F_2 fr$  but the particles are moving in each other slipstream and clustering together which lead to higher velocities than a sliding bed.

**Two layer system:** yes, there is a back-flow

**Sliding flow:** yes



**Run 12****Figure A-18:** Side-view run 12

- Angle pipe:  $70^\circ$
- Particle size: small  $\rightarrow$  5.8/10 mm
- Production pipe: 0.48 kg/s
- Average velocity particles: 0.885 m/s

**Observations run 12** Particles are sliding down, increased suspension but still a sliding flow observed.

**Two layer system:** yes

**Sliding flow:** yes

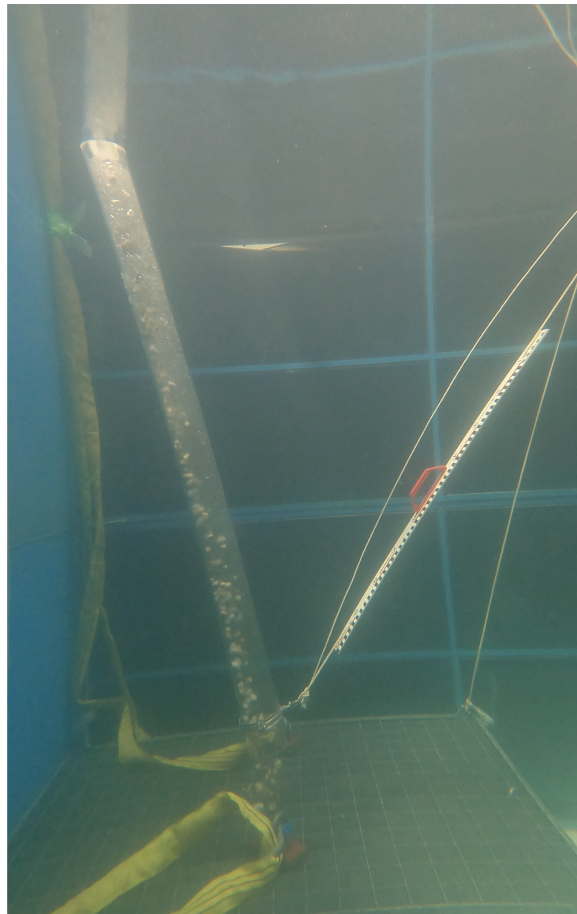


**Figure A-19:** Side-view run 13

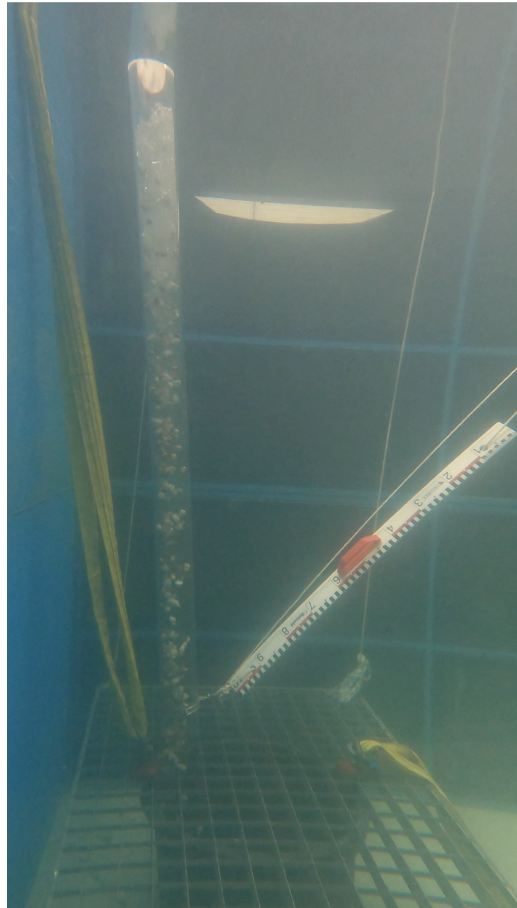
### Run 13

**Observations run 13** Some particles are sliding, there are also many particles in suspension and blown back by the back-flow. This angle,  $78^\circ$ , can be seen as the start of the transition region where a sliding bed still occurs but particles also settle down vertically.

**Two layer system:** Yes

**Sliding flow:** Yes

- Angle pipe:  $78^\circ$
- Particle size: medium  $\rightarrow$  10/20 mm
- Production pipe: 0.5 kg/s
- Average velocity particles: 0.725 m/s

**Run 16****Figure A-20:** Side-view run 16

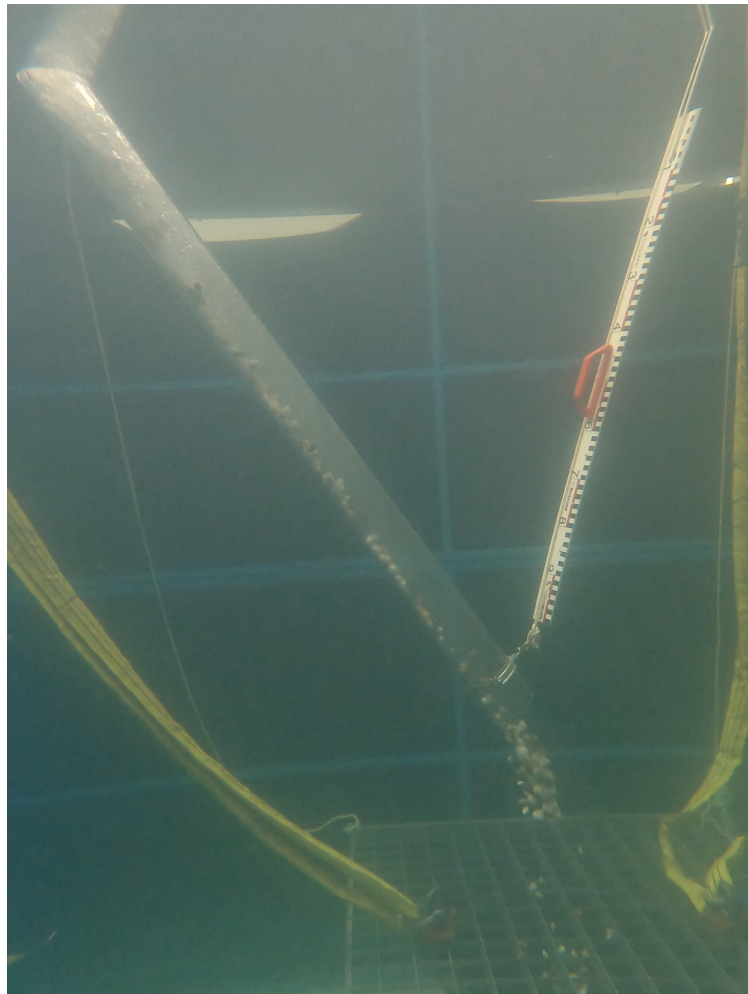
**Observations run 16** It is clear that particles are settling with the hindered settling velocity. However, the small inclination causes the particles in the pipe to move slightly more to one side resulting in a backflow on the other side. This is clearly visible at the bottom at the image A-20, where there are more rocks on the left of the pipe than on the right.

creates a slight back flow with a

**Two layer system:** no

**Sliding flow:** no

- Angle pipe:  $86^\circ$
- Particle size: medium  $\rightarrow$  10/20 mm
- Production pipe: 0.48 kg/s
- Average velocity particles: 0.618 m/s

**Run 17****Figure A-21:** Side-view run 17

**Observations run 17** A clear sliding bed, very thin uniform and constant as can be seen in figure A-21

**Two layer system:** yes

**Sliding flow:** yes

- Angle pipe:  $59^\circ$
- Particle size: medium  $\rightarrow$  10/20 mm
- Production pipe: 0.48 kg/s
- Average velocity particles: 0.726 m/s

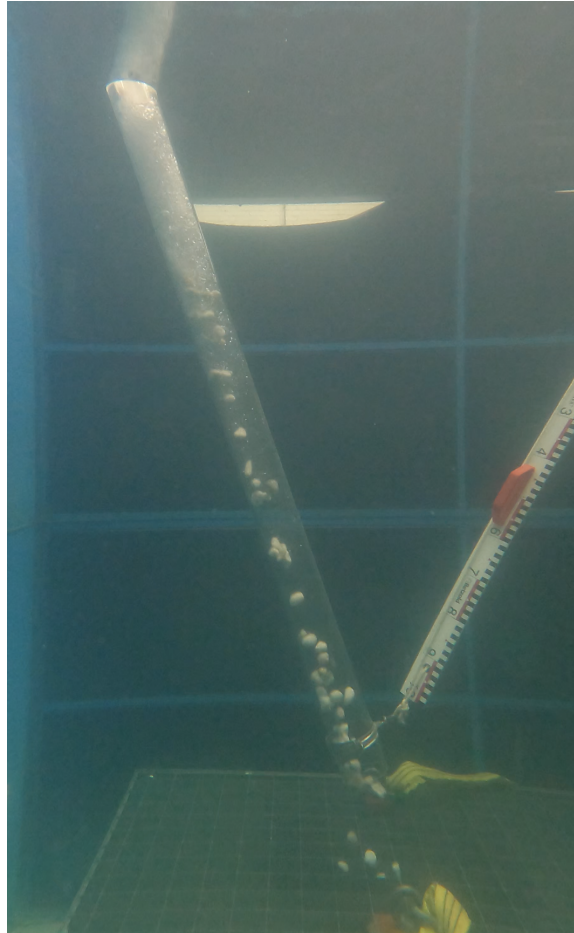


**Figure A-22:** Side-view run 18

### **Run 18**

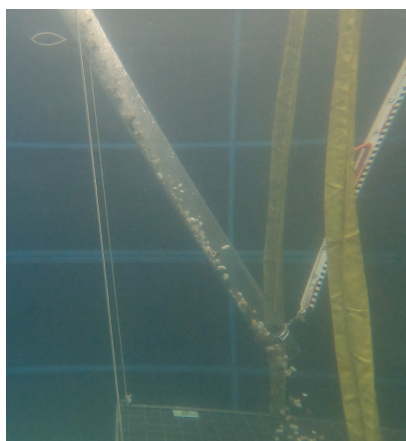
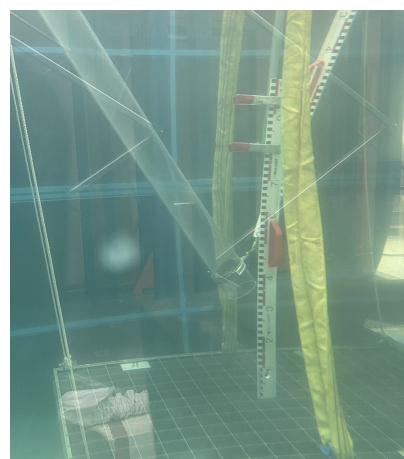
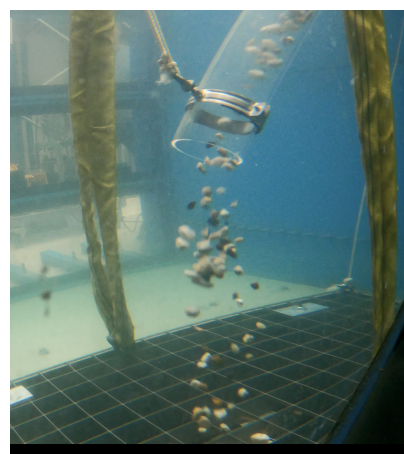
**Observations run 18** The largest particles are moving faster, this causes the particles to cluster together and form some small local sliding beds.  $71^\circ$  is in the transition region between sliding bed and full suspension. Not uniform and not a constant sliding bed regime. Particles tumble and roll down.

**Two layer system:** yes

**Sliding bed:** Yes

- Angle pipe:  $71^\circ$
- Particle size: medium  $\rightarrow$  10/20 mm
- Production pipe: 0.48 kg/s
- Average velocity particles: 0.661 m/s



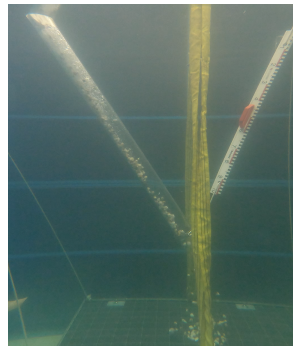
**Run 19****A-7-1 Observation of dispersion lab research****(a)** Run19 sideview**(b)** Run 19 height view**(c)** Run19 dispersion result**(d)** Dispersion view**Figure A-23:** Run 19 observations

**Observations run 19** Run 19 was where the dispersion was measured of the material exiting the fallpipe. The pipe was placed at 32 to 38 cm height, with an inner pipe diameter of 9.4 cm which is about 4 times the diameter. The metal grid where the rocks are fallen into buckets is 6.5 by 6.5 centimetres, almost all particles ended up in 3 by 3 by square buckets.

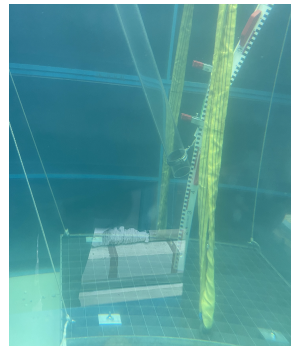
**Two layer system:** yes

**Sliding bed:** Yes

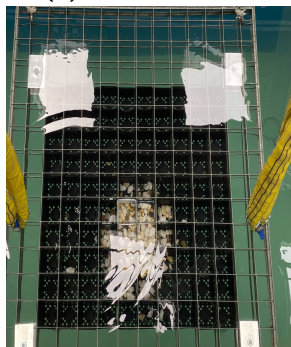
- Angle pipe:  $60^\circ$
- Particle size: medium  $\rightarrow$  10/20 mm
- Average velocity particles: 0.843 m/s



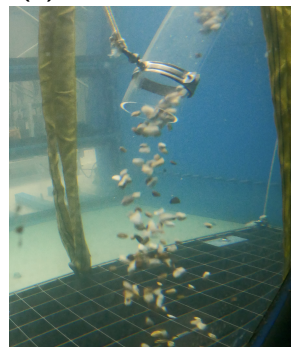
(a) Run20 sideview



(b) Run 20, Height view



(c) Run 20, dispersion result



(d) Run 20, Dispersion view

**Figure A-24:** Run 20**Run 20**

**Observations run 20** Run 20 was where the dispersion was measured of the material exiting the fall pipe. The pipe was placed at 44 to 50 cm height, with an inner pipe diameter of 9.4 cm which is about 5 times the diameter. The metal grid where the rocks are fallen into buckets is 6.5 by 6.5 centimetres, almost all particles ended up in 4 by 4 by square buckets.

**Two layer system:** yes

**Sliding bed:** Yes

- Angle pipe:  $60^\circ$
- Particle size: medium  $\rightarrow$  10/20 mm





---

## Appendix B

---

# Sliding bed model 1 code

This code plots every possible particle velocity and production from every  $\beta$  and  $\alpha$ .

```
1  clc;
2  clear;
3  close all;
4
5  %basic assumption/variables
6  g = 9.81; %Gravity constant
7  d_50 = 15/1000; %Rock/particle diameter(50% of the rocks) [m]
8  rho_w = 1000; %Water density [kg/m^3]
9  rho_s = 2600; %Stone density [kg/m^3]
10 rho_r = (rho_s-rho_w)/rho_w; %relative density [kg/m^3] also desribed as R_sd
11 vis_l = 0.0000013; %Kinematic viscosity Miedema model DHLDDV excel[m^2/
    s])
12 C_fr = 0.416; %assumption friction factor=0.416 bed and pipe,
    miedema book p451 regime 3
13 C_rgh = 0.0015*10^-3; %Roughness plastic—> OMAE2014–23437 epsilon eq:17
    —> warn cast iro
14 w_a = 0; %added water to pipe[m^3/s]
15 C_D = 1; %Form coefficient of rock, Notes rhee p.12
16 m_p = rho_s*4/3 *pi*(d_50/2)^3; %mass of single particle
17
18 %situation dependent variable/inputs
19 L = 2; %Length of pipe
20 D_p = 0.094; %Pipe Diameter
21 lambda_w = d_50/D_p; %Ratio particle size and pipe diameter—> used for
    hindered settling
22 R_e = (3*d_50)/vis_l; %Reynolds number
23 A_p = (pi/4)*D_p^2; %Surface cross section pipe, described in figure 1,
    paper OMAW2014
24 a_wilson = 2.75; %Wilson factor p3 at eq 18 paper OMAW2014
25 n = 2.4; %The value chosen for the hindered sttling exponent
    n = 2.4, which is a value for high particle Reynolds numbers. This value is
    chosen because relative large particles are used for subsea rock installation and
    in scale model.
26
27
28
29 alpha_list = 1:1:90;
30 beta_list = 0:0.01:pi;
31
32
33
34
35 %this loop is with the original bed density [C_vb]
36 for i = 1:length(alpha_list)
37     for ii = 1:length(beta_list)
38         beta = beta_list(ii);
39         alpha = alpha_list(i);
40         A_2 = 0.25*D_p^2*(beta-sin(beta)*cos(beta));
41         A_1 = A_p-A_2;
42         D_H = sqrt((4*A_1)/pi);
43         C_vb = 0.4;
44         F_gx = g*sind(alpha)*rho_r*C_vb*A_2;
45         lambda_12 = (a_wilson*1.325)/(log((0.27*d_50)/D_H)+5.75/R_e^0.9)^2;
46         F_12fl = lambda_12*0.125*(((A_2)*(1-C_vb)/(A_1))+1)^2*sin(beta)*D_p;
```

```

47     F_2fr = ((C_fr*g*cosd(alpha)*rho_r*C_vb*A_p*(beta-sin(beta)*cos(beta))*beta
48             )/(beta*D_p*pi))*D_p*beta;
49     lambda_1= 1.325/(log(0.27*C_rgh/D_H+5.75/R_e^0.9))^2;
50     F_1fl = 0.125*lambda_1*((A_2*(1-C_vb))/A_1)^2*(pi-beta)*D_p;
51     lambda_2= 1.325/(log(0.27*C_rgh/d_50+5.75/R_e^0.9))^2 ;
52     F_2fl = lambda_2*0.125*beta*D_p*(1-C_vb);
53     V_2(i, ii) =sqrt((F_gx-F_2fr)/(F_12fl+F_1fl+F_2fl));
54     if ~isreal(V_2(i, ii)) %Due to the squareroot in V_2 imaginary
55         numbers occur, this line makes those numbers zero's.
56         V_2(i, ii) = 0;
57     end
58     P_o(i, ii)=V_2(i, ii)*A_2*C_vb*rho_s;
59
60     end
61 end
62
63
64
65
66
67 %plot(beta_list, V_2(i,:), 'LineWidth',3)
68 figure(1)
69 surf(beta_list, alpha_list, V_2);
70 title('Velocity sliding bed','fontweight','bold','fontsize',14)
71 xlabel('Beta size of sliding bed[Rad]','fontweight','bold','fontsize',12)
72 ylabel('Alpha, angle pipe[degrees]','fontweight','bold','fontsize',12)
73 zlabel('Velocity [m/s]','fontweight','bold','fontsize',12)
74 grid on
75
76
77 %Draw horizontal lines for a certain production:
78 hold on
79 contour3(beta_list,alpha_list,V_2,[0.6 0.6], '-Y', 'LineWidth',2) % Draw some
80     velocity contour lines at certain V_2
81 hold on
82 contour3(beta_list,alpha_list,V_2,[0.7 0.7], '-b', 'LineWidth',2) % Draw some
83     velocity contour lines at certain V_2
84 hold on
85 contour3(beta_list,alpha_list,V_2,[0.8 0.8], '-r', 'LineWidth',2) % Draw some
86     velocity contour lines at certain V_2
87 hold off
88
89 figure(2)
90 surf(beta_list, alpha_list, P_o);
91 title('Production ','fontweight','bold','fontsize',14)
92 xlabel('Beta size of sliding bed','fontweight','bold','fontsize',12)
93 ylabel('Alpha, angle pipe[degrees]','fontweight','bold','fontsize',12)
94 zlabel('Production [kg/s]','fontweight','bold','fontsize',12)
95 grid on
96
97 %Draw horizontal lines for a certain production:
98 hold on
99 contour3(beta_list,alpha_list,P_o,[0.3 0.3], '-Y', 'LineWidth',2) % Draw Contour At
100     1500 tons/H
101 hold on
102 contour3(beta_list,alpha_list,P_o,[0.5 0.5], '-B', 'LineWidth',2) % Draw Contour At
103     1500 tons/H
104 hold on
105 contour3(beta_list,alpha_list,P_o,[0.7 0.7], '-r', 'LineWidth',2) % Draw Contour At
106     750 tons/H
107 hold off

```

---

## Appendix C

---

### Sliding bed model 1 code: rewritten

This code is mostly similar as but this code uses production as an input and provides the concentration of the bed and the velocity of the particles based on production that is put in the pipe.

```
1  clc;
2  clear;
3  close all;
4
5  %basic assumption/variables
6  g = 9.81; %Gravity constant
7  d_50 = 15/1000; %Rock/particle diameter(50% of the rocks) [m]
8  rho_w = 1000; %Water density [kg/m^3]
9  rho_s = 2600; %Stone density [kg/m^3]
10 rho_r = (rho_s-rho_w)/rho_w; %relative density [kg/m^3] also desribed as R_sd
11 vis_l = 0.0000013; %Kinematic viscosity Miedema model DHLLDV excel[m^2/
    s])
12 C_fr = 0.416; %assumption friction factor=0.416 bed and pipe,
    miedema book p451 regime 3
13 C_rgh = 0.0015*10^-3; %Roughness plastic—> OMAE2014–23437 epsilon eq:17
    —> warn cast iro
14 w_a = 0; %added water to pipe[m^3/s]
15 C_D = 1; %Form coefficient of rock, Notes rhee p.12
16 m_p = rho_s*4/3 *pi*(d_50/2)^3; %mass of single particle
17
18 %situation dependent variable/inputs
19 L = 2; %Length of pipe
20 D_p = 0.094; %Pipe Diameter
21 lambda_w = d_50/D_p; %Ratio particle size and pipe diameter—> used for
    hindered settling
22 R_e = (3*d_50)/vis_l; %Reynolds number
23 A_p = (pi/4)*D_p^2; %Surface cross section pipe, described in figure 1,
    paper OMAW2014
24 a_wilson = 2.75; %Wilson factor p3 at eq 18 paper OMAW2014
25 n = 2.4; %The value chosen for the hindered sttling exponent
    n = 2.4, which is a value for high particle Reynolds numbers. This value is
    chosen because relative large particles are used for subsea rock installation and
    in scale model.
26
27
28
29
30 P_in=0.48;
31 alpha=66;
32
33
34 syms beta
35 A_2 = 0.25*D_p^2*(beta-sin(beta)*cos(beta));
36 A_1 = A_p-A_2;
37 D_H = sqrt((4*A_1)/pi);
38
39 if d_50< 25/1000
40     C_vb=7.7*alpha^-1.15;
41     if d_50< 20/1000
42         C_vb=35.5*alpha^-1.49;
```

```

43         if d_50 < 10/1000
44             C_vb = 9.03*alpha^(-1.045) ;
45         end
46     end
47 end
48     F_gx = g*sind(alpha)*rho_r*C_vb*A_2;
49     x = C_vb*2.5*cos(0.5*beta);

    % efficientie van de 'backflow
50     lambda_12 = 0.83*1.325/(log(0.27*C_rgh/d_50+5.75/R_e^0.9))^2+0.37*(2/(sqrt(2*g
        *D_H*rho_r)))^2.73*(m_p/rho_w)^0.094; % Miedema book 7.3-57 Frdc
        aangenomen dat v1+v2=2
51     F_12fl = lambda_12*0.125*(x*((A_2)*(1-C_vb)/(A_1))+1)^2*sin(beta)*D_p;
52     F_2fr = ((C_fr*g*cosd(alpha)*rho_r*C_vb*A_p*(beta-sin(beta)*cos(beta))*beta
        )/(beta*D_p*pi))*D_p*beta;
53     F_1fl = 0.125*1.325/(log(0.27*C_rgh/D_H+5.75/R_e^0.9))^2*(x*(A_2*(1-C_vb))/
        A_1)^2*(pi-beta)*D_p;
54     F_2fl = x*(1.325/(log(0.27*C_rgh/d_50+5.75/R_e^0.9))^2*0.125*beta*D_p*(1-
        C_vb));
55
56     eqn_beta = (sqrt((F_gx-F_2fr)/(F_12fl+F_1fl+F_2fl))) == P_in/(A_2*C_vb*rho_s);
57     Calculated_beta = vpasolve(eqn_beta,beta, 1.8) % the 1.5 in the equation gives matlab
        a guess where to look for a solution, 1.6 is +/- half pi so half pipe fills bed.
58
59     Calculated_V2 = P_in/(0.25*D_p^2*(Calculated_beta-sin(Calculated_beta)*cos(
        Calculated_beta))*C_vb*rho_s);

```

---

## Appendix D

---

# Sliding bed model 2 code

This code plots every possible particle velocity and production from every  $\beta$  and  $\alpha$ .

```
1  clc;
2  clear;
3  close all;
4
5  %basic assumption/variables
6  g = 9.81; %Gravity constant
7  d_50 = 22/1000; %Rock/particle diameter(50% of the rocks) [m]
8  rho_w = 1000; %Water density [kg/m^3]
9  rho_s = 2600; %Stone density [kg/m^3]
10 rho_r = (rho_s-rho_w)/rho_w; %relative density [kg/m^3] also desribed as R_sd
11 vis_l = 0.0000013; %Kinematic viscosity Miedema model excel[m^2/s])
12 C_fr = 0.2; %assumption friction factor=0.416 bed and pipe,
    miedema book p451 regime 3
13 C_rgh = 0.0015*10^-3; %Roughness plastic—> OMAE2014-23437 epsilon eq:17
    —> warn cast iron: https://www.engineeringtoolbox.com/surface-roughness-
    ventilation-ducts-d_209.html
14 w_a = 0; %added water to pipe[m^3/s]
15 C_D = 1; %Form coefficient of rock, Notes rhee p.12
16 m_p = rho_s*4/3 *pi*(d_50/2)^3; %mass of single particle
17
18 %situation dependent variable/inputs
19 L = 2; %Length of pipe
20 D_p = 0.094; %Pipe Diameter
21 lambda_w = d_50/D_p; %Ratio particle size and pipe diameter—> used for
    hindered settling
22 R_e = (3*D_p)/vis_l; %Reynolds number
23 A_p = (pi/4)*D_p^2; %Surface cross section pipe, described in figure 1,
    paper OMAW2014
24 a_wilson = 2.75; %Wilson factor p3 at eq 18 paper OMOW2014
25 n = 2.4; %The value chosen for the hindered sttling exponent
    n = 2.4, which is a value for high particle Reynolds numbers. This value is
    chosen because relative large particles are used for subsea rock installation (D
    = 0.02 – 0.1 [m]).
26 v_ls_ldv = 1.34*sqrt(2*g*D_p*rho_r)*cosd(80)^(1/3); %5.2.10 The Limit Deposit
    Velocity, from miedema
27
28
29
30 alpha_list = 10:1:90;
31 beta_list = 0.01:0.01:3.13;
32
33 % beta_list = linspace(0.01*pi,pi);
34
35
36 %this loop is with the original bed density [C_vb]
37 for i = 1:length(alpha_list)
38     for ii = 1:length(beta_list)
39         beta = beta_list(ii);
40         alpha = alpha_list(i);
41         A_2 = 0.25*D_p^2*(beta-sin(beta)*cos(beta));
42         A_1 = A_p-A_2;
43         D_H = sqrt((4*A_1)/pi);
44
45         %C_vb based on alpha, different per stone size based on tests
```

```

46 |
47 | if d_50< 25/1000
48 |     C_vb=7.7*alpha^-1.15 ;
49 |     if d_50< 20/1000
50 |         C_vb=35.5*alpha^-1.49;
51 |         if d_50< 10/1000
52 |             C_vb= 9.03*alpha^-1.045 ;
53 |         end
54 |     end
55 | end
56 |     F_gx      = g*sind(alpha)*rho_r*C_vb*A_2;
57 |     x          = C_vb*2.5*cos(0.5*beta);
58 |
59 |     % efficientie van de 'backflow'
60 |     % lambda_12 =(a_wilson*1.325)/(log(0.27*d_50/D_H+5.75/R_e^0.9))^2 ;
61 |     % original kOMAE2014
62 |     paper
63 |     lambda_12 =0.83*1.325/(log(0.27*C_rgh/d_50+5.75/R_e^0.9))^2+0.37*(2/(sqrt(2*g
64 |     *D_H*rho_r)))^2.73*(m_p/rho_w)^0.094; % Miedema book 7.3-57 Frdc
65 |     aangenomen dat v1+v2 =2
66 |     F_12fl = lambda_12*0.125*(x*((A_2)*(1-C_vb)/(A_1))+1)^2*sin(beta)*D_p;
67 |     F_2fr  = ((C_fr*g*cosd(alpha)*rho_r*C_vb*A_p*(beta-sin(beta)*cos(beta))*beta
68 |     )/(beta*D_p*pi))*D_p*beta;
69 |     F_1fl  = 0.125*1.325/(log(0.27*C_rgh/D_H+5.75/R_e^0.9))^2*(x*(A_2*(1-C_vb))/
70 |     A_1)^2*(pi-beta)*D_p;
71 |     F_2fl  = x*(1.325/(log(0.27*C_rgh/d_50+5.75/R_e^0.9))^2*0.125*beta*D_p*(1-
72 |     C_vb));
73 |     %F_2drag = 0.5*rho_w*C_D*sin(beta)*pi*(0.5*d_50)^2*(0.2*sind(alpha))^2; %
74 |     first 0.5 is for particles being in eachother drag u^2 is relative
75 |     velocity, completely vertical there is no water moving with the particles
76 |     V_2(i, ii) =sqrt((F_gx-F_2fr)/(F_12fl+F_1fl+F_2fl));
77 |     if ~isreal(V_2(i, ii))
78 |         V_2(i, ii) = 0;
79 |     end
80 |
81 |     P_o(i, ii)=V_2(i, ii)*A_2*C_vb*rho_s;
82 |
83 | end
84 |
85 | end
86 |
87 | % de alpha, hoek van de pijp begint bij 10 graden en loopt in stappen van
88 | % 1 dus V_2(38,123) is de snelheid bij 48 graden bij een beta van
89 | % 0.01+1236*0.01= 1.23
90 |
91 | %all angles are -10 because an error occurred
92 | V_R4 =V_2(38,113);
93 | V_R7 =V_2(49,126);
94 | V_R12=V_2(60,150);
95 | V_R23=V_2(70,156);
96 |
97 | Velocities_s = [V_R4; V_R7 ;V_R12 ;V_R23];
98 |
99 | P_R4 =P_o(38,113);
100 | P_R7 =P_o(49,139);
101 | P_R12 =P_o(60,151);
102 | P_R23 =P_o(70,157);
103 |
104 |
105 | Productions_s = [P_R4; P_R7; P_R12; P_R23];
106 |
107 | Run_s      = [4;7;12;23] ;
108 | Angle_s    = [48;60;70;80];
109 | Compare_results_small = table(Run_s, Angle_s , Productions_s , Velocities_s)
110 |
111 | V_R2 =V_2(37,123);
112 | V_R5 =V_2(48,151);
113 | V_R17=V_2(48,143);
114 | V_R25=V_2(49,149);
115 | V_R9 =V_2(60,164);

```

---

```

104 V_R13 =V_2(67,182);
105 V_R16 =V_2(75,245);
106
107 Velocities_m = [V_R2; V_R5 ;V_R17 ;V_R25; V_R9; V_R13; V_R16];
108
109 P_R2 =P_o(38,123);
110 P_R5 =P_o(49,151);
111 P_R17 =P_o(49,143);
112 P_R25 =P_o(50,149);
113 P_R9 =P_o(70,164);
114 P_R13 =P_o(68,182);
115 P_R16 =P_o(76,245);
116 Productions_m = [P_R2; P_R5; P_R17; P_R25; P_R9; P_R13; P_R16];
117
118 Run_m = [2;5;17;25;9;13;16] ;
119 Angle_m = [48;59;59;60;71;78;86];
120 Compare_results_medium = table(Run_m,Angle_m,Productions_m, Velocities_m)
121
122
123 V_R4 =V_2(48,113);
124 V_R7 =V_2(59,126);
125 V_R12 =V_2(70,150);
126 V_R23 =V_2(80,156);
127
128 Velocities_l = [V_R4; V_R7 ;V_R12 ;V_R23];
129
130 P_R4 =P_o(48,145);
131 P_R7 =P_o(59,151);
132 P_R12 =P_o(70,185);
133 P_R23 =P_o(80,201);
134
135 Productions_l = [P_R4; P_R7; P_R12; P_R23];
136
137 Run_l = [3;6;18;24] ;
138 Angle_l = [48;59;71;80];
139 Compare_results_large = table(Run_l,Angle_l,Productions_l, Velocities_s)
140
141
142 plot(beta_list , V_2(i,:) , 'LineWidth',3)
143 figure(1)
144 surf(beta_list , alpha_list , V_2);
145 title('Velocity sliding bed')
146 xlabel('Beta size of sliding bed')
147 ylabel('Alpha, angle pipe[degrees]')
148 zlabel('Velocity [m/s]')
149 grid on
150
151
152 %Draw horizontal lines for a certain production:
153 % hold on
154 % contour3(beta_list ,alpha_list ,V_2,[0.3 0.3] , '-r' , 'LineWidth',2) % Draw some
    velocity contour lines
155 % hold on
156 % contour3(beta_list ,alpha_list ,V_2,[0.45 0.45] , '-r' , 'LineWidth',2) % Draw some
    velocity contour lines
157 hold on
158 contour3(beta_list , alpha_list ,V_2,[0.73 0.73] , '-r' , 'LineWidth',2) % Draw some
    velocity contour lines
159 hold off
160
161
162
163 figure(2)
164 surf(beta_list , alpha_list , P_o);
165 title('Production')
166 xlabel('Beta size of sliding bed')
167 ylabel('Alpha, angle pipe[degrees]')
168 zlabel('Production [kg/s]')
169 grid on

```



```
170 |  
171 |%Draw horizontal lines for a certain production:  
172 |% hold on  
173 |% contour3(beta_list,alpha_list,P_o,[0.47*1.5 0.47*1.5], '-r', 'LineWidth',2) % Draw  
    |    Contour At 1500 tons/H  
174 |hold on  
175 |contour3(beta_list,alpha_list,P_o,[0.47 0.47], '-r', 'LineWidth',2) % Draw Contour  
    |    At 1500 tons/H  
176 |% hold on  
177 |% contour3(beta_list,alpha_list,P_o,[0.235 0.235], '-r', 'LineWidth',2) % Draw  
    |    Contour At 750 tons/H  
178 |hold off
```

---

## Appendix E

---

### Sliding bed model 2 code:rewritten

This code is mostly similar as but this code uses production as an input and provides the concentration of the bed and velocity of the particles based on production that is put in the pipe.

```
1 clc;
2 clear;
3 close all;
4
5 %basic assumption/variables
6 g = 9.81; %Gravity constant
7 d_50 = 15/1000; %Rock/particle diameter(50% of the rocks) [m]
8 rho_w = 1000; %Water density [kg/m^3]
9 rho_s = 2600; %Stone density [kg/m^3]
10 rho_r = (rho_s-rho_w)/rho_w; %relative density [kg/m^3] also desribed as R_sd
11 vis_l = 0.0000013; %Kinematic viscosity Miedema model excel[m^2/s])
12 C_fr = 0.2; %assumption friction factor=0.416 bed and pipe,
    miedema book p451 regime 3
13 C_rgh = 0.0015*10^-3; %Roughness plastic—> OMAE2014–23437 epsilon eq:17
    —> warn cast iron: https://www.engineeringtoolbox.com/surface-roughness-
    ventilation-ducts-d_209.html
14 w_a = 0; %added water to pipe[m^3/s]
15 C_D = 1; %Form coefficient of rock, Notes rhee p.12
16 m_p = rho_s*4/3 *pi*(d_50/2)^3; %mass of single particle
17
18 %situation dependent variable/inputs
19 L = 2; %Length of pipe
20 D_p = 0.094; %Pipe Diameter
21 lambda_w = d_50/D_p; %Ratio particle size and pipe diameter—> used for
    hindered settling
22 R_e = (3*D_p)/vis_l; %Reynolds number
23 A_p = (pi/4)*D_p^2; %Surface cross section pipe, described in figure 1,
    paper OMAW2014
24 a_wilson = 2.75; %Wilson factor p3 at eq 18 paper OMOW2014
25 n = 2.4; %The value chosen for the hindered sttling exponent
    n = 2.4, which is a value for high particle Reynolds numbers. This value is
    chosen because relative large particles are used for subsea rock installation (D
    = 0.02 – 0.1 [m]).
26 v_ls_ldv = 1.34*sqrt(2*g*D_p*rho_r)*cosd(80)^(1/3); %5.2.10 The Limit Deposit
    Velocity, from miedema
27
28
29
30 P_in=0.48;
31 alpha=70;
32
33
34 syms beta
35 A_2 = 0.25*D_p^2*(beta-sin(beta)*cos(beta));
36 A_1 = A_p-A_2;
37 D_H = sqrt((4*A_1)/pi);
38
39 if d_50< 25/1000
40     C_vb=7.7*alpha^-1.15;
41     if d_50< 20/1000
```

```

42     C_vb=35.5*alpha^-1.49;
43     if d_50< 10/1000
44         C_vb= 9.03*alpha^-1.045 ;
45     end
46 end
47 end
48 F_gx    = g*sind(alpha)*rho_r*C_vb*A_2;
49 x        = C_vb*2.5*cos(0.5*beta);

        % efficiency of 'backflow
50 lambda_12 =0.83*1.325/(log(0.27*C_rgh/d_50+5.75/R_e^0.9))^2+0.37*(2/(sqrt(2*g
        *D_H*rho_r)))^2.73*(m_p/rho_w)^0.094; % Miedema book 7.3-57 Frdc
        aangenomen dat v1+v2 =2
51 F_12fl   = lambda_12*0.125*(x*((A_2)*(1-C_vb)/(A_1))+1)^2*sin(beta)*D_p;
52 F_2fr    = ((C_fr*g*cosd(alpha)*rho_r*C_vb*A_p*(beta-sin(beta)*cos(beta))*beta
        )/(beta*D_p*pi))*D_p*beta;
53 F_1fl    = 0.125*1.325/(log(0.27*C_rgh/D_H+5.75/R_e^0.9))^2*(x*(A_2*(1-C_vb))/
        A_1)^2*(pi-beta)*D_p;
54 F_2fl    = x*(1.325/(log(0.27*C_rgh/d_50+5.75/R_e^0.9))^2*0.125*beta*D_p*(1-
        C_vb));
55
56 eqn_beta =(sqrt((F_gx-F_2fr)/(F_12fl+F_1fl+F_2fl))) == P_in/(A_2*C_vb*rho_s);
57 Calculated_beta = vpasolve(eqn_beta,beta, 1.4) % the 1.5 in the equation gives matlab
        a guess where to look for a solution, 1.6 is +/- half pi so half pipe fills bed.
58
59 Calculated_V2=P_in/(0.25*D_p^2*(Calculated_beta-sin(Calculated_beta)*cos(
        Calculated_beta))*C_vb*rho_s)

```

---

## Appendix F

---

# Vertical model fallpipe code 1

```
1  clc;
2  clear;
3  close all;
4
5
6  %pipe properties
7  alpha = 90;
8  D_p = 0.094; %Pipe Diameter
9  A_p = (pi/4)*D_p^2; %Surface cross section pipe, described in figure 1,
   paper OMAW2014
10
11 %Particle properties
12 d_50 = 8/1000; %Rock/particle diameter(50% of the rocks) [m]
13 rho_w = 1000; %Water density [kg/m^3]
14 rho_s = 2600; %Stone density [kg/m^3]
15 rho_r = (rho_s-rho_w)/rho_w; %relative density [kg/m^3] also described as R_sd
16 w_a = 0; %added water to pipe[m^3/s]
17 C_D = 0.8; %Form coefficient of rock, Notes rhee p.12
18 lambda = d_50/D_p; %Particle pipe ration
19 n = 2.4; % Hindered settling exponent
20 %basic properties
21 g = 9.81*sind(alpha); %Gravity constant
22
23
24 syms c
25 P_in = 0.48 ; %Production that goes in the pipe.
26 %Velococities
27 W_0 = sqrt((4*rho_r*g*d_50)/(3*C_D)); %single particle
28 W_0p = W_0*(1-lambda^2)*sqrt(1-0.5*lambda); %Hindered particle+wall influenced
29 W_s = W_0p*(1-c)^n; %Hindered particle
30 u_p = W_s+w_a/A_p;
31
32 eqn_1= u_p ==P_in/(rho_s*c*A_p);
33 c_calculated = vpasolve(eqn_1,c,0.08); %equation solver —> get concentration
34
35 V_particle=W_0p*(1-c_calculated)^n %Particle velocoty calculated
```



---

## Appendix G

---

### Vertical model fallpipe code 2

```
1  clc;
2  clear;
3  close all;
4
5
6  %pipe properties
7  alpha = 70;
8  D_p = 0.094; %Pipe Diameter
9  A_p = (pi/4)*D_p^2; %Surface cross section pipe, described in figure 1,
   paper OMAW2014
10
11 %Particle properties
12 d_50 = 15/1000; %Rock/particle diameter(50% of the rocks) [m]
13 rho_w = 1000; %Water density [kg/m^3]
14 rho_s = 2700; %Stone density [kg/m^3]
15 rho_r = (rho_s-rho_w)/rho_w; %relative density [kg/m^3] also described as R_sd
16 w_a = 0; %added water to pipe[m^3/s]
17 C_D = 0.8; %Form coefficient of rock, Notes rhee p.12
18 lambda = d_50/D_p; %Particle pipe ration
19 n = 2.4; % Hindered settling exponent
20 %basic properties
21 g = 9.81*sind(alpha); %Gravity constant
22
23
24 syms c
25 P_in = 0.48 ; %Production that goes in the pipe.
26
27 %Velococities
28 W_0 = sqrt((4*rho_r*g*d_50)/(3*C_D)); %single particle
29 W_0p = W_0*(1-lambda^2)*sqrt(1-0.5*lambda); %Hindered particle+wall influenced
30 W_s = W_0p*(1+c)^n; %Hindered particle
31 u_p = W_s+w_a/A_p;
32
33 eqn_1= u_p ==P_in/(rho_s*c*A_p);
34 c_calculated = vpasolve(eqn_1,c,0.08); %equation solver —> get concentration
35
36 V_particle=W_0p*(1+c_calculated)^n %Particle velocoty calculated
```



# Bibliography

---

- [201, 2012] (2012). Comprehensive Renewable Energy. In Heller, V., editor, *Comprehensive Renewable Energy*.
- [Beemsterboer, ] Beemsterboer, T. N. Modelling the immediate penetration of rock particles in soft clay during subsea rock installation, using a flexible fallpipe vessel. Technical report, Delft University of Technology, Delft.
- [Beemsterboer T.N., 2020] Beemsterboer T.N. (2020). Centrifuge modeling of the impact of local and global scour erosion on the monotonic lateral response of a monopile in sand. *Geotechnical Testing Journal*, 43(5).
- [de Jong, ] de Jong. Hydromechanica\_1\_7\_Comparologie\_in\_maritieme\_techniek\_01.
- [Heller, 2012] Heller, V. (2012). 8.04 - Development of Wave Devices from Initial Conception to Commercial Demonstration. In Sayigh, A., editor, *Comprehensive Renewable Energy*, pages 79–110. Elsevier, Oxford.
- [K.C.Wilson et al., 1992] K.C.Wilson, G.R.ADDIE, and R. CLIFT (1992). *Slurry transport using centrifugal pumps*.
- [Magne Aas et al., ] Magne Aas, P., Andresen, L., Carswell student, W., Grimstad, G., Johansson, J., Petter Jostad, H., Kaynia, A., Langford, T., Lunne, T., Løvholt, F., Madshus, C., Norén-Cosgriff, K., Page, A., Park, J., Saue, M., Schjetne, K., Magnus Sparrevik, P., Strout, J., Sturm, H., and Vanneste, M. Andersen (Technical Expert, Offshore Energy), Lars Andresen (Managing Director), Hans Petter Jostad (Technical Expert, Numerical Modelling), Karl Henrik Møkkelbost (Director, Offshore Energy), Per Magnus Sparrevik (Technical Expert, Subsea Technology) and James Strout. Technical report.
- [Miedema, a] Miedema, S. A. AN ANALYSIS OF SLURRY TRANSPORT AT LOW LINE SPEEDS. Technical report, Delft University of Technology, Delft.
- [Miedema, b] Miedema, S. A. Slurry Transport (2 nd Edition) Fundamentals, A Historical Overview & The Delft Head Loss & Limit Deposit Velocity Framework. Technical report, Delft University of Technology, Delft.
- [Miedema, 2013] Miedema, S. A. (2013). An overview of theories describing head losses in slurry transport: A tribute to some of the early researchers. In *Proceedings of the*



- International Conference on Offshore Mechanics and Arctic Engineering - OMAE*, volume 4 A.
- [Miedema et al., 2021] Miedema, S. A., Wang, F., Chen, X., Wang, F., Hong, G., and Chen, X. (2021). DOMINATING FACTORS IN SLURRY TRANSPORT IN INCLINED PIPES. Technical Report 2.
- [Newitt et al., 1955] Newitt, D. M., Richardson, M. C., Abbott, M., and Turtle, R. B. (1955). Hydraulic conveying of solids in horizontal pipes. *Transactions of the Institution of Chemical Engineers*, 33:93–110.
- [Richardson and Zaki, 1997] Richardson, J. F. and Zaki, W. N. (1997). Sedimentation and fluidisation: Part I. *Chemical Engineering Research and Design*, 75(1 SUPPL.).
- [Rowe, 1987] Rowe, P. (1987). A-convenient-empirical-equation-for-estimation-of-th\_1987\_Chemical-Engineeri. *Chemical Engineer Science*, pages 2795–2796.
- [Schendel et al., 2014] Schendel, A., Goseberg, N., and Schlurmann, T. (2014). EXPERIMENTAL STUDY ON THE PERFORMANCE OF COARSE GRAIN MATERIALS AS SCOUR PROTECTION. *Coastal Engineering Proceedings*, 1(34):58.
- [Schnitzlein and Hofmann, 1987] Schnitzlein, K. and Hofmann, H. (1987). AN ALTERNATIVE MODEL FOR CATALYTIC FIXED BED REACTORS. Technical Report I.
- [The White House, 2021] The White House (2021). Biden Administration Jumpstarts Offshore Wind Energy Projects to Create Jobs.
- [Ulstein, 2010] Ulstein (2010). Flinstone Deepwater rock dumping vessel.
- [Van Rhee, 2018] Van Rhee, I. C. (2018). Lecture Notes OE44045. Technical report, Tu Delft.
- [Wentink et al., 2022] Wentink, P., Jongeling, D., Verhagen, L., and Berg ten, F. (2022). Efficient rock placement for offshore wind turbine foundation. Technical report, Technical University Delft, Delft.
- [Wilson and Wilson, 2006] Wilson, K. C. and Wilson, K. C. (2006). *Slurry transport using centrifugal pumps*. Springer.

# Glossary

---

## List of Acronyms

<b>IFP</b>	inclined fall pipe
<b>GLDD</b>	Great Lakes Dredge & Dock Company, LLC
<b>SBM1</b>	Sliding bed model 1
<b>SBM2</b>	Sliding bed model 2
<b>VFM1</b>	Vertical fallpipe model 1
<b>VFM2</b>	Vertical fallpipe model 2

## List of Symbols

$A_1$	Cross-section surface water in pipe [ $m^2$ ]
$A_2$	Cross-section surface bed pipe [ $m^2$ ]
$c_{vb}$	volumetric concentration of bed[-]
$i$	Hydraulic gradient [-]
$c$	volumetric concentration[-]
$F_l$	Durand and Condolios Limit Deposit Velocity coefficient
$L_{pipe}$	Length pipe [m]
$n$	Hindered settling exponent
$F_W$	Weight bed [KN]
$F_{1,fl}$	Force between fluid and pipe wall [KN]
$F_{12,fl}$	Force between fluid and bed [KN]
$F_{2,fl}$	Force on bed due to pore fluid [KN]
$F_{2,fr}$	Force on bed due to friction[KN]
$F_W$	Weight bed KN
$O_{12}$	Width contact bed/water in pipe [ $m$ ]
$O_1$	Contact arc-length water and pipe [ $m$ ]
$O_2$	Contact arc-length water and pipe [ $m$ ]
$P_i$	Production in fallpipe[ $kg/s$ ]

---

$P_o$	Production out fallpipe [ $kg/s$ ]
$V_m$	Mixture velocity
$V_{sl}$	Slip
$V_s$	Solid velocity
$c_{vs}$	Spatial volumetric Concentration [-]
$c_{vt}$	Delivered (transport)volumetric Concentration [-]
$d_{50}$	Mass median diameter [m]
$u_w$	Velocity of water [ $m/s$ ]
$u_p$	Velocity of Particle [ $m/s$ ]
$u_*$	Friction velocity [ $m/s$ ]
$\beta$	Angle of the bed [ $rad$ ]
$\lambda_w$	Ratio diameter rock and pipe [-]
$\lambda_{12}$	Moody friction factor on bed [-]
$\lambda_2$	Moody friction factor on pipe wall [-]
$\nu$	Kinematic viscosity water [ $m^2/sec$ ]
$\omega_s$	Hindered settling velocity of particle [ $m/s$ ]
$\rho_l$	Density of liquid [ $kg/m^3$ ]
$\rho_s$	Density of solid [ $kg/m^3$ ]
$\tau_{1,fl}$	Shear stress from between fluid and pipe wall above bed [kPa]
$\tau_{12,fl}$	Shear stress bed-fluid [kPa]
$\tau_{2,fl}$	Shear stress from fluid in between bed and pipe wall [kPa]
$\tau_{2,fr}$	Shear stress from sliding friction bed and pipe wall [kPa]
$\varepsilon$	Pipe wall roughness [m]
$w_0$	Single particle settling velocity [ $m/s$ ]
$w_{0,p}$	Hindered by wall fallpipe settling velocity [ $m/s$ ]